SEDIMENTOLOGICAL AND GEOCHEMICAL STUDIES OF BARAIL SANDSTONES IN AND AROUND NGOPA VILLAGE, SAITUAL DISTRICT, MIZORAM.

A THESIS SUBMITTED IN PARTIAL FULFILMENT OF THE REQUIREMENTS FOR THE DEGREE OF DOCTOR OF PHILOSOPHY.

ORIZEN MS DAWNGLIANA

MZU REGD. NO.: 1807389

PH.D. REGD. NO.: MZU/Ph.D/1291 of 27.07.2018

DEPARTMENT OF GEOLOGY

SCHOOL OF EARTH SCIENCES AND NATURAL RESOURCES MANAGEMENT.

DECEMBER, 2022.

SEDIMENTOLOGICAL AND GEOCHEMICAL STUDIES OF BARAIL SANDSTONES IN AND AROUND NGOPA VILLAGE, SAITUAL DISTRICT, MIZORAM.

BY

Orizen MS Dawngliana
Department of Geology

Dr. Jimmy Lalnunmawia
Supervisor

Submitted
In partial fulfilment of the requirement of the Degree of Doctor of Philosophy in Geology of Mizoram University, Aizawl.

DEPARTMENT OF GEOLOGY

MIZORAM UNIVERSITY

(***A Central University established by an Act of Parliament***)

भौमिकी विभाग, मिज़ोरम विश्वविद्यालय

Mizoram : Aizawl - 796 004

मिज़ोरम : आइज़ोल – ७९६००४

Reach to us:
www.mzu.edu.in
geologymzu@gmail.com
geology@mzu.edu.in
9862329703

Dated Aizawl 19th December 2022

CERTIFICATE

This is to certify that the thesis entitled "Sedimentological and Geochemical studies of Barail sandstones in and around Ngopa Village, Saitual District, Mizoram." by Mr Orizen MS Dawngliana, Ph.D. Regn. No. MZU/Ph.D./1291 of 27.07.2018, for the award of Doctor of Philosophy in Geology of Mizoram University has been written under my guidance.

He has fulfilled all the requirements laid down in the Ph.D. regulations of the Mizoram University. The thesis is the result of his investigation into the subject. Neither the thesis as a whole nor any part of it was ever submitted to any other University for any research degree.

Dated: 19th December, 2022
Place: Aizawl

(DR. JIMMY LALNUNMAWIA)
Supervisor

DECLARATION

MIZORAM UNIVERSITY

DECEMBER, 2022

I, Orizen MS Dawngliana, Ph.D. Regn. No. MZU/Ph.D./1291 of 27.07.2018 hereby declare that the subject matter of this thesis is the record of work done by me, that the contents of this thesis did not form basis of the award of any previous degree to me or to do the best of my knowledge to anybody else, and that the thesis has not been submitted by me for any research degree in any other University/Institute.

This is being submitted to the Mizoram University for the degree of Doctor of Philosophy in Geology.

(ORIZEN MS DAWNGLIANA)
Research Scholar

(DR. JIMMY LALNUNMAWIA)
Head

(DR. JIMMY LALNUNMAWIA)
Supervisor

ACKNOWLEDGEMENT

'The mind of man plans his way but the Lord direct his step'. First and foremost, I would like to thank God almighty for His unfailing love, and for directing my path, leading me to this prestigious institution. The time that I spent in Mizoram University will always be emphasized out in my life journey. It was indeed a splendid, mesmerizing, terrific yet nerve wrecking and challenging moments making it such a beautiful wholesome life experience.

My deepest gratitude goes to my supervisor Dr. Jimmy Lalnunmawia, Department of Geology, Mizoram University for his enormous understanding, patience and enthusiasm to guide me throughout this research journey. I am incredibly privileged to receive a numerous encouragements, helpful suggestions and motivations despite his busy schedule and moreover, the risks he had taken to be present in the department amidst covid-19 pandemic. His punctuality and kindness will always capture admiration and respect. I bid him every success and greater achievements in his future. I would also like to express my gratitude towards all the teachers and office staff of the Department of Geology, Mizoram University for their support, cooperation and providing all the facilities required for the research work.

I would also like to express my sincere gratitude to my research project funding agency, DST-SERB (EEQ/2016/000655) without whom it would not be possible to complete this research.

I would also like to thank the Director and Geochemical Division, CSIR-National Geophysical Research Institute (NGRI), Hyderabad for allowing me to perform geochemical analysis in their Laboratory. I would also like to thank all the Scientists, Research scholars, Laboratory technical persons, Project assistants etc. of Geochemical Division, NGRI for allowing me to take part in sample preparation and analysis in their laboratory, helping me in better understanding and knowledge on XRF and ICP-MS machines.

I express my sincere thanks to Dr. Bubul Bharali Department of Geology, Pachhunga University College for teaching me Software application for my research and his suggestions and guidance for data interpretation using softwares. I extend my gratitude towards V. Lalramdina and Lalremruati, the current Research scholars, Department of Geology for their assists and company during my research fieldwork. I would also like to thank Laltluanpuii, current Ph.D scholar for preparing Geological Map of my study area using ArcGIS.

I would also like thank my family, my parents, my uncles and all the family members for their patience, understanding, financial, moral support and their prayers during the entire course of my research study.

Date : 19th December 2022
Place : Aizawl

(ORIZEN MS DAWNGLIANA)
Research Scholar

TABLE OF CONTENTS

LIST OF TABLES

LIST OF FIGURES

LIST OF PLATES

CHAPTER 1
INTRODUCTION

1.1 INTRODUCTION

Along the Eastern margin of North East India, Cenozoic rocks are well developed and formed part of a distinctive convergence tectonic setting. The current study focused on Barail Group of rocks which were formed in the Surma Basin. The basin is also sometimes referred to as the northern extension of Bengal Basin. Geologically, Mizoram is a part of the Neogene Surma Basin which is now surrounded by a belt of folded, elongated hill ranges with an arcuate shape that are convex to the west. "The area of Mizoram covers around 21,081 Sq.km stretching between latitudes 22˚00'N and 24˚30'N and longitudes 92˚15'E and 93˚25'E". The N-S trending hill ranges developed along the Indo-Burmese Ranges (IBR)/Chittagong-Tripura Fold Belt (CTFB) as a result of collision between Indian Plate and the Burmese Plate. The Cenozoic Stratigraphic succession of Mizoram is classified into Barail, Surma and Tipam Groups of rocks (Table 1.1). Among the among these group of rocks, Barail Group of rocks is the oldest lithostratigraphic unit being Oligocene in age having thickness of about 3000 m. The Lower to Middle Miocene Surma Group of rocks in Mizoram are separated into the Bokabil Formation and Bhuban Formation. The Bhuban Formation, which reaches a thickness of roughly 5,000 m, is the most developed lithostratigraphic unit in Mizoram. The other subdivisions of this Formation are represented by the Lower, Middle, and Upper Bhuban Units. The whole sedimentary column of the Formation is constituted by repeated succession of arenaceous and argillaceous facies. Sandstone, siltstone, mudstone and their admixtures in varying quantities are the principal lithologies exposed along with few pockets of fossiliferous rock, calcareous sandstone, intraformational conglomerate and siltstone (Tiwari and Kachhara, 2003).

Several experts in the fields of sedimentology and palaeontology have investigated the sedimentary rocks that make up the entire geology of Mizoram. The Barail Group of rocks spanned sizable amount of Assam, Manipur, Nagaland and a

sizable portion of facies in eastern Mizoram. Many scholars have carried out numerous investigations in the above areas and they have been divided into three subgroups: “Laisong, Jenam, and Renji”. But the presence of the Barail Group of rocks in Mizoram has been the subject of intense controversy. According to research done by the Geological Society of India (GSI), this rock sequence is a member of the Barail Group. “The 3000m overall thickness of the Barail sedimentary rock is primarily made up of thick sandstones intercalated with thinly laminated shale” (Behra *et al*. 2011).

A fair amount of sedimentological studies have been done in the recent past years in Surma, Tipam and Barail Group of rocks in Mizoram. The research conducted in the Barail Group of rocks in Mizoram focused on magnetostratigraphic studies by C. Lalremruatfela (2019) and a few small-scale studies on whole-rock geochemistry (Hussain and Bharali, 2019) and Malsawmtluangkima Hauhnar *et. al*. (2021) in Champhai District. Numerous researchers have studied the Barail Group of rocks in neighbouring states including Assam, Manipur and Nagaland using geochemistry and petrography (Srivastava and Pandey, 2011; Sen *et al*., 2012; Ramamoorthy and Ramasamy, 2015; Kichu and Srivastava, 2018). However, no comprehensive study in the field of geochemistry as well as petrology has been conducted in these areas. A few of the methods and techniques that have been utilized to determine the provenance, depositional environment, tectonic settings and intensity of weathering include geochemistry, heavy mineral and petrographic analysis. The source rock, depositional environment, tectonic settings and weathering conditions of the exposed rocks of the Barail Group in the Ngopa area will be interpreted using the Grain size analysis, petrography, heavy mineral analysis and geochemical studies that will be presented in this thesis.

1.2 LOCATION AND ACCESSIBILITY OF THE STUDY AREA

The study area is situated in the northeastern corner of Saitual District, Mizoram, NE India. The area is lying close to the border of Manipur and Myanmar. The distance of the Study area from Aizawl, the Mizoram state capital, is around 170 km. The study area is covered by Survey of India in its toposheet No.84 E/1 and 84 E/2 (Between Tuiphal bridge 23°48'32.53"N, 93° 9'39.46"E and Kawlbem Village

23°52'16.13"N, 93°18'27.76"E). The study area is approachable by National Highway NH-104B. All the samples taken from the area are named as BNG, where B is Barail and NG indicates Ngopa.

1.3 PHYSIOGRAPHY

The easternmost state of India, Mizoram, shares border with Bangladesh and Myanmar on its West and East side respectively. Geographically, it is a curving N-S anticlinal hill range with a surface area of 21,081 Sq. km and an average elevation of 1,000 metres above mean sea level. Phawngpui located in Lawngtlai District, popularly known as The Blue Mountain, is thought to be the state's the highest mountain peak which elevated at 2157 m above mean sea level. Typically, the topography consists of steep gorges and valleys. The major rivers that follow the valleys often flow either northward or southward. Tlawng (Dhaleswari), Tuirial (Sonai), Tuivawl, and Tut (Gutur), which flow toward Assam's Barak Valley, are some of the state's significant rivers. In addition, significant rivers that flow south include Chhimtuipui (Koladyne) and Khawthlangtuipui (Karnafuli/Karnaphuli) which originate in the southernmost corner of Mizoram.

1.4 CLIMATE

Mizoram enjoys a fairly comfortable temperate climate with winter temperatures which average between 11–21°C and summer temperatures which average between 20–30°C. The entire region is prevailed by the monsoon climate with average annual rainfall of 250 mm. Winter is typically fairly dry due to no rainfall.

1.5 SCOPE OF THE STUDY

The entire study area may be assumed as part of the Assam-Arakan basin which encompasses a sizable continental mass that includes parts of Bangladesh, northeastern India and Myanmar. This basin extends across more than 100,000 Sq.km in India including Assam, Mizoram, Meghalaya, Tripura, Manipur and a portion of Arunachal Pradesh. Due to its complicated geological structure and advantageous hydrocarbon generation and accumulation framework, the investigated area attracts interest from both the academic community and Industrial corporations.

In recent times, a few exploration company had undertaken operation of hydrocarbon resources in Mizoram. The suggested location has good exposure of Oligocene rocks. The study area lacks a scientific data base with reference to petrographical and geochemical characterization. It calls for a combined petrographical-geochemical analysis that is integrated with other proxies in order to understand the framework of Surma Basin.

The Schuppen Belt which is an indication of oil and gas calls for vigorous research activities in the thrust belt region of northeast India. However, the exploration programme in this portion of the country is not sufficient due to the regional complicacy and unstable hilly topography and lack of detailed knowledge on its structural and sedimentological characteristics. The oil exploration and production companies will be more effective in their strategy for hydrocarbon exploration in Mizoram if more scientific approach with the help of proper and detailed understanding of the attitude of the rocks, reconstruction of depositional history integrated with geochemical analysis and other factors are taken into account.

1.6 OBJECTIVES OF THE STUDY

1. To prepare lithological column of the study area.
2. To do systematic classification of the sandstones exposed in the study area.
3. To determine weathering history, depositional environment and tectono-provenance of the sandstone in the study area.

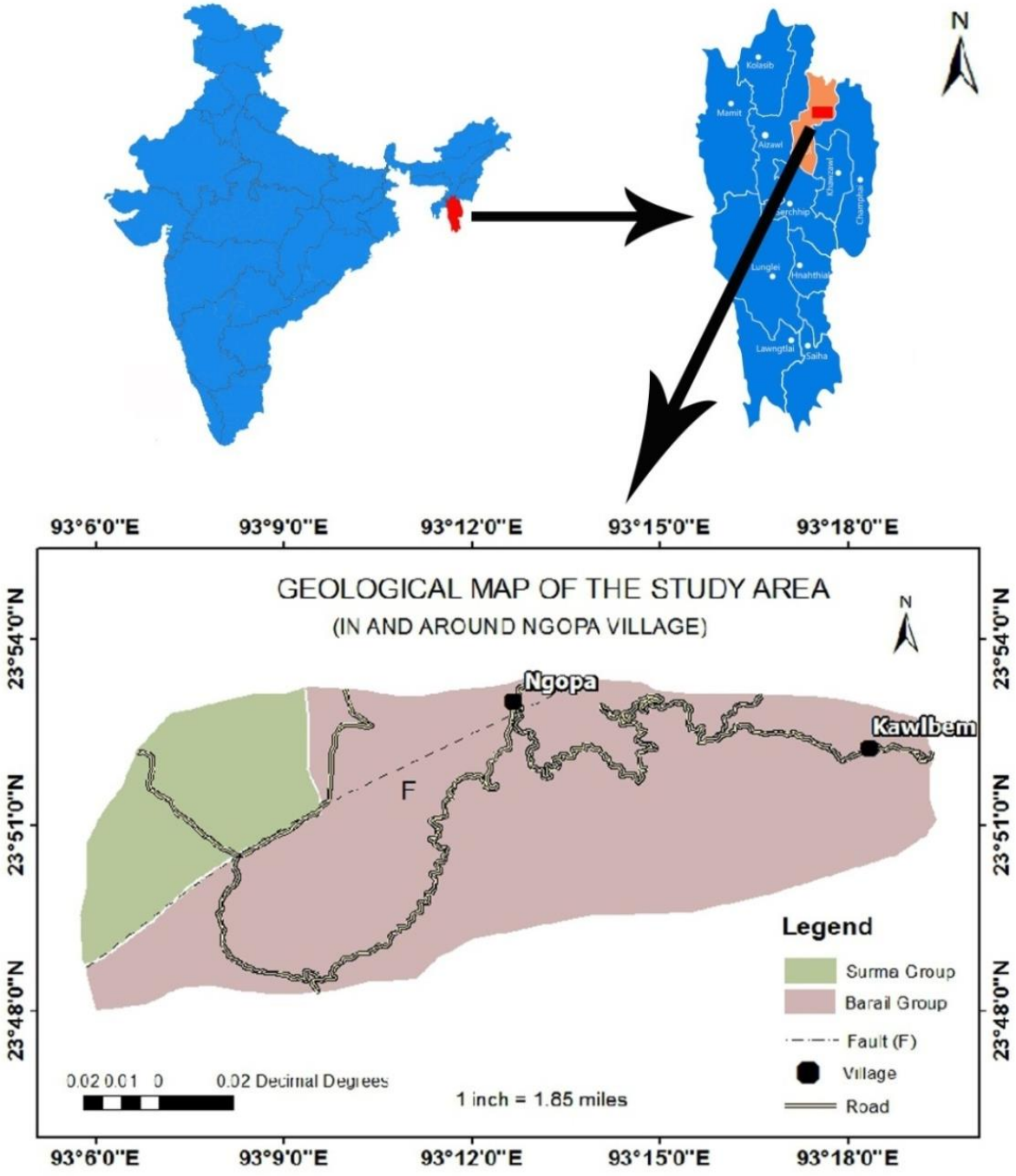

Fig. 1.1: Location and Geological Map of the study area

CHAPTER 2
LITERATURE REVIEW

A complete literature review was conducted as part of the current study in the project. According to the goals and objectives of the present work, literature survey on the related topic is conducted with the help of journals at national and international level and only certain related literatures were reviewed.

There are only few geochemical and petrological investigations in Mizoram that focused on "provenance, tectonic settings and paleoweathering of the source region". However, certain outstanding contributions made by the early workers have provided a chance to comprehend the regional perspective of the basin (Ganju, 1975; Banerjee *et al*., 1979; Nandy *et al*., 1983; Dasgupta, 1984). According to Tiwari *et al*. (2011), Skolithos and Cruziana ichnofacies were found in the Bhuban Formation of Aizawl. They also claimed that the foreshore zone had high energy environment whereas the shoreface and offshore zone had low energy conditions. Rajkonwar *et al*. (2013) also hypothesised, based on ichnofossils that the Middle Bhuban Unit exposed in and around Aizawl was subjected to varying energy conditions in the foreshore to shoreface/offshore zone of shallow marine environment. According to magnetostratigraphic studies by Tiwari *et al*. (2007) and Malsawma *et al*. (2010), the Upper Bhuban Unit had sedimentation rate higher than that of the Middle Bhuban Unit. Both the Units of Bhuban Formations were deposited in a variety of environments, ranging from shallow marine to pro-delta facies.

Lalmuankimi *et al. (*2011) carried out geochemical analysis of Upper Bhuban sandstones of Mizoram to decipher the tectonic settings and weathering conditions of the source region. Their result of CIA data indicated higher values than the Upper Continental Crust, which suggested that the source region was extensive weathered. The geochemical characteristics indicated that the Upper Bhuban sandstones were deposited in an active continental margin setting. They came to the conclusion that "the sandstones are arkose, litharenite and wacke". Lalnunmawia *et al*. (2014) conducted a provenance analysis of the Bhuban sandstones exposed in Durtlang Road, Aizawl and suggested that "the sandstones originated from igneous and

metamorphic sources, most likely from the Himalaya Orogen and the Indo-Burmese collision zones". Litharenite and sublitharenite are the two classifications for the examined sandstones. Through petrography and heavy minerals, Bharali *et al*. (2017) were able to determine the source rock, tectonic settings and paleoclimate of Upper Bhuban Unit. Based on their research, "sandstones are categorised as litharenite and wacke which were deposited in shallow marine environments and are thought to have been formed from sediments that came from felsic source rock. The sediments are transported from the tectonic source area of active continental margin to the Recycled Orogen, where they are moderately weathered under semi-humid to humid climatic conditions".

Sandstone exposed in the Champhai-Mualkawi area of the Champhai District, Mizoram, was examined in 2018 by Hauhnar and colleagues using petrography. They concluded that the studied sandstones are "very fine to fine grained sublitharenite, litharenite and feldspathic litharenite". It is hypothesised that the examined sandstones were formed by reworking sedimentary rocks, acidic to basic igneous rocks and low- to high-grade metamorphic rocks. In their study of the whole rock geochemistry of Tertiary sediments from the Mizoram foreland basin, Hussain and Bharali (2019) classified the rocks as "quartzarenite and sublitharenite" based on their mineralogy. According to the "Chemical Index of Alteration" (CIA) and "Chemical Index of Weathering" (CIW) values, the source rock for the Barail and Surma sandstone was moderately weathered. Chondrite normalised REE studies of the Surma and the Barail sandstone inferred "felsic magmatic source".

Numerous researchers have also conducted sedimentological studies on the Barail Group of rocks exposed in North East India. Sen *et al*. (2012) performed geochemical analysis of shales of Barail Group found in and around Mandardisa, north Cachar Hills, Assam and came to the conclusion that the Barail sandstone is likely formed from felsic source rock of the Upper Continental Crust, which is dominated by granitic rocks. The tectonic settings of the Barail sandstone are indicated by the CaO-K2O-Na2O ternary plot as "Active continental margin". The CIA data showed "increasing chemical maturity and moderate to high degree of chemical weathering under humid climatic conditions".

Srivastava S.K. (2013) investigated the major element geochemistry of the Barail sandstone in Jotsoma, Nagaland. The analysis revealed a transitional tectonic setting when combined with petrography and exhibits "arid to semi-arid/semi-humid climate during deposition". Ramamoorthy and Ramasamy (2015) also conducted research on the provenance of Barail sandstones exposed in Kohima, Nagaland. The Barail sandstone of Kohima is categorised as "Quartz arenite" based on modal analysis, and its provenance as a "Continental block". According to the petrographic research, the sediments came from metamorphic schist and granitic terrain. They hypothesized that humid climate prevailed at the period when the Barail sediments were deposited.

Petrography and geochemical study of Palaeogene sandstone of Kohima was also conducted by Srivastava *et al*. (2018). Based on their finding, "Quartz predominates in the Palaeogene sandstone followed by rock fragments and feldspar". Geochemical and petrographic analysis showed "transitional regime with a mixed-provenance and semi-humid environment". In and around Jotsoma Village, Kohima Nagaland, Kichu and Srivastava (2018) examined the diagenetic process of Barail sandstone. Their investigated sandstone shows diagenetic characteristics such as "authigenesis, overgrowth, deformation and bending of flaky mineral as well as various compaction effects". A derivation of mixed source sediments is suggested by their petrographic analysis.

Rahman and Suzuki (2007) conducted geochemical analyses of the Surma Group of Miocene in the Bengal Basin of Bangladesh. The examined sandstone was thought to have been formed from felsic source rock based on the "elemental ratio and chondrite normalised REE pattern with negative Eu anomaly". With the help of different tectonic discriminant diagrams, the tectonic settings of the Surma Group in the Bengal basin were suggested as "Active continental margin to Passive margin with signs of Recycled provenance". The provenance and tectonic settings of Tipam sandstone exposed in the Sita Kunda area, Upper Assam were examined by Sarma and Chutia (2013). Tipam sandstones are classed as "subarkose" based on petrography, and also a diamond plot of provenance showed that they originated from "middle, upper, and low rank metamorphic source rocks". The triangular QmFLt diagram displayed mixed and dissected arc types, suggesting that the

investigated rocks were derived from Recycled Orogen. The ZTR maturity index of Tipam Sandstone showed predominance of tourmaline and zircon, suggesting that it originated from both igneous and metamorphic source rocks. Chutia and Sarma (2013) studied the geochemical composition and source area weathering of Tipam sandstone from few oil fields in the Upper Assam Basin. According to the research, Tonalite, Granodioritic and K-Metasomatism of rocks dominate the Tipam Sandstone and the CIA implied substantial weathering of the source area.

Lalnunmawia *et al*. (2016) performed petrography and heavy mineral analyses on Upper Bhuban sandstones exposed along Aizawl to Reiek road and Tuirial road sections. The study revealed that the sandstones from these areas are "fine to medium grained" and are classified as "litharenite and sublitharenite". It was discovered that the sediments were deposited during marine transgression in a "deltaic to shallow marine environment". The study showed "rapid sedimentation". They found out that the sedimentary provenance being lithologically complex, probably of the surrounding Recycled Orogen of eastern Himalayan region and the adjoining Indo-Burmese range.

To ascertain the provenance, numerous researchers have examined the heavy mineral assemblages in the tertiary succession, the analysis of heavy mineral assemblages was conducted by Chenkual *et al*. (2010) in the Teidukhan anticline, Kolasib district, Mizoram, and they suggested that the sediments were derived from various rocks such as volcanic rocks and pegmatite to high rank metamorphic source and reworked sediments. By examining heavy minerals, Ralte (2012) investigated the provenance of Tipam sandstone near Buhchang village in Kolasib district, Mizoram. The occurrence of heavy minerals indicated cosmopolitan nature which was made up of different detrital grains of volcanic, sedimentary and metamorphic sources. According to Zoramthara *et al.* (2015), the Tipam sandstone of Buhchang village, Kolasib was deposited in a mixed source environment, with river processes predominating over marine processes.

Uddin *et al*. (2007) performed a heavy mineral constraint on the provenance of Cenozoic sediments. Their research showed that the sediments in Assam and the Bengal Basin during the Oligocene period originated from distinct sources, the Himalaya's developing orogenic belt for the Bengal Basin and the Indian craton for

the Assam. The Assam basin, on the other hand, suggested an "earlier and more nearby redeposition of Himalayan detritus, whereas sediments from the Bengal basin suggested a younger depocenter" based on their analysis of the heavy minerals.

Heavy minerals in Cenozoic silt from the Bengal basin, Bangladesh were examined by Uddin and Lundberg in 1998. "Low to intermediate grade metamorphic, silicic igneous rocks and meta-sedimentary rocks" were suggested as the source rocks based on heavy mineral content of the Eocene and Oligocene Barail Group. As a result, the abundance of stable minerals and lack of heavy minerals point to extensive chemical weathering. Further, they have concluded the Indo-Burmese or proto-Himalayan mountains as the provenance.

Srivastava and Pandey (2011) conducted provenance analysis of the Oligocene Barail sandstone in and around Jotsoma, Nagaland. According to petrography, Barail sandstones are classed as "sublitharenite". They are mostly composed of an angular to subrounded monocrystals of non-undulatory quartz. The heavy minerals that have been found are euhedral and spherical, giving them a cosmopolitan appearance. Heavy mineral assemblages and petrography both point to Recycled Orogen provenance.

Numerous studies using geochemical and petrological methods have been conducted in the nearby Bengal Basin and north eastern regions of India. Najman *et al*., (2008) used biostratigraphy, petrography, geochemistry, isotope and seismic techniques to investigate the Paleogene record of Himalayan erosion in the Bengal Basin of Bangladesh. They came to the conclusion that the Barail Formation of deltaic sandstones, which range in age from "Late Eocene to early Miocene (38 Ma to 21 Ma)" is the first substantial source of Himalayan-derived detritus to enter the Bengal basin. Devi and Mondal (2008) investigated the provenance and tectonic settings of the Barail (Oligocene) and Surma (Miocene) Group in the Surma-Barak basin, Manipur. These Barail and Surma sandstones are formed from the collision-suture fold belt and are categorised as sublitharenite and litharenite respectively. The Surma sandstone was attributed to "Quartzose Recycled Orogen and Transitional Recycled Orogen". The provenance was believed to be Craton Interior and Quartzose Recycled Orogen. They hypothesized that the source areas of these two Formations have a "humid and semi-humid climate". Barail and Surma sandstones are thought to

have originated from “Collision suture and Fold Thrust belt” according to the provenance ternary diagram.

Hossain *et al*. (2010) investigated the petrography and whole-rock geochemistry of the Tertiary Sylhet succession (Northeastern Bengal Basin of Bangladesh). According to their study, the Barail and Surma succession are dominated by sedimentary and metamorphic lithic fragments and rich in quartz but low in feldspar contents. They inferred “Recycled Orogen” tectonic provenance. The decreasing CIA value of Barail to Surma Group suggested “rapid influx of detritus to the Sylhet basin at Late Eocene rather than the Neogene”.

The provenance, tectonic context and source weathering of contemporary fluvial sediments of the Brahmaputra-Jamuna River were studied by Bhuiyan *et al*. (2011). According to their work, the sediments are mostly quartzose with traces of volcanic debris and low grade metamorphic, recycled sedimentary fragments and feldspar. The tectonic provenance was inferred as “Recycled Orogen”. They concluded that sediments of the Brahmaputra-Jamuna River are geochemically classified as “litharenite” and are thought to have come from an “active continental margin”. The furthered concluded that the rocks were originated from felsic source rock. They suggested that the chemically immature sediments from the Brahmaputra and Jamuna rivers exhibited little chemical weathering. According to Roy and Roser (2012), the tertiary sequence in the Shahbajpur-1 well, Hatia trough, Bengal basin, Bangladesh, have their provenance of homogeneous felsic source that is primarily from Himalayan debris and recycled sediments. The CIA values indicated an active state situation caused by Himalayan uplift and moderately weathering condition.

Bracciali *et al*. (2015) used a variety of methods, including U-Pb detrital zircon and rutile, isotopic (Sr-Nd and Hf) and petrography to explain the shift in origin of the neogene paleo-Brahmaputra deposit of the Surma basin. According to the study, the uplift of the Tibetan Plateau has increased river gradients and stream strength which led to the Yarlung Tsangpo river being captured by the Brahmaputra. The three methods suggested that detrital minerals arrived as a result of Cenozoic metamorphism with input from Yarlung Tsangpo.

The geochemistry of Tipam Sandstones found in and around the Dilli Area, Sivasagar District, Assam was investigated by Baruah *et al*. (2017) and they

suggested that the sediments are thought to have originated from granitic (felsic) parent rocks. They classified sandstone as sublitharenite to wacke. They assumed that the Tipam sandstone of the Dilli region originated in the tectonic conditions of an active continental edge.

Somasekhar *et al.* (2018) investigated the geochemical and petrological properties of the siliciclastic rocks of Chitravati Group of the Cuddapah Supergroup to find out provenance and depositional environment. The textural and compositional maturity of the examined sandstones was discernible. They find out that the investigated sandstone exhibited moderate to strong weathering. Their investigation inferred that the source rock are the granitoid of Cuddapah basin, which also implied that the tectonic settings were "passive to active continental margin settings" with concurrent "volcanism and sedimentation".

By using petrographical and geochemical methods, Chaudhuri *et al*. (2020) investigated the compositional change in the Mesozoic sedimentary record during the evolution of the pericratonic rift basin of Kutch. The investigation indicated the felsic source rocks with the help of different parameters like dominance of arkosic sandstone, zircon concentration, trace element abundance and ratio and enrichment of LREE with negative Eu anomaly. The study hypothesized "intermediate to intense weathering in the source area with immature to mature sediments". The tectonic settings analysis suggested that the Kutch Basin are derived in passive margin settings during the Mesozoic Era.

CHAPTER 3
MATERIALS AND TECHNIQUES

In order to achieve the objectives of the research work, the following methods and techniques are employed throughout the course of the study.

3.1. LITERATURE REVIEW

The first stage in each research project is a literature review. From the library and the internet, literatures that are pertinent to the current study are gathered. Any literature related to the present work, either in terms of methodology and application or similarity in discipline of the research provide vital information and help in the present work. Literature aids in identifying the limitations and gaps in earlier works. Thesis, scientific reports and research articles have all been compiled from the Central Library and Library of the Department of Geology, Mizoram University. In addition, certain literature resources were collected from INFLIBNET (https://www.inflibnet.ac.in), ResearchGate (https://www.researchgate.net) and Shodganga (https://shodhganga.inflibnet.ac.in). The literatures collected are briefly reviewed and presented in Chapter 4.

3.2. FIELD WORK, MAPPING AND LITHOCOLUMN PREPARATION

A thorough field assessment was conducted in the study area; Tuiphal river to Kawlbem Village, Saitual District while Ngopa is the central part of the study area. The activities during fieldwork may be briefly enumerated as follows:

a) Field analysis on sedimentary structures, lithology and detailed mapping of the litho units exposed in the study area.
b) Collection of rock samples, recording of field data on attitudes of rock like dip and strike, dip direction and thickness of the litho units and field photography.

During fieldwork, GSI toposheet No.84 E/1 and 84 E/2 was carried to mark sample location and the study area as a whole. The study area was traversed across strike and along strike to cover maximum rock exposure. During field study, 40

sandstone samples are collected from different horizons which are named as BNG, where B is Barail and NG indicates Ngopa.

The lithocolumn and geological map of the study area was prepared using free computer software such as SedLog v3.1 integrated with QGIS v3.10. The maps are prepared with the help of different lithological information recorded during field work. The toposheet of the study area is georeferenced and updated with GPS coordinates (Using Global Mapper Software) of the actual GPS data collected during field work. The geological map of the study area is shown in Chapter 4.

3.3 LABORATORY ANALYSIS

For laboratory analysis, fresh and representative 20 samples are sorted out from the total collections. The various laboratory analyses employed during the study includes:

1) Granulometric Analysis
2) Petrographic Analysis
3) Heavy Mineral Analysis
4) Preparation of powder samples for different Geochemical Analysis.

Finally, an effort has been made to comprehend the characteristics and tectonic setting, the provenance, paleoclimatic conditions, various weathering parameters, and the depositional setting of the Barail Group of rocks in the study area with the help of these laboratory investigations combined with field observations.

3.3.1 GRANULOMETRIC ANALYSIS

Granulometric analysis was carried out in Sedimentology Laboratory in the Department of Geology, Mizoram University. The selected 20 samples are prepared for Granulometric Analysis with the help of electrically operated automatic sieve shaker machine in the Department of Geology, Mizoram University which is procured under DST-SERB project (EEQ /2016/000655). A 1 kg of the samples was disintegrated into individual grains which are homogenized with the help of coning technique. Out of the disintegrated samples, a 100 g of the carefully prepared samples are taken for sieving. To adhere to the necessary grade scale, different grades of ASTM sieves such as 35, 45, 60, 80, 120, 170, 230, 325 are employed and

finally collected in pan. The ASTM sieves are placed with the coarsest mesh size at the top and the finest mesh sizes at the bottom above collecting pan. After sieving for 10 minutes, the fractions that are left on each sieve are individually packed, numbered, accurately weighted and documented.

The natures of grains that make up clastic sediments are important for textural parameter. They are related with both the depositional processes and the hydrodynamics of transportation. The understanding of transportation agencies and the depositional environment from the grain size analysis has been attempted in a number of ways (Folk and Ward, 1957; Friedman, 1961, 1967; Inman, 1949, 1952; Klovan, 1966; Moss, l962, 1963; Visher, 1965, 1969; Sahu, 1964; Passega, 1957, 1964). Folk and Ward (1957) highlighted the dependency of different size characteristics in the Brozos River bar. Friedman (1961, 1967, 1979) was the first person who recognized the bivariant scatter plot of different size parameters in distinguishing between various depositional environments.

Various plotting such as Bivariate scatter plots, Cumulative curve, log-Probability curve, log-log plot and CM pattern are prepared in the present study.

3.3.2 PETROGRAPHIC ANALYSIS

Petrographic analysis was carried out in Optical Laboratory in the Department of Geology, Mizoram University. Out of the 40 collected samples, 38 thin sections were prepared and used for petrographic analysis. 20 thin sections were selected for detailed studies such as mineral modal analysis and micro textural studies. All the microscopic analysis are carried out with the help of LeicaDM2700 P polarizing microscope equipped with Leica DFC420 camera and Leica Image Analysis software (LAS- v4.6). The petrographic modal analysis was conducted using Gazzi-Dickinson (1966) method. The modal analysis was done with the help of PETROGLITE Stepping Stage (cf. Ingersoll *et al*., 1984). The diagenetic alterations and detail mineralogical analyses have been made. Petrographic classification, tectonic setting, and provenance-related interpretations have been made using the modal analysis data. The microscopic equipments are installed in the Department of Geology, Mizoram University under DST-SERB funded project (EEQ/2016/000655).

3.3.3 HEAVY MINERALS ANALYSIS

Heavy mineral analysis was carried out in Sedimentology Laboratory in the Department of Geology, Mizoram University. Funnel separation method with principle of gravity settling was employed in which Bromoform was used as medium of seperation. The analysis involves disintegration of rock samples, separation with heavy liquids, grain mounting and identification of separated heavy mineral grains. The procedures of Heavy mineral separation are explained in the following.

1) The samples are disaggregated into pieces and soaked in water for two to three days and then dried in an oven at 110 °C. The dried samples were again disaggregated gently and 100 mesh fractions were separated through sieving.
2) 50 g of samples from step 1 is taken and treated with 10% HCl which is gently heated in a beaker to remove calcite and Fe-oxide cementing materials.
3) After gentle heating in step 2, the samples were washed with distilled water to remove soluble salts and then boiled in Sodium bicarbonate in treatment with Hydrogen peroxide.
4) The solutions were then drained and washed with distilled water and then with absolute alcohol. And then leave the sample to dry on a hot plate at 100 °C.
5) A 250 ml funnel with stop coke was half-filled with Bromoform. The samples were carefully poured into it such that the samples were uniformly distributed into the liquid. The lid of the funnel was closed to prevent oxidation of the Bromoform
6) After 35 minutes, the heavy minerals are suppose to be settled at the bottom of the funnel. Then the stop coke was opened quickly and closed immediately after the settled minerals are drained off. The stop coke was immediately closed to prevent the subsequent flow of light minerals.
7) The drained heavy minerals were filtered in a funnel with a filter paper which was later cleaned into a petridish with the help of acetone.
8) After washing the separated samples with Acetone, it was dried, mounted on a glass slide using Canada balsam and identified under the microscope in the Optical laboratory in the Department of Geology, Mizoram University.
9) The heavy minerals were counted and calculated into percentage for statistical analysis (Hubert, 1962).

3.3.4 GEOCHEMICAL ANALYSIS

The Geochemical analysis involved preparation of samples for different analytical techniques. The sample preparation in the form of powder was performed in Geochemical Laboratory, Department of Geology, Mizoram University. Powdering was done with manual grinding using Agate mortar and pestle. For XRF analysis, the samples are ground into as fine as 200 ASTM mesh size while for the HR-ICP-MS, the samples are ground as fine as talcum powder. Further preparations of samples for analysis are performed in the Geochemical Laboratory of CSIR-National Geophysical Research Institute (NGRI), Hyderabad, India. Trace and rare earth elements are analyzed using HR-ICP-MS and the major elements are analyzed using XRF.

3.3.4 (a) **Sample Preparation for High Resolution Inductively Coupled Plasma Mass Spectrometry (HR-ICP-MS) analysis (Closed system)**

The selected rock samples are ground down to a size of talcum powder (600 ASTM) mesh. Each Sample, along with the standards, is placed in a fresh Teflon beaker separately weighing 0.05 g. The Teflon sample container is filled with 10 ml of a 7:3 combination of HF and HNO_3. The powdered components are then fully dissolved by heating the samples for 48 hours at 150 °C. The samples are given two drops of perchloric acid after cooling for 48 hours ($HClO_4$). The samples were cooked in oven until they precipitated into paste (free of liquids). After that, 10 ml of 1:1 HNO_3 mixture added to the sample which is in a paste form. The samples are then heated to 150 °C for about 45 minutes, allowed to cool for a while, and then diluted into 250 ml.

10 ml of HNO_3, 5 ml of Rh (Rhodium) and 250 ml of final make-up water were added into a clean 250 ml beaker. After thoroughly shaking of the mixture, 5 ml of the prepared sample is pipetted into a 50 ml test tube and make-up water is added until the 50 ml markings was reached. The sample is then ready for analysis using the HR-ICP-MS device.

3.3.4 (b) **Sample preparation for Wavelength Dispersive X- ray fluorescence spectrometry (WD-XRF) analysis**

The samples are prepared into disc pellet using collapsible aluminium cup by pressed pellet method. In the method, the aluminium cup was partially filled with H_3BO_3 (Boric acid powder) and over which the powdered rock samples of 200 ASTM mesh size are evenly scattered. This is done to ensure that all of the Boric powders are covered by powdered sample. A hydraulic compressor was used to compress the prepared sample to form pressed pellet. The pressed pellets were prepared by two cycles of 25 tonnes hydraulic pressure at an interval of 5 seconds between the cycles. The powdered materials become compact and intact. Then, the samples are ready for WD-XRF analysis.

3.3.4 (c) **Procedure for calculation of Lost on Ignition (LOI)**

Before the samples are put into them, the crucibles (container) are cleaned, their weights are precisely measured and then 1gm of powdered samples are added for each sample separately. After that, crucibles containing samples are then exposed for about an hour to a 950 °C flame inside a kiln. After an hour, they are removed and then cooled down in a sealed container filled with silica crystals to prevent moisture from getting inside the samples. The weight of the heated sample and the crucibles are noted. Comparison was made between the two weights of the Samples + Crucible before and after heating. The distinction yields LOI values.

CHAPTER 4
GEOLOGICAL FRAMEWORK

4.1REGIONAL GEOLOGY

Nandy (2017) divided the tectonic and geology of north-eastern India into eight provinces, namely "Eastern Himalayan Collision Belt, Diorite-granodiorite complex of Mishmi Block, the Meghalayan Plateau and Mikir Hills, the Indo-Myanmar Collision Belt, the Brahmaputra Valley and the Bengal Basin". The rocks in these provinces, which cover the whole geological age, are found in close geographical connection. "The Patkoi-Naga-Manipur-Chin Hills-Arakan Yoma, which has a westerly convex-arctic belt with a NW-SE tendency at its southern apex and extremes and an ENE-WSW trend at its northern terminus, is affected by the Indo-Myanmar collision". The N-S trending Shan-Sagaing fault, the Sino-Myanmar high land and the Eastern Boundary Thrust, which represents the Palaeogene-Neogene age, are the boundaries of the central Myanmar sedimentary basin, which is 200 km wide and 1 400 km long. According to Nandy (2017), two prominent molasses basin namely "Tipam and Surma basin" formed close to the Oligocene in the Indo-Myanmar collision belt. The fold belt of the Surma basin had its origin in the southern region of Meghalaya while the Tipam molasse originated in the northern part of Upper Assam. The Paleogene subduction-accretionary complex, which includes Eocene-Disang flysch facies and Oligocene-Barail sub-flysch facies along the Chin Hills through Arakan Yoma Flysch facies, was represented by the outer arcades of the Indo-Myanmar tectonic ridge and the Andaman-Mentawai ridge. The Disang and Jaintia Group were covered by the arenaceous Barail Group of rocks, which were assumed conformable to the Oligocene Period. Nandy (2017) claimed that the rocks of Barail Group span a total of around 200 km, from Jaintipur in the east via Jatinga gorge to the region of Kohima. The outcrop extends from Kohima towards the south following the eastern border of the State of Mizoram. The Barail rocks of Lower Assam are subdivided into Upper Renji characterized by massive sandstone, Middle Jenum characterized by alternating beds of sandstone, shale, and

carbonaceous shale, and the Lower Laisong characterized by sandstone and subordinate shale.

Entire sequence of tertiary sediments from the Himalayan and Indo-Myanmar ranges, as well as more recent alluvium deposits from the Ganga-Brahmaputra delta, are found in the Bengal basin. It includes Bangladesh, W.Bengal, and the northern portion of the Bay of Bengal. Since the Cretaceous Period, the India Plate has collided with Eurasia and Burma to form the Bengal basin (Mitchell and Reading, 1986; Uddin and Lundberg, 1998). One of the greatest delta complexes in the world covering an area of more than 200,000 Sq.km was developed in the Bengal Basin of Bangladesh. The orogenic sediments from the Indo-Burmese Ranges to the east and the eastern Himalayas to the north mostly deposit the sediments (Uddin and Lundberg, 1999). Uddin and Lundberg (1998) hypothesized that the Oligocene Barail sediments are derived from proto-Himalaya and the Miocene Surma sediments from granitic sources based on petrographic research. According to Hossain *et al*. (2010) and Rahman *et al*. (2014) carried out geochemical analysis of rocks from the Bengal Basin and concluded that the Surma and Barail sediments were primarily produced from felsic source rock in the Himalaya.

4.2. GENERAL GEOLOGY AND STRATIGRAPHY OF MIZORAM

The westerly convex arcuate belt, or the Patkoi-Naga-Manipur-Chin Hills-Arakan Yoma section of the Indo-Myanmar mobile belt, includes Mizoram, also known as the Chin Hills (Nandy, 2017). The Surma group of rocks cover the majority of Mizoram's orogenic phase, which is thought to be the southern extension of the Neogene Surma basin. Typically “shallow marine and deltaic complexes with recurrent transgressive-regressive patterns” make up the Surma sediments. The post-Barail unconformity, which is then faulted to the east, surrounds the Surma basin (Nandy, 2017). A groundbreaking study by Nandy and Sarkar (1973) and Mukherjee and Saxena (1973) on the sedimentary structure, lithology, and sedimentation history of Mizoram suggest that turbidity current action causes sedimentation to occur in the deep sea flysch environment. The entire sedimentary succession of Mizoram is constituted by rhythmic alternate bands of Palaeogene-Neogene arenaceous and argillaceous rocks, with each group of rocks having unique

lithologlogical component. The lithology includes pockets of calcareous sandstone, shell-limestone, and intraformational conglomerate in addition to siltstone, sandstone, shale silty sandstone, mudstone, and their combinations in variable proportions (Tiwari and Kachhara, 2003). This sequence broke up into several roughly N-S trending, longitudinally dipping synclines and anticlines (Ganju, 1975; Ganguly, 1975, 1983). The rock sequence has a strike direction of N-S with a dip that ranges from 20 to 50 degrees either east or west.

According to Karanakaran (1974) and Ganju (1975), the upper Miocene to lower Pliocene rocks of the Tipam group are classified as Barail (Oligocene), Surma (lower to middle Miocene), and the tertiary succession of Mizoram is commonly separated into these three groups. A few ONGC employees, including Ganju (1975), Ganguly (1985), and Shrivastava *et al*. (1979), excluded the Barail formation from Mizoram, although other employees, including Nandy (1972) and Nandy *et al*. (1983) stated the Barail formation was present in the eastern section of Mizoram. The current study, however, was crucial in studying this contentious subject.

The Oligocene Barail sediments of Mizoram are composed of a thick (+3000m) sequence of fine to very fine-grained, minor siltstone and silty-shale, as well as the presence of carbonaceous sandstone, according to Karunakaran (1974) and Ganju (1975). Where sandstone, silty shale, and siltstone are interbeds, they are often pale-gray to brown in hue. Sedimentary structures including ripples, flute casts, and other similar formations are primarily seen in this region, along with a thin streak of carbonaceous materials that is occasionally visible.

The Surma Group of rocks, which are exposed extensively in neighbouring states like “Tripura, Cachar, West Manipur, the Chittagong Hill tract of Bangladesh, and the Arakan Coastal Area of Myanmar”, range from the Upper Oligocene to the Miocene age. Within Mizoram, they occupy thickness of +5950m. The Bokabil and Bhuban Formations are subdivided into the Mizoramian Surma Group based on the quantity of sandstone and shale (Evans, 1932). Once more divided into the Lower, Middle, and Upper Bhuban subgroups, the Bhuban Formation has a thickness of more than 7000m (Nandy, 2017). They are primarily composed of argillaceous and arenaceous rocks with siltstone and shale.

Table 4.1. Stratigraphic Succession of Mizoram (Modified after Karunakaran, 1974 and Ganju, 1975).

<table>
<tr><th>Age</th><th>Group</th><th>Formation</th><th>Unit</th><th>Generalized lithology</th></tr>
<tr><td>Recent</td><td>Alluvium</td><td>-</td><td>-</td><td>Silt,clay and gravel</td></tr>
<tr><td colspan="5">Unconformity</td></tr>
<tr><td>Early Pliocene to Late Miocene</td><td colspan="2">TIPAM (+900m)</td><td>-</td><td>Friable sandstone with occasional clay bands</td></tr>
<tr><td colspan="5">——————————Conformable and transitional contact——————————</td></tr>
<tr><td rowspan="8">Miocene to Upper Oligocene</td><td rowspan="8">S
U
R
M
A
(+5950m)</td><td>BOKABIL (+950m)</td><td>-</td><td>Shale, siltstone and sandstone</td></tr>
<tr><td colspan="3">———Conformable and transitional contact———</td></tr>
<tr><td rowspan="3">B
H
U
B
A
N</td><td>Upper Bhuban (+1100m)</td><td>Arenaceous predominating with sandstone, shale and siltstone</td></tr>
<tr><td colspan="2">–Conformable and transitional contact–</td></tr>
<tr><td>Middle Bhuban (+3000m)</td><td>Argillaceous and predominating with shale, siltstone shale alternations and sandstone.</td></tr>
<tr><td colspan="2">–Conformable and transitional contact–</td></tr>
<tr><td>Lower Bhuban (+900m)</td><td>Arenaceous predominating with sandstone and silty shale</td></tr>
<tr><td colspan="5">——————————Unconformity obliterated by faults——————————</td></tr>
<tr><td>Oligocene</td><td>BARAIL (3000m)</td><td>-</td><td>-</td><td>Shale, siltstone and sandstone</td></tr>
<tr><td colspan="5">——————————Lower contact not see——————————</td></tr>
</table>

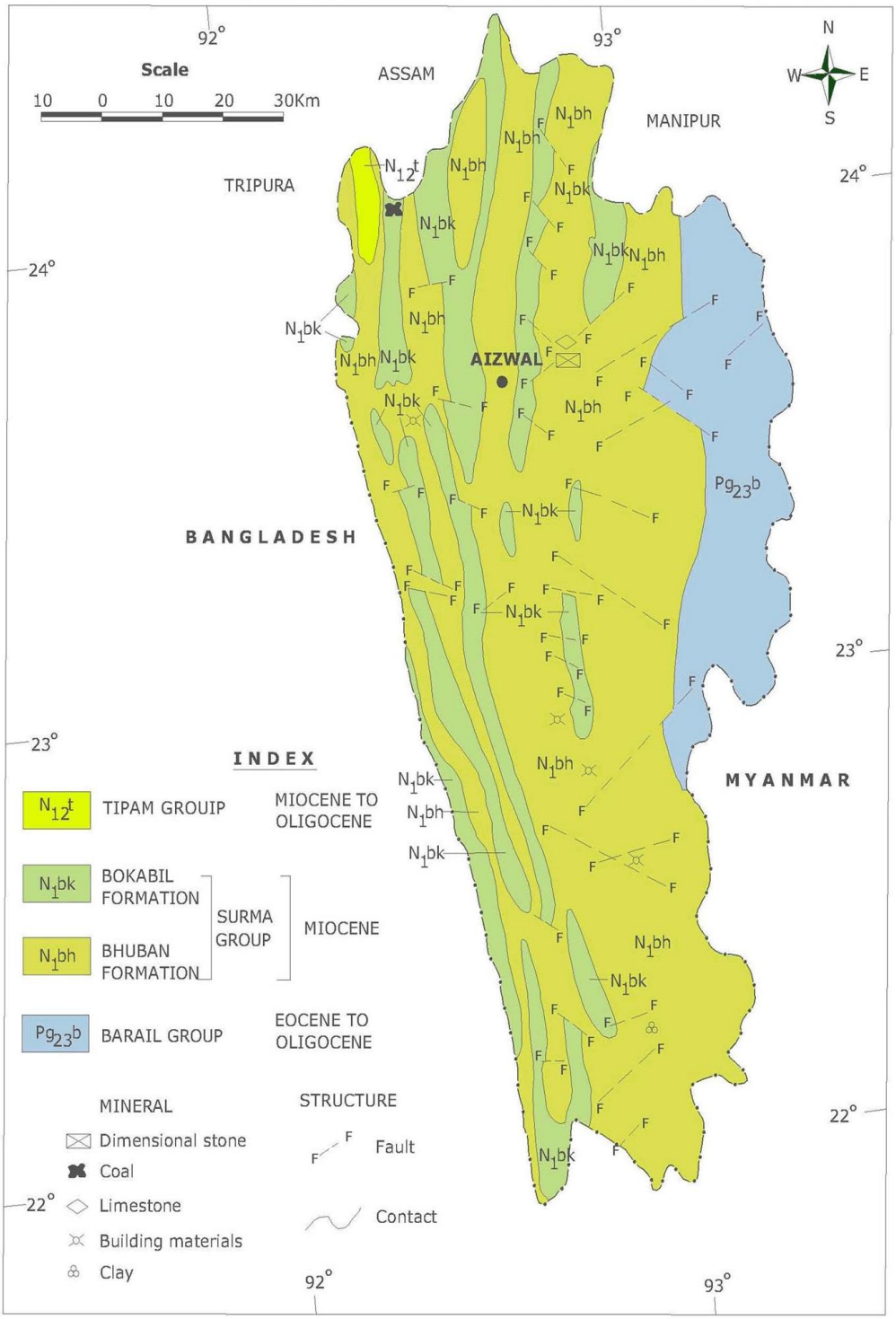

Fig. 4.1 Geological map of Mizoram (Behra *et al*., 2011).

The Bokabil Formation of the Surma Group was deposited along synclinal cores in the northern section of Mizoram. All of the formation ranges in thickness from 1000 to 1500 m and is primarily composed of argillaceous, soft and grey, laminated shale, siltstone/shale alternation and calcareous siltstone. The Bokabil Formation of Mizoram is constituted by different components of sedimentary rock like shale, silt shale, thinly laminated siltstone, thinly bedded sandstone and buff colored, fine to medium grained friable sandstones all of which have undergone varying degrees of weathering. "The Bokabil Formation of the Surma Group is unconformably overlain by rocks from the Tipam Group, which range in age from Early Pliocene to Late Miocene". Petrified wood are often observed and medium to coarse ferruginous sandstone make up the majority of their composition. "The heart of the shallow synclinal trough of the northwest Mizoram, eastern Tripura-Cachar, and Chittagong fold belts is where the litho-units of the whole Tipam rocks are found. The 900 m thick Tipam Group of Mizoram is made of friable sandstone with sporadic clay bands". The regional geology of Mizoram after Behra *et al.* (2011) is shown in Fig. 4.1.

4.3 GEOLOGY AND LITHOLOGICAL COLUMN OF THE STUDY AREA

The present study region, which includes Ngopa village and its surroundings, is covered by approximately +3000 m thick Barail Group of rocks. The atudy area extended within a road section between Tuiphal river bridge to Kawlbem village. The lithological columns are created along this section based on field observations (Figures 4.2 a-c).

Based on geological field work and field observation, the study area of Ngopa and its adjoining areas are found to be made up of sandstone, siltstone, and shale, and these rocks occur as rhythmic beds in varying proportions of thickness. Figure 4.3 (a & b) showed field photos and rock exposures in the study area. The majority of shale are splintery and crumpled type and all rock types show inter-bedded relationship. The sandstones are compact, hard and have fine to very fine grain size. They are predominantly buff in color. The field observations showed that the sandstone, siltstone and shale boundaries show transitional contact. Although sandstones are typically massive, some of the sedimentary structures like different kinds of ripple marks, burrows, ball and pillow structures, load casts, rain drop structures, lens, cross

laminations, ripped up clasts, liesegang etc. are exceptionally well preserved (Figure 4.4 a&b). The sandstones are occasionally found thickly bedded while in other cases they are also thinly bedded and intercalated with laminated siltstones, silty shale, or shale. The buff-colored variant of the sandstones, in particular, have high biotite composition which results in a "high leaching of Fe from these ferromagnesian minerals" giving the rock its reddish-brown color. The buff colored sandstones are therefore highly micaceous in characteristics. There are bioturbated preservations in the form of burrows in some of the sandstone beds which may suggest and support the hypothesis of a shallow depositional environment with an oxidizing environment and supportive environment for living organisms where sun light could reach. According to general lithology, the shale components are exceedingly fine and cannot be identified using a hand lens of 10x or even under the microscope. They are frequently referred to as crumpled shale due to their brittleness and highly fracturing property.

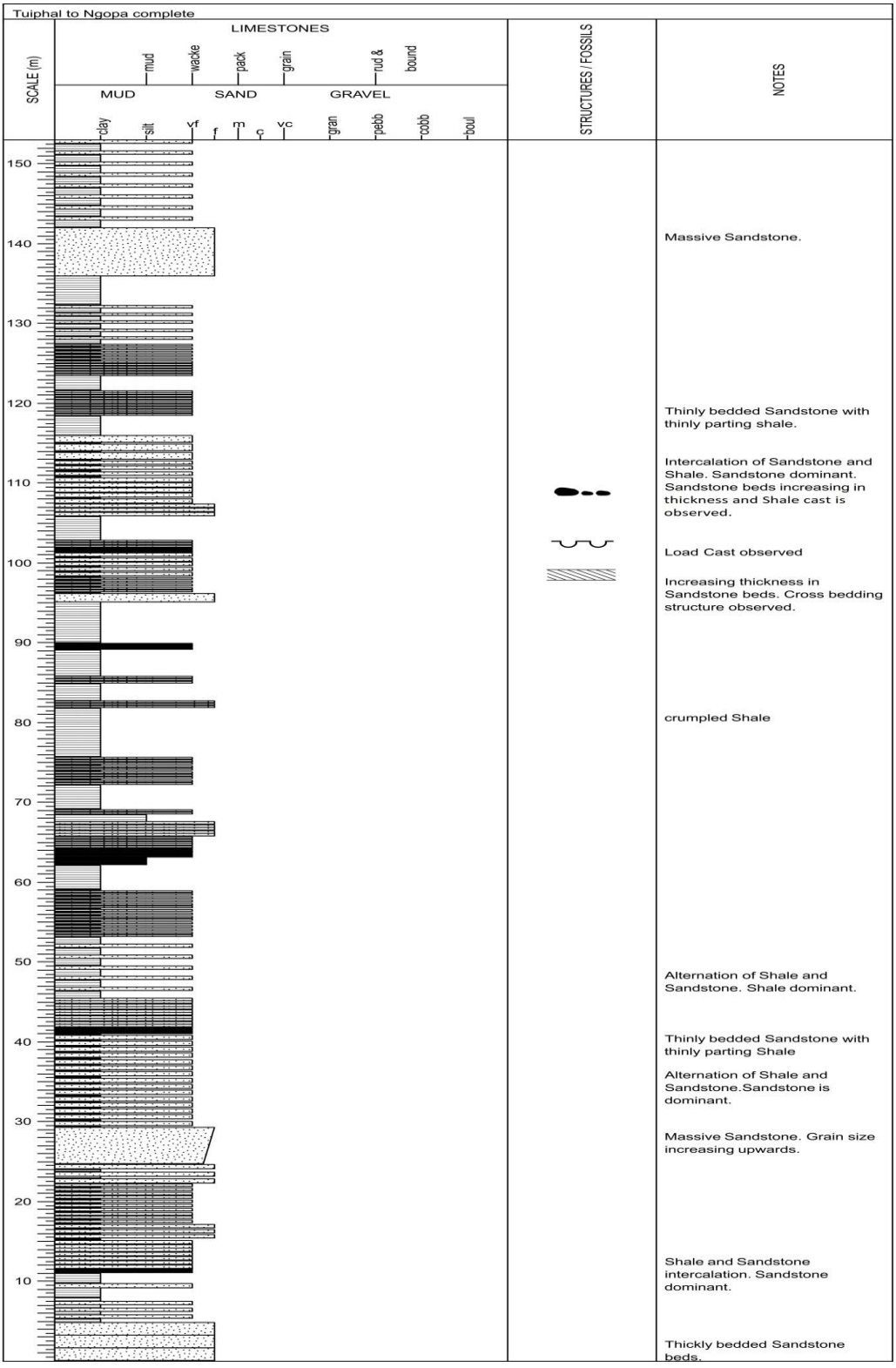

Fig. 4.2 (a) Lithological column of Tuiphal bridge to Ngopa village, Mizoram.

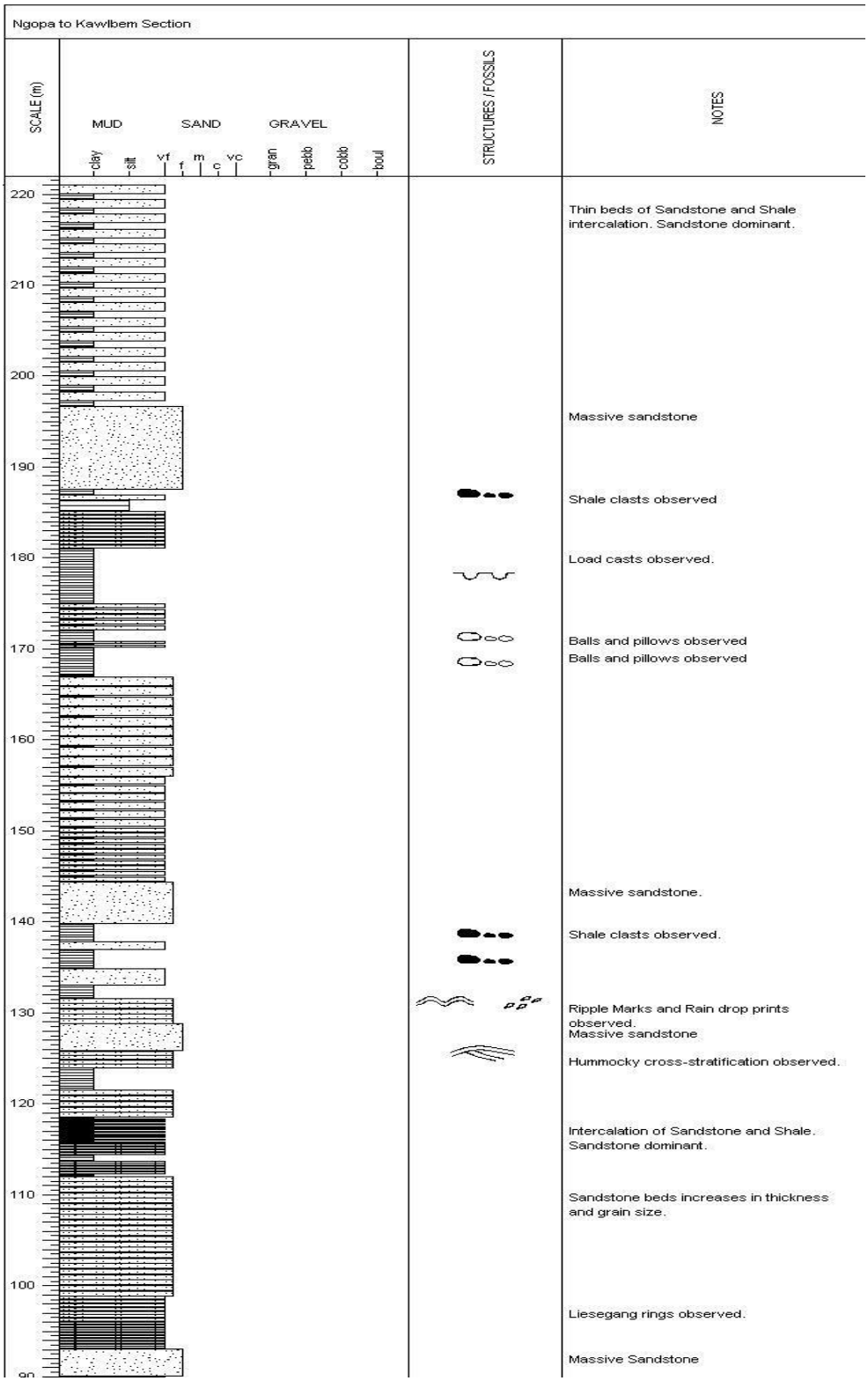

Fig. 4.2 (b) Lithological column of Ngopa village to Kawlbem Village, Mizoram (column continue in next page).

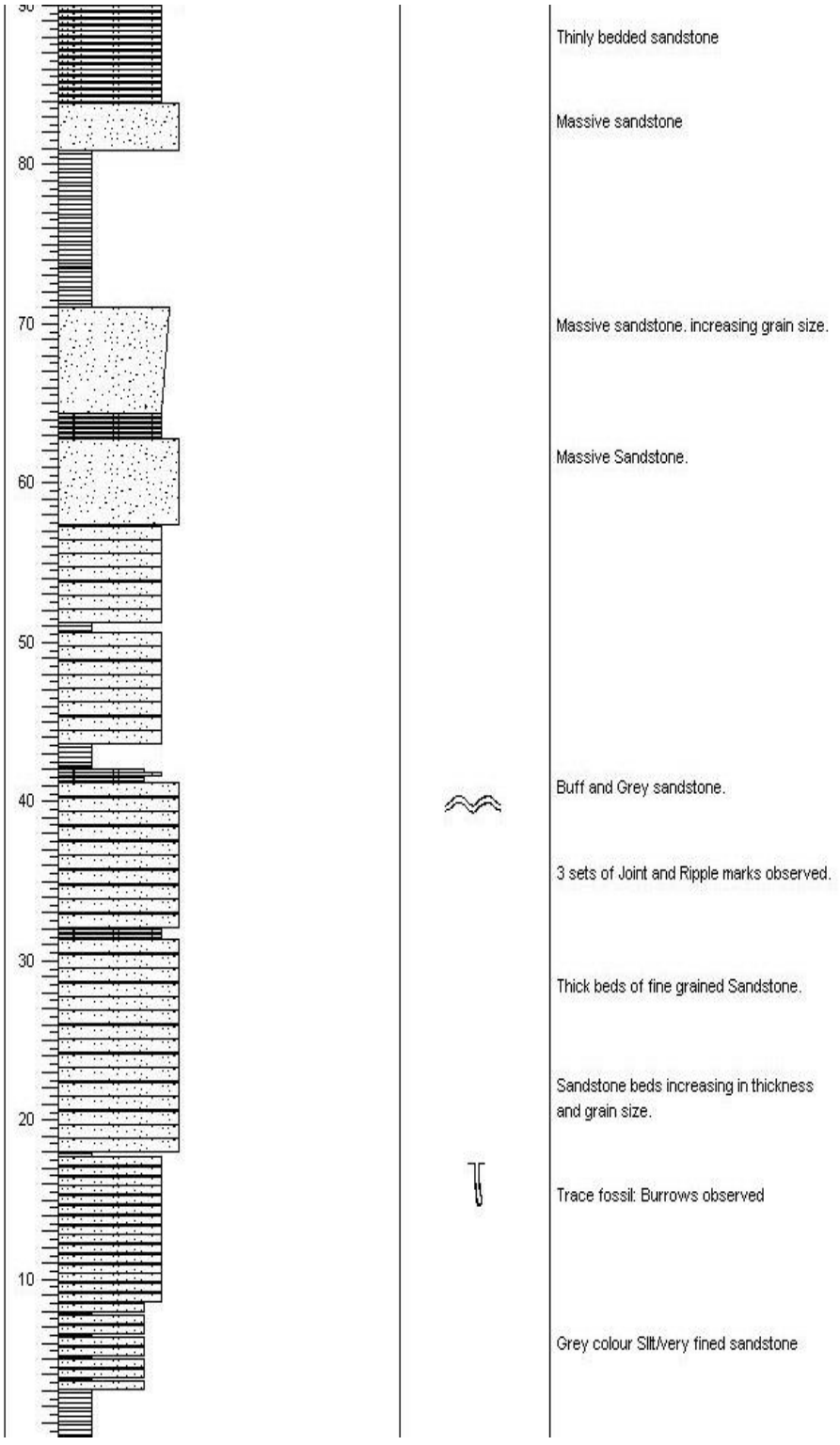

Fig. 4.2 (c) Lithological column of Ngopa village to Kawlbem Village, Mizoram.

Fig.:4.3 (a) Intercalation of sandstone and thinly bedded shale of Barail rocks exposed between Ngopa and Kawlbem Village, Mizoram.

Fig. 4.3 (b) Intercalation of sandstone and thinly bedded shale of Barail rocks exposed at Kawlbem Village, Mizoram.

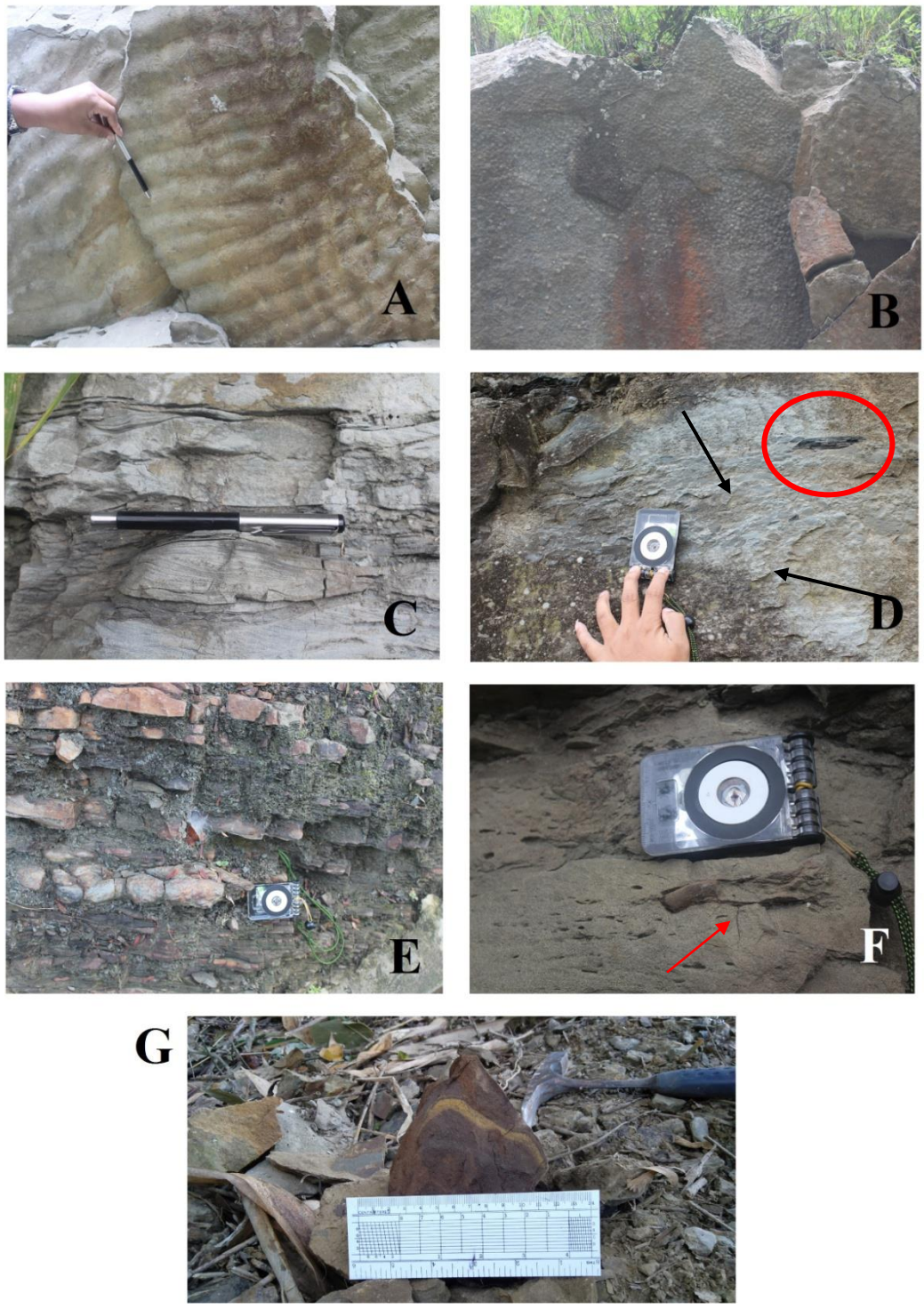

Fig.: 4.4 (a): Observed sedimentary structures in the study area of Ngopa (Mizoram): A - Ripple marks, B - Rain drop imprints, C - cross lamination, D - Coal fragment (red circle) and shale clasts (arrows), E - Ball and pillow structure, F - Burrows, G - Leisegang.

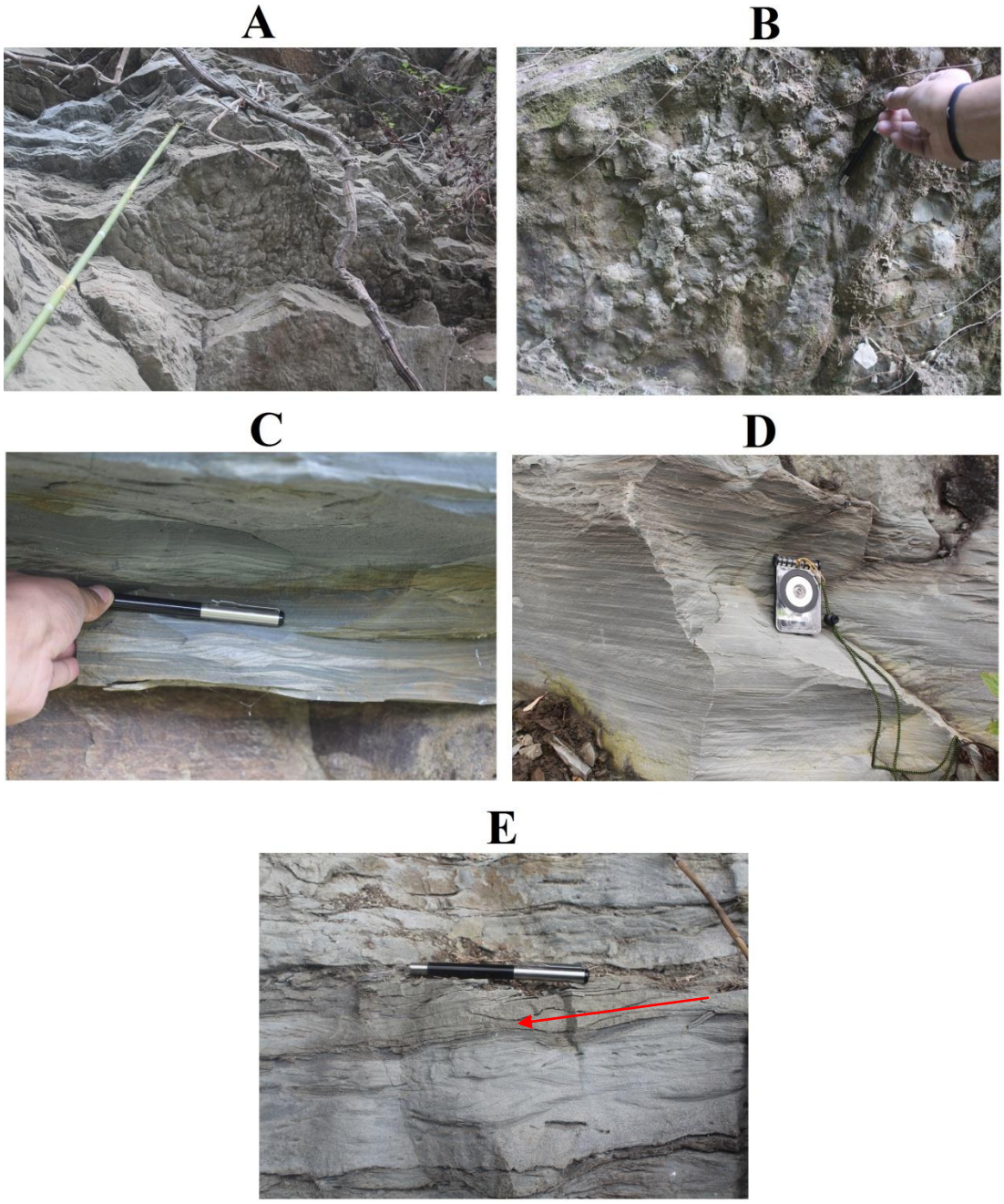

Fig.: 4.4 (b): Observed sedimentary structures in the study area of Ngopa (Mizoram): A&B – Load structures, C – Planar cross bedding and Shale laminations, D –Shale lamination, E – Small scale trough cross bedding and shale lamination (arrow).

CHAPTER 5
TEXTURAL ANALYSIS

5.1. INTRODUCTION

Granulometric analysis is a traditional tool that provides additional information about sediment transport, energy conditions, and depositional environment (Udden, 1914; Wentworth, 1922; Otto, 1939; Keller, 1949; Inman and Chamberlain, 1955; Srivastava and Mankar, 2009). It can also be described as a method for determining the relative proportions of different-sized particles in sediments. Many workers have attempted to use grain size parameters to determine environments of deposition (Uden, 1914; Wentworth, 1931; Krumbein, 1937; Keller, 1945; Folk, 1954; Folk & Ward, 1957; Passega, 1957, 1964, 1977; Friedman, 1961; Visher, 1969; Roy & Biswas, 1975).

According to Friedman and Johnson, 1982, Textural parameters of a sediment rock include individual grain shape, roundness, grain-size and their particle arrangement, which is packing ad fabric. A study of this textural element can provide a clue to their environment of deposition.

Since the size distribution is related with the physical forces for transportation and deposition, it is one of the most important parameter for the study of the nature of deposition for clastic sediments. The distribution of the grain size is considered to be influenced by their environment of deposition.

In textural studies, sieving is the most common technique for long period. (Blatt *et al*.1980). In the present study, emphasis was given for textural studies relating to size, sorting, skewness and kurtosis of Barail sandstones of Ngopa area. The data obtained were then utilized further to interpret the provenance and their environment of deposition. The relationships of sediments that are inter dependent of various textural attributes of the Ngopa area sediments were studied with the help of bivariate plots. Size analysis of the sediments can serves as an essential tool to understand their mechanism of transportation and environment of deposition (Moiola and Weiser,

1968). A huge number of early workers have contributed to grain size studies including Udden (1898, 1914), Wentworth (1922, 1929), Krumbein and Pettijohn (1938) and Otto (1939). Doeglas (1946) has also demonstrated that grain size distributions are mixture of two or more populations generated by varying transport conditions. From their Textural analysis study from Mustand Island, Texas, Mason and Folk (1958) suggests that a plot of skewness versus kurtosis was useful in differentiating between beach and Aeolian flat. The Scatter plots of mean size versus Standard Deviation and Skewness versus standard deviation were useful in differentiating between beach sand and dune or river sands. Friedman (1961, 1967) these apart, Visher (1969) and his co-workers demonstrated that each cumulative curve comprises a number of straight-line segments of different slopes which represent truncated Log-Gaussian sub populations.

Table 5.1 Frequency of weight retained (out of 100g) in each Mesh sizes and collecting pan for each sample of Barail sandstones, Ngopa area, Saitual Dist., Mizoram.

Sample No./ASTM	35	45	60	80	120	170	230	325	pan
BNG-1	11.43	9.05	28.04	16.95	19.42	2.17	8.23	0.83	1.02
BNG-2	6.39	14.89	26.07	16.76	14.39	7.93	9.24	0.81	1.21
BNG-3	11.27	13.68	16.74	19.13	12.27	8.7	10.26	1.06	5.39
BNG-4	9.87	8.57	12.17	13.74	13.22	17.19	19.79	1.87	1.78
BNG-5	8.74	12.01	18.63	21.99	13.55	7.76	9.73	0.98	5.1
BNG-6	16.29	16.24	13.25	8.38	26.67	6.09	2.91	3.22	4.16
BNG-7	5.98	11.28	17.85	15.31	14.81	14.27	13.57	0.69	5.39
BNG-8	11.44	12.68	27.63	19.8	7.67	7.37	9.15	1.07	1.52
BNG-9	14.07	17.27	16.03	8.03	4.86	8.21	21.79	3.16	5.63
BNG-10	5.19	8.63	17.81	23.56	17.13	11.86	10.05	1.37	3.57
BNG-11	9.78	13.77	11.95	8.51	9.49	19.08	18.15	2.38	3.55
BNG-12	18.35	15.21	13.67	8.97	17.23	7.12	13.81	2.83	1.45
BNG-13	11.18	11.92	16.76	15.62	13.45	12.72	13.83	2.14	2.35
BNG-14	9.44	16.68	27.01	15.08	5.72	6.03	13.7	0.87	3.72
BNG-15	8.71	14.61	15.21	9.51	7.41	26.69	9.85	2.2	4.51
BNG-16	6.95	12.94	13.83	9.85	10.01	19.8	19.33	1.82	4.7
BNG-17	12.89	15.67	18.45	21.13	8.93	7.96	10.01	1.56	2.38
BNG-18	11.88	13.72	18.01	13.83	12.12	13.28	7.76	3.6	4.21
BNG-19	10.88	10.89	15.04	14.08	13.5	15.46	13.16	2.8	2.76
BNG-20	8.7	10.01	18.63	22.99	13.55	9.76	8.73	1.01	5.1

Table 5.2: Cumulative weight percentage of Barail sandstones, Ngopa area, Mizoram

Sample/Φ	**1**	**1.5**	**2**	**2.5**	**3**	**3.5**	**4**	**4.5**
BNG-1	11.77	21.08	49.95	67.4	87.39	89.62	98.1	98.95
BNG-2	6.54	21.78	48.47	65.63	80.36	88.47	97.93	98.76
BNG-3	11.44	25.33	42.32	61.75	74.2	83.04	93.45	94.53
BNG-4	10.05	18.78	31.17	45.16	58.63	76.13	96.28	98.19
BNG-5	8.87	21.07	39.98	62.31	76.07	83.95	93.83	94.82
BNG-6	16.76	33.46	47.09	55.71	83.15	89.41	92.41	95.72
BNG-7	6.03	17.41	35.41	50.85	65.79	80.18	93.87	94.56
BNG-8	11.63	24.53	52.63	72.77	80.57	88.06	97.37	98.45
BNG-9	14.2	31.64	47.82	55.93	60.84	69.13	91.13	94.32
BNG-10	5.23	13.94	31.89	55.65	72.93	84.88	95.02	96.4
BNG-11	10.12	24.36	36.73	45.53	55.35	75.09	93.87	96.33
BNG-12	18.6	34.02	47.88	56.97	74.44	81.66	95.66	98.53
BNG-13	11.18	23.11	39.87	55.5	68.95	81.67	95.51	97.65
BNG-14	9.61	26.59	54.08	69.42	75.25	81.38	95.33	96.21
BNG-15	8.71	23.63	39.04	48.67	56.18	83.22	93.2	95.43
BNG-16	7	20.04	33.98	43.91	54	73.95	93.43	95.26
BNG-17	13.02	28.85	47.49	68.84	77.86	85.91	96.02	97.6
BNG-18	12.07	26.01	44.31	58.37	70.68	84.18	92.06	95.72
BNG-19	11.04	22.09	37.34	51.63	65.32	81.01	94.36	97.2
BNG-20	8.83	19	37.92	61.26	75.02	84.93	93.8	94.82

5.2 GRAPHICAL REPRESENTATION OF GRAIN-SIZE DISTRIBUTION

The data obtained from the grain size analysis can be presented graphically in the form of Histogram, frequency curve and cumulative-frequency curve.

5.2.1 **Histogram**

Histogram is the simplest method of representing grain size data and they represent frequency-distribution data of the studied clastic sediments of Barail from Ngopa area. It is a simple bar graph in which weight percent of sediment in each size is plotted as rectangle. The bars are arranged vertically along horizontal scale which marks various class limits. However, they cannot be used to determine statistical parameters and the sieve interval (Mesh sizes) selected greatly affects their shape. Histogram is useless for detailed analysis (Friedman and Johnson, 1982).

Histogram plot of the present work is shown in fig. 5.1(A to D). All of the Histogram shows unimodal nature

5.2.2 **The frequency distribution curve**

Frequency distribution curve is generated by plotting the various grain sizes (In percentage). It is a plot of frequency where some variables occur within arbitrarily defined subclass of a poThe class limits are transcribe in a Phi units (Friedman and Johnson, 1982). Frequency values are put along the ordinate (y-axis) while the phi values are plotted along abscissa. The highest point of the frequency curve gives the modal values (Friedman and Johnson, 1982).

Figure 5.2 A-D shows the frequency distribution curves of the studied Barail sandstone samples. The samples show Unimodal nature.

5.2.3 **The cumulative frequency curves**

The cumulative frequency curves are differing from simple frequency curve. They represents the sum of all the percentages of the adjacent previous (coarser) size classes. The cumulative curves have many advantages over the frequency curve whereas: They test for normality of a distribution, their statistical measure is more

accurate, standard deviation of the distribution is marked by slope of the line as a function (steep slope means low standard deviation value and gentle slope means high deviation value) and also, if there are separate subpopulations, they are identifiable as straight line segments (Visher, 1969).

The log-probability graph of cumulative frequency curve of particle sizes come out as three or even more straight-line segments with different slopes separated by sharp breaks, these breaks reveals the mechanisms of deposition of sediment particles. Sediments deposited by rolling or sliding are marked by a coarser end the suspension deposition are depicted by a finer end segments. Sediment particles which are transported by a jumping or saltation behaviour are also depicts by the largest segment in the centre (Fridman and Johnson, 1982).

The log-probability graph plot (Fig. 5.3) of the studied samples show that there are three to four sub-popoulations which were produced mainly by three transportation modes such as; rolling and sliding and saltation.

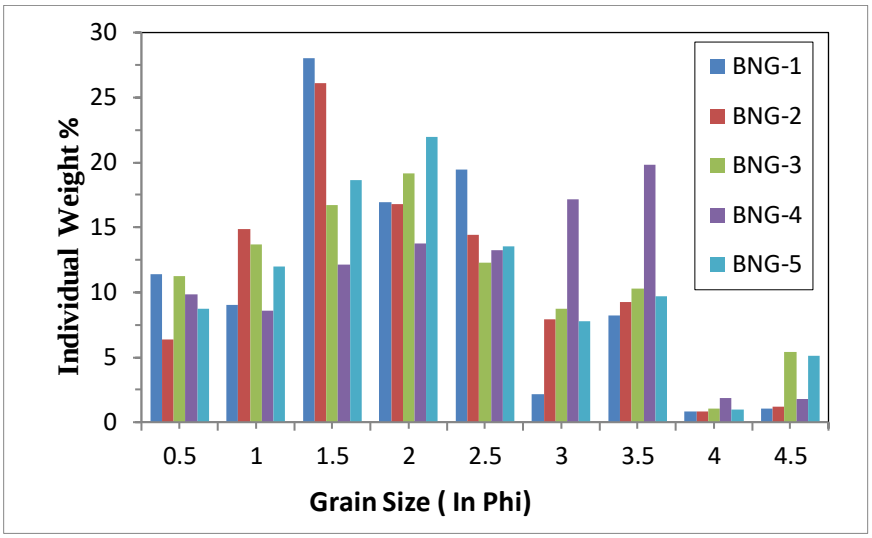

Fig. 5.1 (A): Histogram of BNG-1, BNG-2, BNG-3, BNG-4 and BNG-5

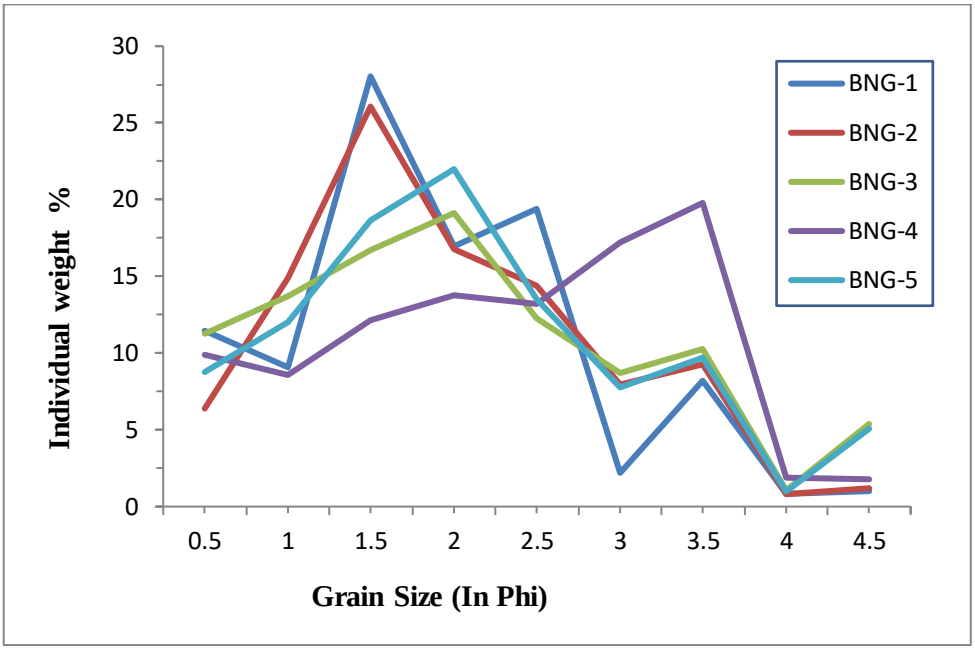

Fig. 5.2 (A): Frequency distribution curve of BNG-1, BNG-2, BNG-3, BNG-4 and BNG-5

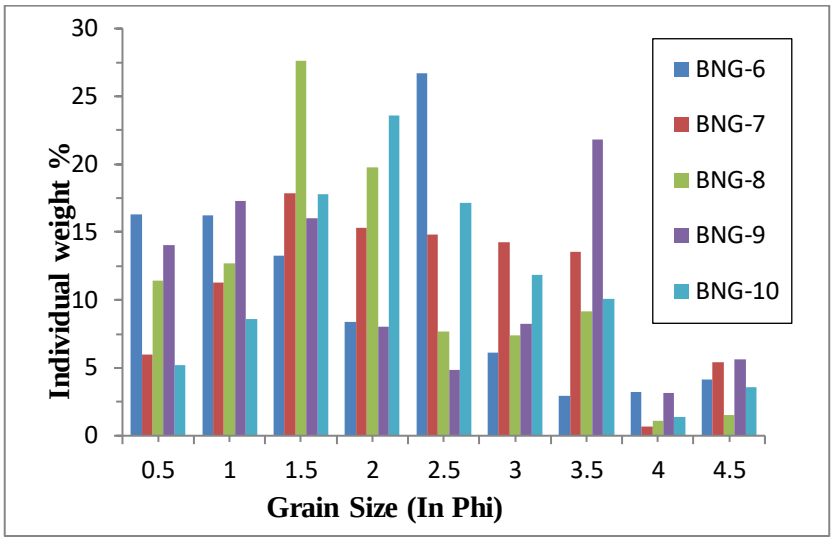

Fig. 5.1 (B): Histogram of BNG-6, BNG-7, BNG-8, BNG-9 and BNG-10

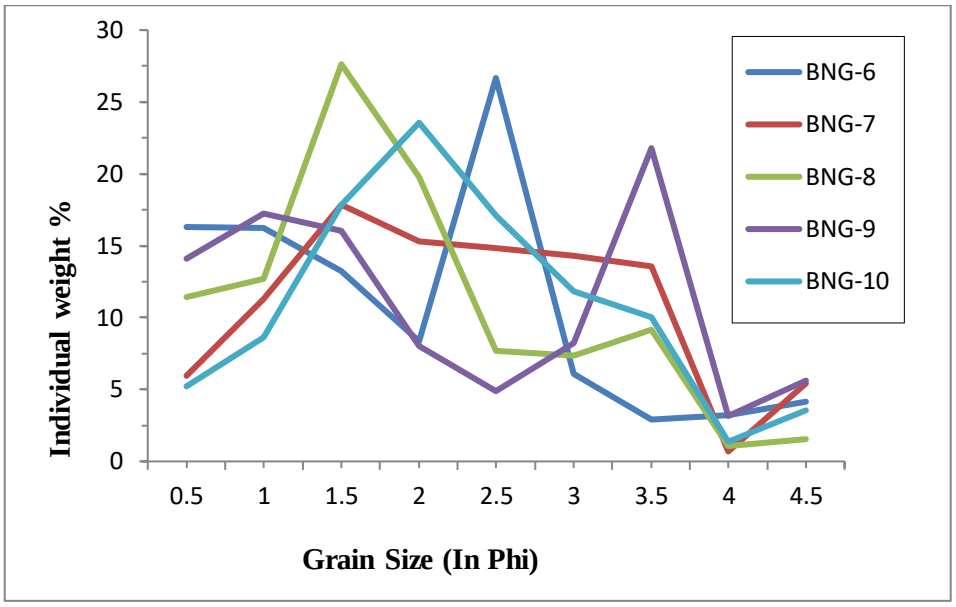

Fig. 5.2 (B): Frequency distribution curve of BNG-6, BNG-7, BNG-8, BNG-9 and BNG-10.

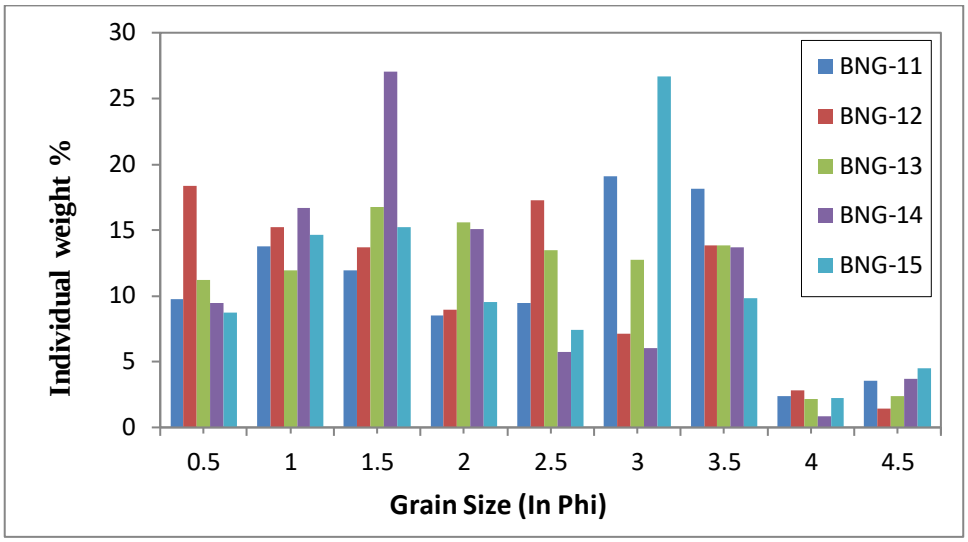

Fig. 5.1 (C): Histogram of BNG-11, BNG-12, BNG-13, BNG-14 and BNG-15

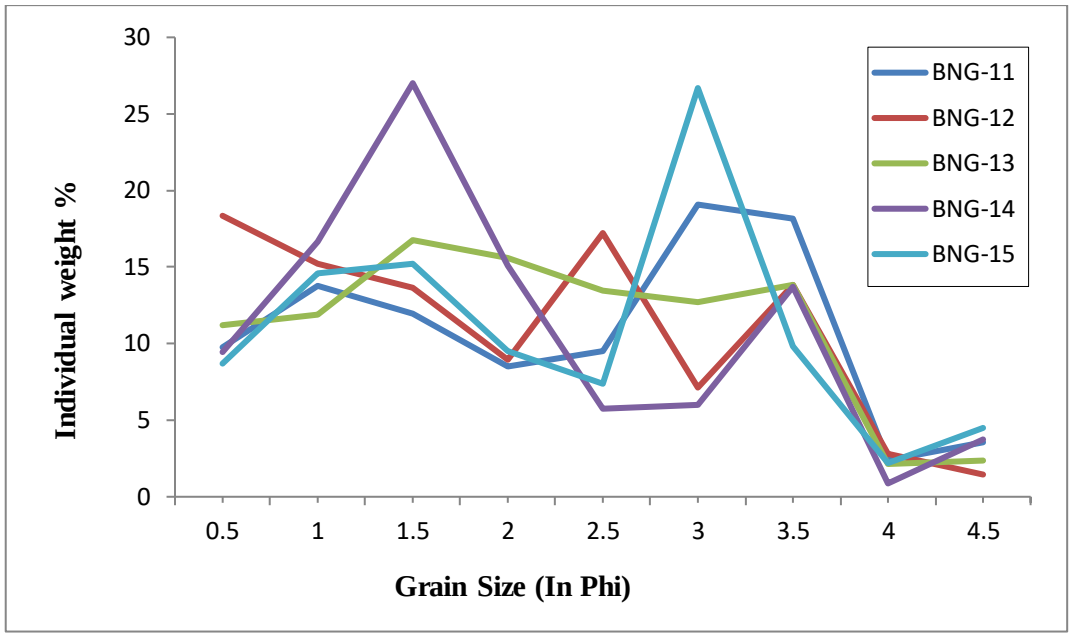

Fig. 5.2(C): Frequency distribution curve of BNG-11, BNG-12, BNG-13, BNG-14 and BNG-15.

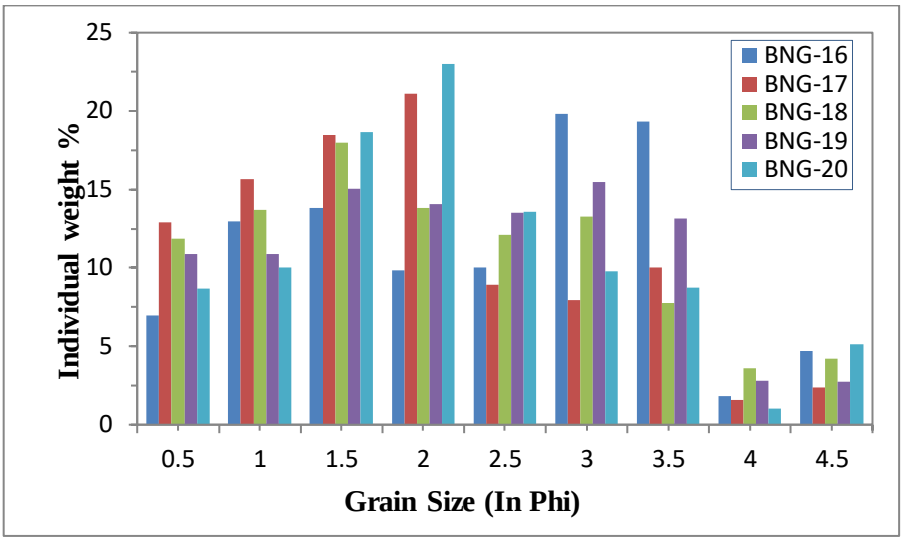

Fig. 5.1 (D): Histogram of BNG-16, BNG-17, BNG-18, BNG-19 and BNG-20

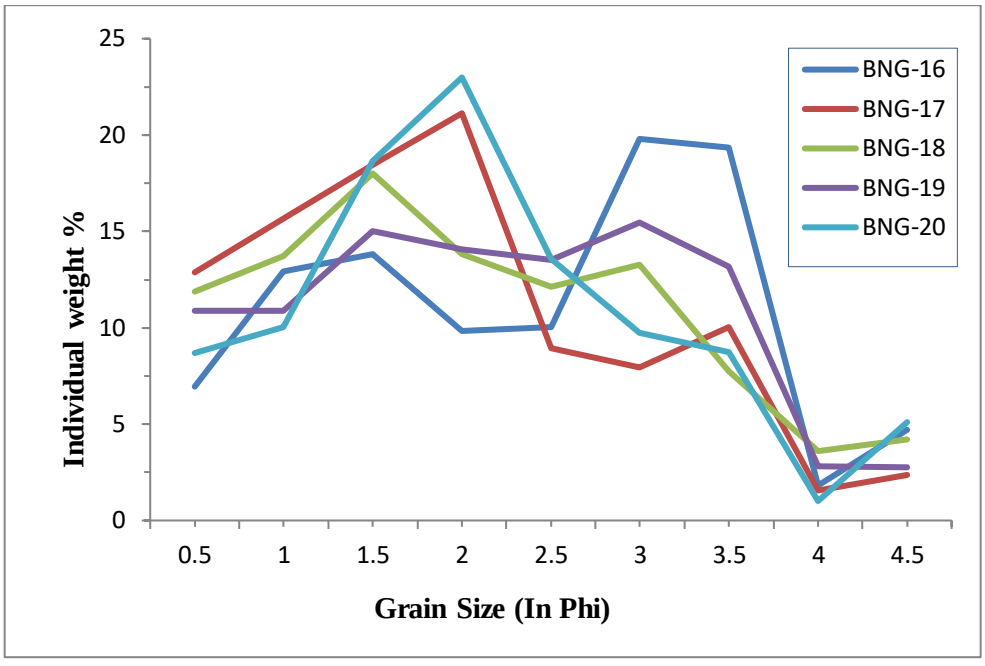

Fig. 5.2(D): Frequency distribution curve of BNG-16, BNG17, BNG-18, BNG-19 and BNG-20.

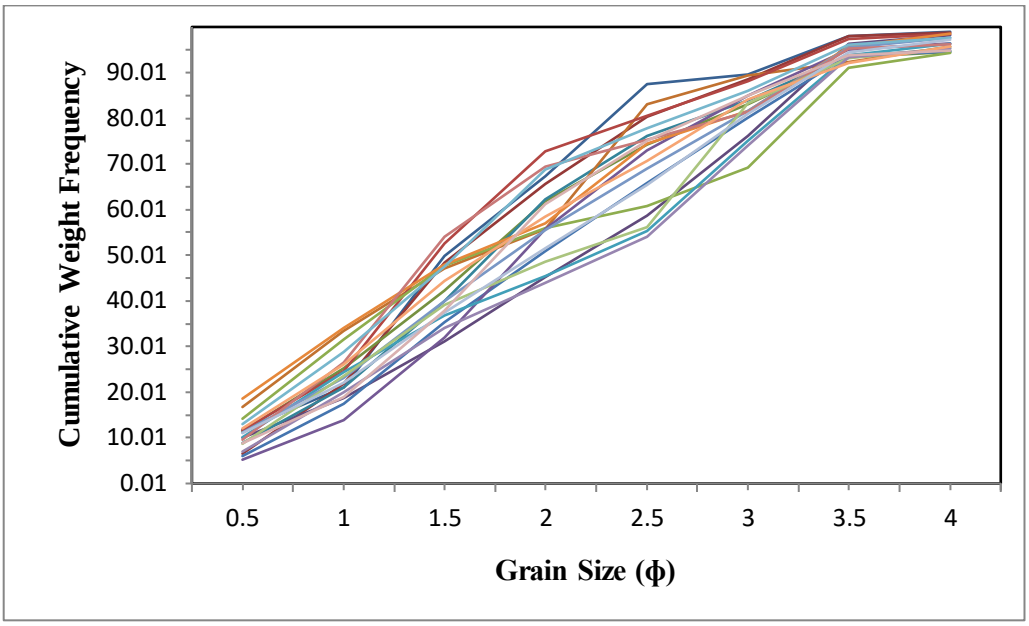

Fig. 5.3: Cumulative frequency curve of arithmetic probability showing traction, saltation and suspension of Barail sandstones (Visher,1969)

5.3 STATISTICAL PARAMETERS OF GRAIN SIZE

5.3.1. **Graphic Mean Size (Mz)**

The graphic mean measures the measure of an average particle size of the sediment and it is influenced by source of supply, the environment and the velocity (of current) of the depositing media (Sahu, 1964). It can be calculated by the formula proposed by Folk and Ward (1957) :

$Mz = (\Phi 16 + \Phi 50 + \Phi 84)/3$

The Graphic Mean size value of the present study ranges from 2.1 to 2.63Φ with an average of 2.36. This shows that all the samples are fine grained sediment. (Table 5.3)

5.3.2 **Graphic Standard Deviation (σ_1)**

Graphic standard deviation **(σ_1)** measures the sorting or uniformity of the grains and it indicates the state of the energy conditions prevailing during

sediments transportation in the basin. It is calculated by the formula proposed by Folk and Ward (1975) :

[σ_1=(Φ84-Φ16)/4 + (Φ95-Φ5/6.6)]

From the present analyzed samples, 80% are poorly sorted (σ_1: 1 - 2) and 20% samples are moderately sorted (σ_1: 0.71 – 1) Table 5.3. Folk and Ward (1957) suggested classification of sorting based on Standard deviation values

ϕ Values from	**To**	**Equal**
0.00	0.35	Very well sorted
0.35	0.50	Well sorted
0.50	0.71	Moderately well sorted
0.71	1.00	Moderately sorted
1.00	2.00	Poorly sorted
2.00	4.00	Very poorly sorted
4.00	above	Extremely poor sorted

5.3.3 **Graphic Skewness (Ski)**

Graphic Skewness (Ski) is the measure of degree of asymmetry in the frequency curves in favour of domination of fine or coarse-grained fractions. It has been calculated by formula proposed by Folk and Ward (1975):

[Ski= (Φ84 + (16Φ-2Φ50) / 2 (Φ84-Φ16) + (Φ5+Φ95-2Φ50) / 2(Φ95-Φ5)]

Table Table 5.3 shows that the present studied samples of sandstones show that 55% of the samples are near symmetrical (Ski = 0.10 to -0.10), 25% positively skewed (Ski = -0.11 to -2.01) and 15% negative skewed (Sk= -0.10 to -0.30) and 5% stongly positive skewed (Sk= 1.0 to 0.3). Data shows that maximum samples are near symmetrical ranging in Skewness values from 0.10 to -0.10 and considerable amounts of sample are positively skewed. This means that the sediments were deposited in a mixed environment. Folk and Ward suggested the following different classes of skewness based on Skewness values

Values from	To	Mathematically:	Graphically Skewed to the:
+1.00	+0.30	Strongly positive skewed	Very Negative phi values, coarse
+0.30	+0.10	Positive skewed	Negative phi values
+0.10	- 0.10	Near symmetrical	Symmetrical
- 0.10	- 0.30	Negative skewed	Positive phi values
- 0.30	- 1.00	Strongly negative skewed	Very Positive phi values, fine

5.3.4 **Graphic Kurtosis (K_g)**

Kurtosis (K_G) measures the peakedness of the frequency curve, Cadigan (1961). It is calculated by formula proposed by Folk and Ward (1975):

$[K_G= (\Phi 95- \Phi 5)/2.44(\Phi 75- \Phi 25)]$

Kurtosis limits suggested by Folk and Ward (1957):

Phi Values from	To	Equals
0.41	0.67	Very platykurtic
0.67	0.90	Platykurtic
0.90	1.11	Mesokurtic
1.10	1.50	Leptookurtic
1.50	3.00	Very Leptokurtic
3.00	above	Extremely Leptokurtic

Kurtosis is a quantitative measure of shape of the frequency curve, and the ratio between the sorting in the tail and central portion of the curve. In a frequency curve, if the central portion is better sorted than the tail portion, the curve is said to be leptokurtic nature (excessively peaked), but if the tail portion is better sorted than the central portion, it is called platykurtic nature(flat peaked) and the curve is called mesokurtic if both the tail and centre portions are equal. The analyzed sample comprises 40% to be of mesokurtic nature, 35% to be platykurtic and 15% leptokurtic and 10% Very leptokurtic.

Table 5.3: Statistical parameters of Grain size.

Sample No.	Graphic Mean (Mz)	Inclusive Graphic Standard Deviation (σ1)	Inclusive Graphic Skewness (SK)	Graphic Kurtosis (KG)
BNG-1	2.1	0.88	0.03	1.19
BNG-2	2.3	0.89	0.2	0.99
BNG-3	2.53	1.09	0.17	0.97
BNG-4	2.56	1.06	-0.19	0.82
BNG-5	2.36	1.08	0.24	1.17
BNG-6	2.1	1.12	-0.04	1.12
BNG-7	2.56	1.06	0.01	0.92
BNG-8	2.13	0.98	0.16	1.09
BNG-9	2.4	1.26	0.18	0.73
BNG-10	2.46	0.97	0.1	1.06
BNG-11	2.6	1.16	-0.21	0.79
BNG-12	2.2	1.23	-0.07	0.8
BNG-13	2.43	1.06	0.06	1.99
BNG-14	2.26	1.04	0.38	1
BNG-15	2.36	1.08	-0.1	0.84
BNG-16	2.63	1.14	-0.22	0.82
BNG-17	2.16	1.06	0.07	1.07
BNG-18	2.33	1.16	0.08	1
BNG-19	2.43	1.11	0	0.87
BNG-20	2.32	1.23	0.08	1.28

5.4 RELATIONSHIP BETWEEN TEXTURAL PARAMETERS

5.4.1 **Mean (mz) vs Standard deviation (σ_1)**

Friedman (1967) proposed a binary plot in which the graphic mean (Mz) values is plotted against standard deviation (σ_1) to distinguish river and beach sands. The studied samples showed that the sediments were deposited under a fluvial environment as represented in the Figure 5.4 thereby indicating the deposition in a river environment.

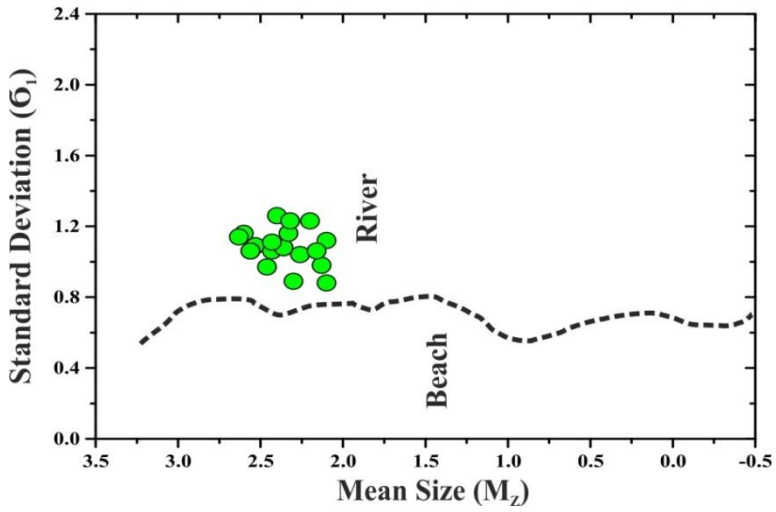

Figure 5.4: Mean Size vs Standard Deviation binary plot of Barail sandstoes, Ngopa area, Mizoram. After Friedman (1967)

5.4.2 **Skewness (sk_i) vs Kurtosis (k_g)**

Friedman (1961) also proposed a binary plot to interprete the depositional condition in which Skewness (Ski) is plotted against Kurtosis (K_G). The Barail sandstones are showing the mixed environment condition where river environment condition dominates beach environment by little (Figure 5.5**)**. So, it can be interpreted that the sediments were deposited in beach environment by the influence of flowing rivers as well as marine waves.

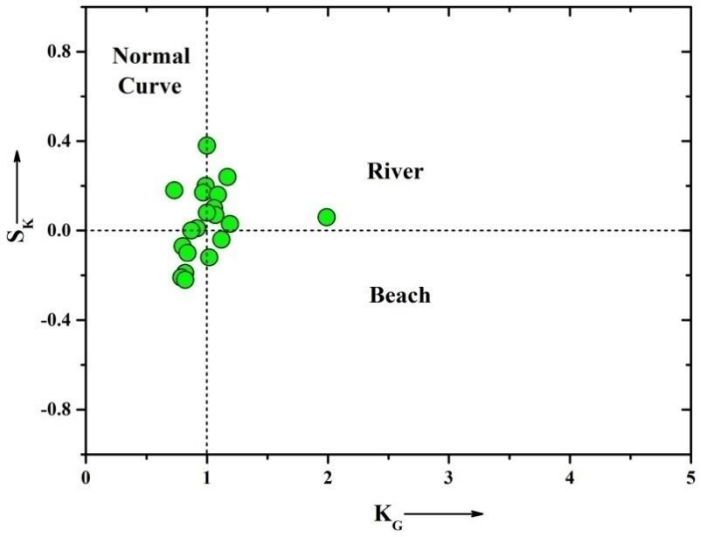

Figure 5.5: Kurtosis vs Skewness binary plot of Barail sandstone from Ngopa area, Mizoram. After Friedman (1961)

5.4.3 **Mean (mz) vs Standard deviation (σ_1)**

Binary plot proposed by Goldberry (1980) of Mean (Mz) versus Standard Deviation (σ_1) shown in the Figure 5.6 also indicates that the samples falls in and just outside the wave processes margins. So, according to the plot, we can say that the sediments at the time of deposition were influenced mainly by wave processes.

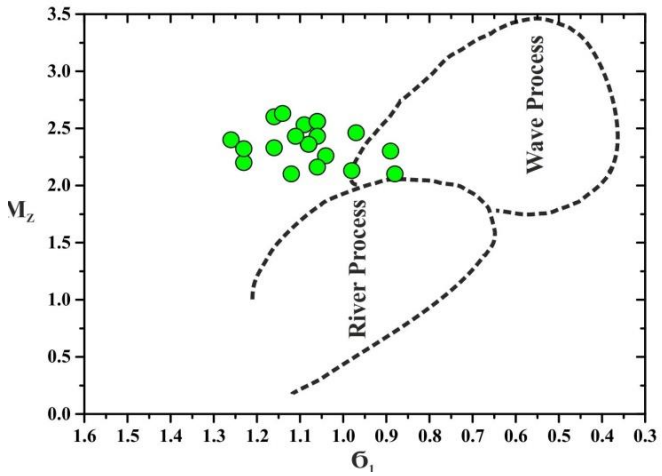

Figure 5.6: Standard deviation vs Mean Size binary plot after Goldberry (1980)

5.4.4 **Skewness (ski) vs Kurtosis (k_g)**

Thompson et al. (1972) also proposed another bivariate plot of Skewness (Ski) vs Kurtosis (K_G) which demarcates the energy condition prevailing at the time of deposition along with the particle size. The analyzed Barail sandstone samples ranges from fine to medium sand and deposited in a higher energy condition. So it can be concluded that the sediments were deposited in a transitional to shallow marine depositional settings (Figure 5.7).

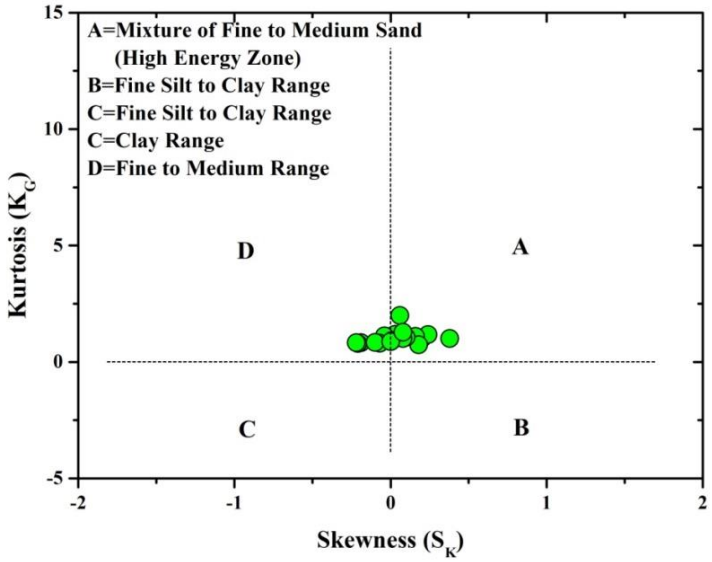

Figure 5.7: Skewness vs Kurtosis binary plot after Thompson (1972)

5.4.5 **Mean Diameter (Mz) Vs Standard Deviation (σ_1)**

Another bivariate plot of mean diameter vs standard deviation proposed by Glaister and Nelson (1974) reveals the trend of deposition of the sediments. The samples are clustered towards braided bar condition of deposition (Figure 5.8).

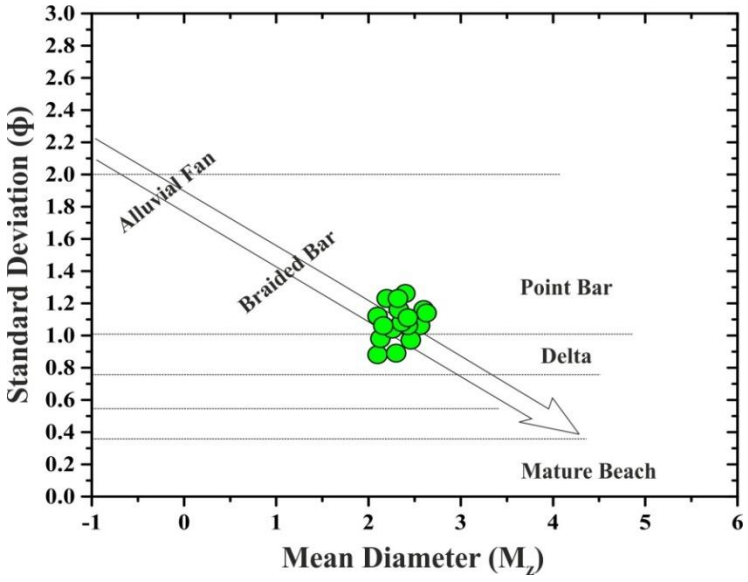

Figure 5.8: Mean Diameter vs Standard Deviation binary plot of Barail sandstone from Ngopa area, after Glaister and Nelson (1974)

5.4.6 **log-log Plot**

In order to interprete the depositional environment, Sahu (1964) proposed a plot based on grain size values by using the bivariate plot of $\sqrt{\sigma_{1-2}}$ vs $(K_G/Mz)*\sigma_{12}$. While plotting in Log-Log plot (Figure 5.9) it is observed that most of the Barail samples of present study are deposited in shallow marine condition with few samples under deltaic conditions.

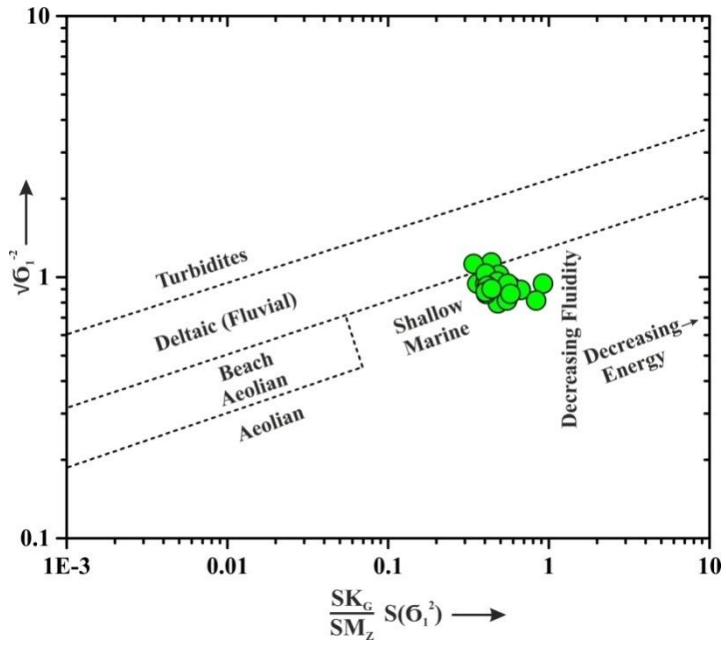

Figure 5.9: Log log plot of Barail sandstones after Sahu (1964)

5.4.7 **Standard Deviation (σ_1) Vs Mean Size Diameter (Mz)**

Another bivariate scattered plot of Standard deviation (σ_1) vs Mean size Diameter (Mz) proposed by Folk and Ward (1957) also reveals that the Barail sandstones are fine sand and they are moderately sorted to poorly sorted. This indicates a continuous reworking of sediments by wave and currents (Fig. 5.10).

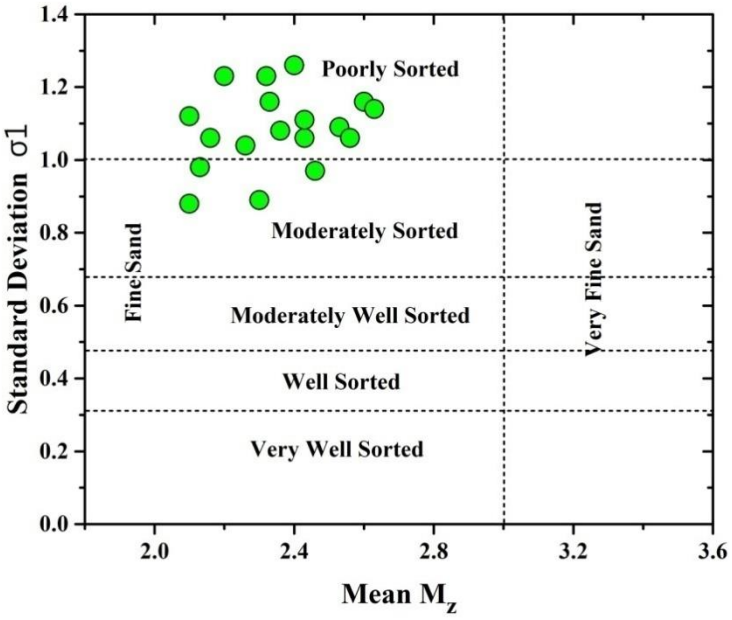

Fig. 5.10: Binary scattered plot of Mean size (M_z) vs standard deviation (σ_1) after Folk and Ward (1957).

5.4.8 **Mean Size (M_z) Vs Skewness (S_k)**

Another bivariate plot (5.11) of Moaoila and Weiser (1968), Mean size (M_z) vs standard deviation (σ_1) also shows that the Barail sandstones were deposited in a mixed environment of River and Beach.

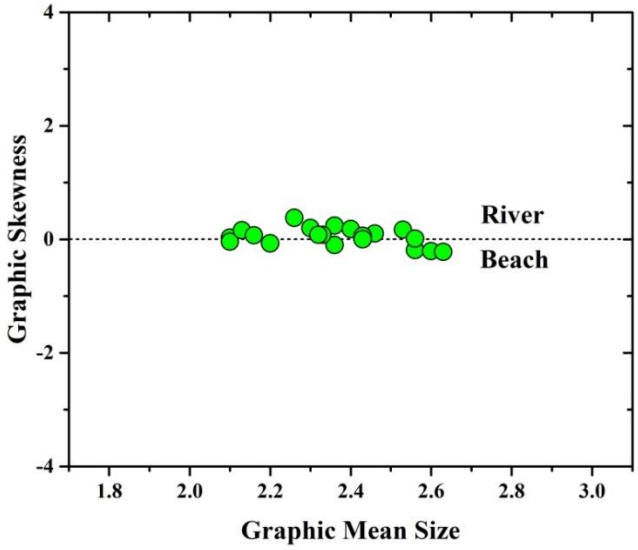

Fig. 5.11: Bivariate plot of Graphic Mean size vs Graphic skewness after Moiola and Weiser (1968).

5.4.9 **Study Of Linear Discriminant Function**

In order to distinguish sediments from aeolian, shallow agitated marine, beach and fluvio-deltaic environments, Sahu (1964) established certain discriminant functions based on graphical parameters of Folk and Ward (1957).

The following linear discrimination is various environments proposed by Sahu (1964):

$Y_1 = -3.5688M_z + 3.7016\sigma_1^2 - 2.0766S_{ki} + 3.1135K_G$

$Y_2 = 15.6534\ M_z + 65.7091\ \sigma_1^2 + 18.1071\ S_{ki} + 18.5043\ K_G$

$Y_3 = 0.2852\ M_z - 8.7604\ \sigma_1^2 - 4.8932\ S_{ki} + 0.0482\ K_G$

$Y_4 = 0.7215\ M_z - 0.4030\ \sigma_1^2 + 6.7322\ S_{ki} + 5.2927\ K_G$

Y_1 values: < -2.7411 = Aeolian Deposition

Y_1 values: > -2.7411 = Beach Deposition

Y_2 values: <65.3650 = Beach Deposition

Y_2 values: >65.3650 = Shallow Agitated Marine

Y_3 values: <-7.4190 = Fluvial Deposition

Y_3 values: >-7.4190 = Shallow Agitated Marine Deposition

Y_4 values: <9.8433 = Turbidity Current Deposition

Y_4 values: >9.8433 = Fluvial Deltaic Deposition

The discriminant functions of present sediments is shown in the Table 5.4 A&B. According to this discriminant functions,Y1 values of all the Barail samples indicates Beach deposition, where Y2 values shows shallow agitated marine deposits. The Y3 values of majority of the samples showed Fluvial deposits and some sample falls in Shallow agitated marine deposits where Y4 values shows Turbidity currents. Considering all the above parameters of linear discriminant functions and observations it can be interpreted that the depositional environment was shallow marine or Beach depositional where they are influenced by Fluvial action.

Using these linear discriminant values, Sahu (1964) proposed Binary discriminant plot for the depositional environment of swediments. Figure 5.12 (A-C) shows Binary plots of the studied Barail sediment samples.

Table 5.4 (A): Classification of different depositional environment by Sahu (1962, 1964).

Sample No.	Y1	Result	Y2	Result
BNG-1	-0.99	Beach Deposition	106.32	Shallow agitated Marine Deposition
BNG-2	-2.61	Beach Deposition	109.99	Shallow agitated Marine Deposition
BNG-3	-1.96	Beach Deposition	138.7	Shallow agitated Marine Deposition
BNG-4	-2.03	Beach Deposition	125.64	Shallow agitated Marine Deposition
BNG-5	-0.96	Beach Deposition	139.58	Shallow agitated Marine Deposition
BNG-6	0.72	Beach Deposition	135.3	Shallow agitated Marine Deposition
BNG-7	-2.13	Beach Deposition	131.11	Shallow agitated Marine Deposition
BNG-8	-0.99	Beach Deposition	119.52	Shallow agitated Marine Deposition
BNG-9	-0.79	Beach Deposition	158.66	Shallow agitated Marine Deposition
BNG-10	-2.2	Beach Deposition	121.76	Shallow agitated Marine Deposition
BNG-11	-1.4	Beach Deposition	139.93	Shallow agitated Marine Deposition
BNG-12	0.38	Beach Deposition	147.38	Shallow agitated Marine Deposition
BNG-13	1.56	Beach Deposition	149.78	Shallow agitated Marine Deposition
BNG-14	-1.74	Beach Deposition	131.83	Shallow agitated Marine Deposition
BNG-15	-1.28	Beach Deposition	127.32	Shallow agitated Marine Deposition
BNG-16	-1.57	Beach Deposition	137.75	Shallow agitated Marine Deposition
BNG-17	-0.36	Beach Deposition	128.71	Shallow agitated Marine Deposition
BNG-18	-0.39	Beach Deposition	144.84	Shallow agitated Marine Deposition
BNG-19	-1.4	Beach Deposition	135.1	Shallow agitated Marine Deposition
BNG-20	1.14	Beach Deposition	160.86	Shallow agitated Marine Deposition

Table 5.4 (B): Classification of different depositional environment by Sahu (1962, 1964).

Sample No.	Y3	Result	Y4	Result
BNG-1	-6.27	Shallow agitated marine deposit	7.7	Turbidity current deposition
BNG-2	-7.21	Shallow agitated marine deposit	7.93	Turbidity current deposition
BNG-3	-10.47	Fluvial Deposition	7.62	Turbidity current deposition
BNG-4	-8.14	Fluvial Deposition	4.46	Turbidity current deposition
BNG-5	-10.66	Fluvial Deposition	9.04	Turbidity current deposition
BNG-6	-10.14	Fluvial Deposition	6.67	Turbidity current deposition
BNG-7	-9.12	Fluvial Deposition	6.33	Turbidity current deposition
BNG-8	-8.54	Fluvial Deposition	8	Turbidity current deposition
BNG-9	-14.07	Fluvial Deposition	6.17	Turbidity current deposition
BNG-10	-7.98	Fluvial Deposition	7.68	Turbidity current deposition
BNG-11	-9.98	Fluvial Deposition	4.1	Turbidity current deposition
BNG-12	-12.24	Fluvial Deposition	4.74	Turbidity current deposition
BNG-13	-9.35	Fluvial Deposition	12.24	Fluvial Deltaic Deposition
BNG-14	-10.64	Fluvial Deposition	9.05	Turbidity current deposition
BNG-15	-9.01	Fluvial Deposition	5.01	Turbidity current deposition
BNG-16	-9.52	Fluvial Deposition	4.23	Turbidity current deposition
BNG-17	-9.52	Fluvial Deposition	7.24	Turbidity current deposition
BNG-18	-11.47	Fluvial Deposition	6.97	Turbidity current deposition
BNG-19	-10.06	Fluvial Deposition	5.86	Turbidity current deposition
BNG-20	-12.92	Fluvial Deposition	8.38	Turbidity current deposition

The binary plots (Sahu, 1964) of Y1 vs Y2 clearly support the above discussion. And the binary plot Y2 vs Y3 suggest mainly a fluvial deposition. Also, Y3 vs Y4 also shows Fluvial/Turbidity current.

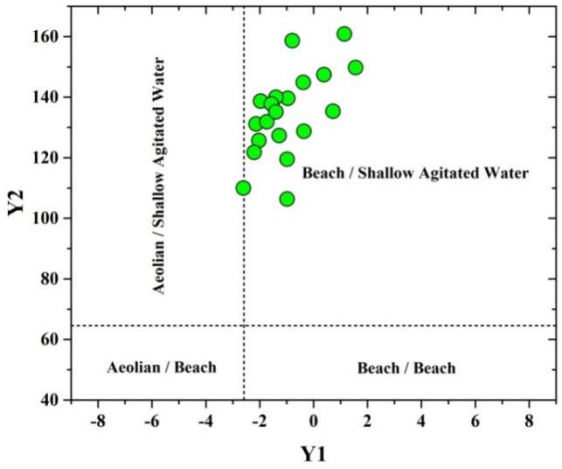

Fig.: 5.12 (A): A Linear discrimination function plot of Y2 vs Y1 of Barail sandstones Ngopa area (Sahu, 1964)

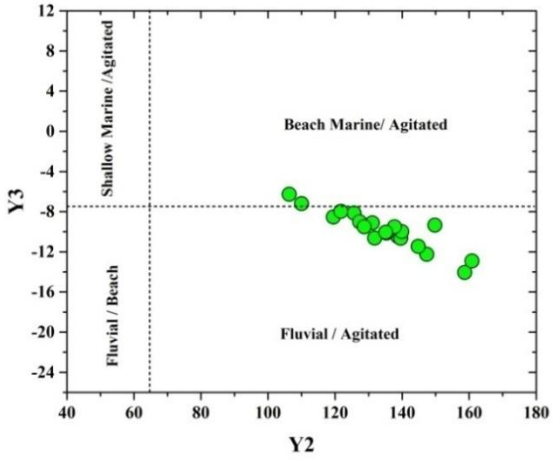

Fig.: 5.12 (B): A Linear discrimination function plot of Y2 vs Y3 of Barail sandstones Ngopa area (Sahu, 1964).

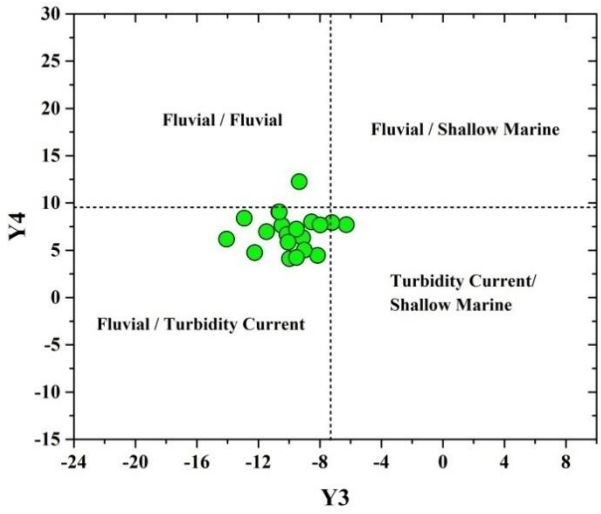

Fig.: 5.12 (C): A Linear discrimination function plot of Y2 vs Y3 of Barail sandstones Ngopa area (Sahu, 1964).

5.5 DISCUSSION AND INTERPRETATION

Grain size analysis has been employed to find out the distribution and deposional environment of Barail sandstones exposed in and around Ngopa village, Saitual District. Histogram and frequency curve shows a unimodal nature with a peak around 1.5Φ and 3 – 3.5Φ. This character alone also can interpret that the analysed Barail sandstones were derived in mixed environment of marine and fluvial.

The log-probability curve plot also shows that three subpopulations are presents which are present by three modes of transportations: rolling and sliding population, saltation population and suspension populations. It can be concluded from the curve that sorting is good in saltation population, fair in rolling and sliding population and poor in suspension populations.

Statistical parameters of Grain size such as Inclusive graphic mean, inclusive graphic standard deviation, inclusive graphic skewness and Kurtosis shows that the Barail sandstones of the study area are fine grained sand which were poorly sorted. And it is also evident that the sediments were deposited in a mixed environment.

Interrelationship between grain size parameters were plot as a scattered bivariate diagram plots, they are used to depict the depositional environments and their behaviour. Various bivariate scattered plots of Inclusive Graphic Mean size (M_z) vs Inclusive graphic Skewness (S_k) after Friedman (1967), Goldberry (1980), Glaister and Nelson (1974) and Folk and Ward (1957) reveals that the Barail sediment samples collected from Ngopa area is deposited in a mixed environment of Beach and River. They were deposited by wave processes under the influence of river action. They were deposited in a Braided bar towards Delta. The sediments were moderately sorted to poorly sorted. A bivariate plots of Inclusive graphic Skewness (S_k) vs Kurtosis (K_G) after Friedman (1961) and Thompson (1972) reveals that the Barail sediments are fine to very fined grained and were deposited in a mixed environment of both river and Beach environment. This is also supported by bivariate plot of Inclusive graphic Skewness (S_k) vs graphic Mean size (M_z) plot suggests by Moiola and Weiser (1968) where it shows that the Barail sediments were deposited in mixed environment of both River and Beach environment. Log-Log plot after Sahu (1964) also shows that majority of the Barail sandstone were deposited in a shallow marine environment while few samples were clustered in Deltaic environment.

Calculations of Linear discrimination functions proposed by Sahu (1964) are also employed in order to depict the depositional environment of Barail sandstones of the study area. Based on these calculations, the Y1 values of all of the studied samples were categorized in Beach deposition. Y2 values shows Shallow marine deposits, Y3 values showed that majority of the samples were deposited in a fluvial environment deposition while few samples were put in shallow agitated marine deposits. Y4 value shows that the sediments of the studied samples were of Turbidity current depositions. Furthermore, Sahu used these linear discrimination values again to plot bivariate scattered plots in which, Y1 vs Y2 plot suggests Beach/Shallow agitated environment deposition and Y2 vs Y3 suggests Fluvial/agitated and 10% shows Beach marine/agitated environment deposition. According to Y3 vs Y4 plot, the sediments were deposited by Fluvial/Turbidity currents.

Based on the above Granulometric study of Barail sandstones from Ngopa area, it can be concluded that the sediments seemed to be deposited in beach/shallow marine environment under the influence of river action.

CHAPTER 6
PETROGRAPHY

6.1. INTRODUCTION

Petrography to a great extent is based on the study of the various aspects of the section of rocks which can either be thin or transparent. It can be defined as a branch of Petrology that focuses on a detailed description of rocks. To find out their source rock, tectonic settings as well as depositional environment, the petrography of terrigenous rocks can serves as significant information. The characteristics of detrital grains which have undergone modification or some changes can give us idea about the tectonic setting and their provenance (Dickinson, 1985). Nevertheless, different factors like the transport mechanism, climate, relief, depositional environment as well as diagenesis can make alterations to the sandstone's composition. Using point counting methods, the detrital framework grains are quantified to get the sandstone provenance. (Dickinson and Suczek, 1979). Crooks (1974) and Schwab (1975) deliberately studied the interrelation between quartz rich rock with passive continental margin. For the first time, Sorby (1880) and Mackie (1896) works on thin section petrography and they performed detailed investigation of quartz varieties. Different properties like inclusion, extinction, poly-crystallinity, mineral grains' shape and their resistance towards weathering (Quartz) ascertain the place of origin, the provenance of sediments. Krynine (1940, 1946) categorized Quartz grains' provenance as sedimentary, igneous and metamorphic. The depositional environment of sandstone is specified by their susceptibility of feldspar towards mechanical wear in weighing up with other detrital grains. Judd (1886) revealed that high concentration of feldspar mineral in sandstone manifests the paleoclimatic condition and their relief.

To find out the provenance, tectonic settings and climatic conditions of sandstone, a thorough study of mineral compositions, textural characteristics and diagenesis are necessary to be conducted with the help of Petrographic analysis apart from Geochemical studies. Detrital grains were analyzed using modal analysis and were plotted using different discrimination plots in order to find out the analyzed

sandstones' classification, their provenance, tectonic settings as well as climatic condition of the source area.

6.2 PETROGRAPHIC DESCRIPTION OF BARAIL SANDSTONES

For petrography, a total of 40 sandstone samples were collected from the study area, i.e., in and around Ngopa Village. Mineral constituents and their texture were analyzed using LeicaDM2700 P polarizing microscope equipped with Leica DFC420 camera and Leica Image Analysis software (LAS- v4.6). Based on petrographic analysis under the microscope, the size of detrital framework are fine- to very fine-grained sandstone and they are "poorly sorted to well sorted". The observation also shows that the detrital grains are "sub-angular to angular, sub-rounded to rounded" (Plate 6.1 B&C). The textural analysis indicated that the grains are closely packed and extremely compacted, interlocked and cemented by cementing materials like silica and ferruginous. Quartz, feldspar and rock fragments are the primary detrital grains. The rocks also commonly contain Micas. Some heavy mineral inclusions are also observed in the thin sections (Plate 6. 2 B).

The modal count of Barail sandstones from Ngopa area, Mizoram are tabulated in Table 6.1 and the microphotographs of the rock thin sections are shown in Plate 6.1 and 6.2. A comprehensive description of minerals observed during petrographic analysis is discussed in the following section.

6.2.1. **Quartz**

They are the most abundant minerals among primary detrital grains and they constitutes up to 51.58 - 75.32% having average concentrations 67.34% (Table 6.2). The majority of quartz grains are subhedral and sub angular in shape, but rounded grains are sometimes observed. Monocrystalline quartz and polycrystalline quartz are the two varieties of Quartz observed in thin sections. Monocrystalline quartz accounts for 42.94 – 72.79% with an average 62.97% out of the entire framework grains. They are divided into "undulatory quartz and non-undulatory quartz".

The non-undulatory Quartz constitutes up to an average of 9.83%. The undulatory quartz are those which display extinction angle greater than 5˚ (Basu *et al.*,1975). Comparably, the undulatory quartz tends to break into small grains as they are thermodynamically less stable than non-undulatory quartz (Blatt *et al.*, 1980).

The undulatory extinction of quartz is commonly observed in most of the grains (6.1 E) which is due to deformation of the mineral after crystallization (Boggs, 2009). Undulatory quartz constitutes an average of 53.13% which surpasses the concentrations of non-undulatory quartz variety. The grain boundaries of some grains display suture and concavo-convex contact which specifies igneous and metamorphic source rock (Plate 6.1 C) Sub-rounded quartz grains often display secondary overgrowth which is due to silica precipitation following diagenesis. Some quartz grains often display fracture (Plate 6.2 F) which indicates igneous and metamorphic source rock which had gone through certain tectonic effects (Moss, 1972 and Pettijohn *et al*., 1972). The Polycrystalline quartz constitutes 0.65 – 11.37% with an average of 4.37% (Table 6.1, Plate 6.2 A).

6.2.2. **Feldspar**

Among the primary detrital grains, feldspar is the third prevalent grain after Rock fragment and followed by mica. They constitutes 1.96 – 11.52% with an average of 5.42 % (Table 6.1). Plagioclase feldspar and K-feldspar are found in all of the analyzed rock samples. Varieties of K-feldspars like Microcline (Plate 6.2 C) as well as Orthoclase (Plate 6.2 E) are commonly found. In addition, perthitic intergrowth of plagioclase and K-feldspar are also frequently observed (Plate 6.2 E&F). Orthoclase is distinctively identified by its cloudy appearance with dust-looking alteration (Plate 6.2 E). Microcline stipulates tartan twinning (Plate 6.2 C) and an intergrowth of microcline with albite have also been detected. Characteristics of albite twinning (Plate 6.1 F & 6.2 C) can be seen in Plagioclase and they are less abundant than K-feldspar.

6.2.3. **Lithic Fragments or Rock Fragments**

Lithic fragments or Rock fragments are made up of two or more mineral grains which can be made of sedimentary, igneous or metamorphic rocks. They offer crucial information for figuring out the provenance and tectonic settings. They accounts for the second most abundant detrital grains, showing 9.95 – 23.83% with an average of 16.66% in the sandstone samples (Table 6.1). Schists and gneisses are metamorphic fragments commonly observed in all the rock thin sections (Plate 6.1 F). They are typically aggregates of malformed quartz, feldspar and mica minerals.

6.2.4. Chert

“Chert is a chemically precipitated sedimentary rock, essentially mono-mineralic and composed chiefly of microcrystalline and/or chalcedonic quartz with subordinate mega-quartz and minor amounts of impurities” (Folks, 1980). From petrography of Barail sandstone, chert contributes 0 – 6.05% with an average of 1.56 % (Plate 6.2 A). This detrital grains are commonly observed in all the Barail sandstones. The grains are usually well rounded and free from any fractures and any inclusions. Their characteristic appearance indicates reworked nature or transportation from long distance.

6.2.5. **Micas**

The detrital grains of Micas such as Muscovite and Biotite (Plate 6.1 D) are essentially found in all Barail sandstones under the microscope. Both can easily be identified with the help of their distinct characteristics like flaky nature and parallel extinction. Muscovite percentage is higher in all the samples than that of Biotites, which is due to the fact that Muscovites are more resistant to weathering. In the majority of the sandstone samples, Muscovites are deformed into kink bands which are frequently observed in the rock samples. The bending is caused by diagenetic effects of pressure (6.2 D).

6.2.6. **Matrix and Cementing Material**

Matrix are the fine-grained materials or clay (less than 0.03 mm) found in some of the sandstones. The Barail sandstones contains good amount of matrix which are composed of miscellaneous minerals which may comprises of microcrystaline quartz, very fine iron ore, micas, etc., which are which are not possible to identify even under the microscope. They occupy voids and inter-granular spaces. Cement is the chemically precipitated materials that bind the grains in clastic rock. The Barail sandstones are found to be well cemented, either siliceous or ferruginous. Detrital grains of analyzed rock samples from the study area are primarily cemented together by ferruginous cementing materials, while silica cementation is less frequent.

6.2.7. **Accessory Minerals**

Heavy minerals (Plate 6.2 B) are also found in addition to other detrital framework grains in Barail sandstones. These minerals are not counted or described in detail due to their low percentages.

Table 6.1: Data of Modal analysis of Barail sandstones, Ngopa area, Mizoram where, Q_{mu}: Monocrystalline undulatory quartz, Q_{mnu}: Monocrystalline non undulatory quartz, Q_{mt}: Total monocrystalline quartz, $Q_{p\ 2\text{-}3}$: Polycrystalline quartz with 2-3 grains per quartz, $Q_{p\ >3}$: Polycrystalline quartz with Qp >3 grain per quartz, Q_{pt}: Total polycrystalline quartz, Q: Total no. of Quartz, Kf: K-feldspar, NaF/CaF: Plagioclase feldspar, Ft: Total no. of feldspar, L/R: Lithic fragments or Rock fragments (sedimentary, metamorphic and volcanic).

Sl. No	Sample No.	Quartz type						Total Quartz	Feldspar		Rock/ Lithic Fragments	Chert	Cement	Matrix	Micas	Others
		Monocrystalline Quartz			Polycrystalline quartz											
		Q_{Mnu}	Q_{Mu}	Q_{Mt}	$Q_{P2\text{-}3}$	$Q_{P>3}$	Q_{Pt}	$Q=(Q_{Mt}+Q_{Pt})$	Alkali Felds. (Kf)	Plag. (NaF/CaF)						
1	BNG-1	10.09	32.85	42.94	2.59	6.05	8.64	51.58	8.93	2.59	10.74	6.05	8.72	4.23	2.74	4.42
2	BNG-2	6.64	47.83	54.47	1.86	4.03	5.89	60.36	3.41	1.86	9.95	3.41	4.23	6.31	7.12	3.35
3	BNG -3	14.76	44.57	59.33	1.21	3.01	4.22	63.55	2.41	1.2	11.25	1.51	2.92	4.62	9.64	2.9
4	BNG-4	7.31	41.23	48.54	1.46	4.39	5.85	54.39	3.8	3.22	14.4	1.17	1.92	3.56	11.29	6.25
5	BNG-5	11.31	53.26	64.57	3.64	3.54	7.18	71.75	4.37	2.36	13.69	1.84	1.38	1.59	3.02	0
6	BNG-6	15.21	38.98	54.19	4.11	7.26	11.37	65.56	5.16	2.24	15.09	2.87	1.22	2.33	3.16	2.37
7	BNG-7	16.29	42.02	58.31	3.9	1.63	5.53	63.84	3.58	0.98	23.83	0.33	1.97	2.36	2.28	0.83
8	BNG-8	11.63	48.5	60.13	2.66	2.99	5.65	65.78	4.32	1.33	21.2	1.33	1.87	2.62	0.33	1.22

Cont..

Cont..

9	BNG-9	8.26	51.19	59.45	5.07	4.27	9.34	68.79	5.89	3.58	16.03	0.66	1.32	0.84	2.07	0.82
10	BNG-10	6.05	57.84	63.89	1.27	0.64	1.91	65.8	3.82	2.55	15.74	1.27	1.42	2.37	4.45	2.58
11	BNG-11	9.45	54.38	63.83	4.72	0.63	5.35	69.18	4.4	1.89	16.07	0.31	0.56	1.29	5.66	0.64
12	BNG-12	5.13	62.13	67.26	1.29	0.32	1.61	68.87	1.6	1.92	20.16	0	1.76	0.52	3.85	1.32
13	BNG-13	8.67	63.7	72.37	1.65	0.63	2.28	74.65	3.3	1.33	18.08	0.33	0.33	0.66	0.99	0.33
14	BNG-14	7.84	59.15	66.99	0.65	0	0.65	67.64	3.27	1.33	22.09	1.63	0.82	1.54	0.33	1.35
15	BNG-15	7.28	63.61	70.89	0.95	0.32	1.27	72.16	2.53	2.21	15.81	0.63	0.33	1.26	5.07	0
16	BNG-16	12.38	56.31	68.69	1.34	2.42	3.76	72.45	1.97	0.66	17.65	1.64	0.42	2.04	1.64	1.53
17	BNG-17	9.51	63.28	72.79	0.33	0.98	1.31	74.1	2.29	0.66	17.03	2.3	0.33	1.32	1.64	0.33
18	BNG-18	6.56	64.26	70.82	0	0.98	0.98	71.8	0.98	0.98	21.29	0.66	1.34	0.98	1.64	0.33
19	BNG-19	7.47	61.04	68.51	0	0.65	0.65	69.16	3.25	1.95	18.27	0.97	1.32	2.16	2.59	0.33
20	BNG-20	14.8	56.57	71.37	2.96	0.99	3.95	75.32	3.62	0.66	14.8	2.3	0.66	1.32	1.32	0

Table 6.2: Recalculated percentile values of total Quartz, Feldspar and Rock fragments of Barail sandstones, Ngopa area, Mizoram.

Sample No.	Quartz (Total)	Feldspar	Rock Fragments	Sum (Qtot+F+RF)	Total Quartz (Q) (Recalculated %)	Feldspar (F) (Recalculated %)	Rock Fragments (R) (Recalculated %)
BNG-1	51.58	11.52	10.74	73.84	69.85	15.60	14.54
BNG-2	60.36	5.27	9.95	75.58	79.86	6.97	13.16
BNG-3	63.55	3.61	11.25	78.41	81.05	4.60	14.35
BNG-4	54.39	7.02	14.4	75.81	71.75	9.26	18.99
BNG-5	71.75	6.73	13.69	92.17	77.85	7.30	14.85
BNG-6	65.56	7.4	15.09	88.05	74.46	8.40	17.14
BNG-7	63.84	4.56	23.83	92.23	69.22	4.94	25.84
BNG-8	65.78	5.65	21.2	92.63	71.01	6.10	22.89
BNG-9	68.79	9.47	16.03	94.29	72.96	10.04	17.00
BNG-10	65.8	6.37	15.74	87.91	74.85	7.25	17.90
BNG-11	69.18	6.29	16.07	91.54	75.57	6.87	17.56
BNG-12	68.87	3.52	20.16	92.55	74.41	3.80	21.78
BNG-13	74.65	4.63	18.08	97.36	76.67	4.76	18.57
BNG-14	67.64	4.6	22.09	94.33	71.71	4.88	23.42
BNG-15	72.16	4.74	15.81	92.71	77.83	5.11	17.05
BNG-16	72.45	2.63	17.65	92.73	78.13	2.84	19.03
BNG-17	74.1	2.95	17.03	94.08	78.76	3.14	18.10
BNG-18	71.8	1.96	21.29	95.05	75.54	2.06	22.40
BNG-19	69.16	5.2	18.27	92.63	74.66	5.61	19.72
BNG-20	75.32	4.28	14.8	94.4	79.79	4.53	15.68

Table 6.3: Recalculated percentile value of Monocrystalline quartz, feldspar and rock fragments of Barail sandstones, Ngopa area, Mizoram.

Sample No.	Monocrystalline Quartz (Qmt)	Feldspar	Rock Fragments	Sum (Qmt+F+RF)	Monocrystalline Quartz	Feldspar	Rock Fragments
BNG-1	42.94	11.52	10.74	65.2	65.86	17.67	16.47
BNG-2	54.47	5.27	9.95	69.69	78.16	7.56	14.28
BNG-3	59.33	3.61	11.25	74.19	79.97	4.87	15.16
BNG-4	48.54	7.02	14.4	69.96	69.38	10.03	20.58
BNG-5	64.57	6.73	13.69	84.99	75.97	7.92	16.11
BNG-6	54.19	7.4	15.09	76.68	70.67	9.65	19.68
BNG-7	58.31	4.56	23.83	86.7	67.25	5.26	27.49
BNG-8	60.13	5.65	21.2	86.98	69.13	6.50	24.37
BNG-9	59.45	9.47	16.03	84.95	69.98	11.15	18.87
BNG-10	63.89	6.37	15.74	86	74.29	7.41	18.30
BNG-11	63.83	6.29	16.07	86.19	74.06	7.30	18.64
BNG-12	67.26	3.52	20.16	90.94	73.96	3.87	22.17
BNG-13	72.37	4.63	18.08	95.08	76.11	4.87	19.02
BNG-14	66.99	4.6	22.09	93.68	71.51	4.91	23.58
BNG-15	70.89	4.74	15.81	91.44	77.53	5.18	17.29
BNG-16	68.69	2.63	17.65	88.97	77.21	2.96	19.84
BNG-17	72.79	2.95	17.03	92.77	78.46	3.18	18.36
BNG-18	70.82	1.96	21.29	94.07	75.28	2.08	22.63
BNG-19	68.51	5.2	18.27	91.98	74.48	5.65	19.86
BNG-20	71.37	4.28	14.8	90.45	78.91	4.73	16.36

PLATE 6.1

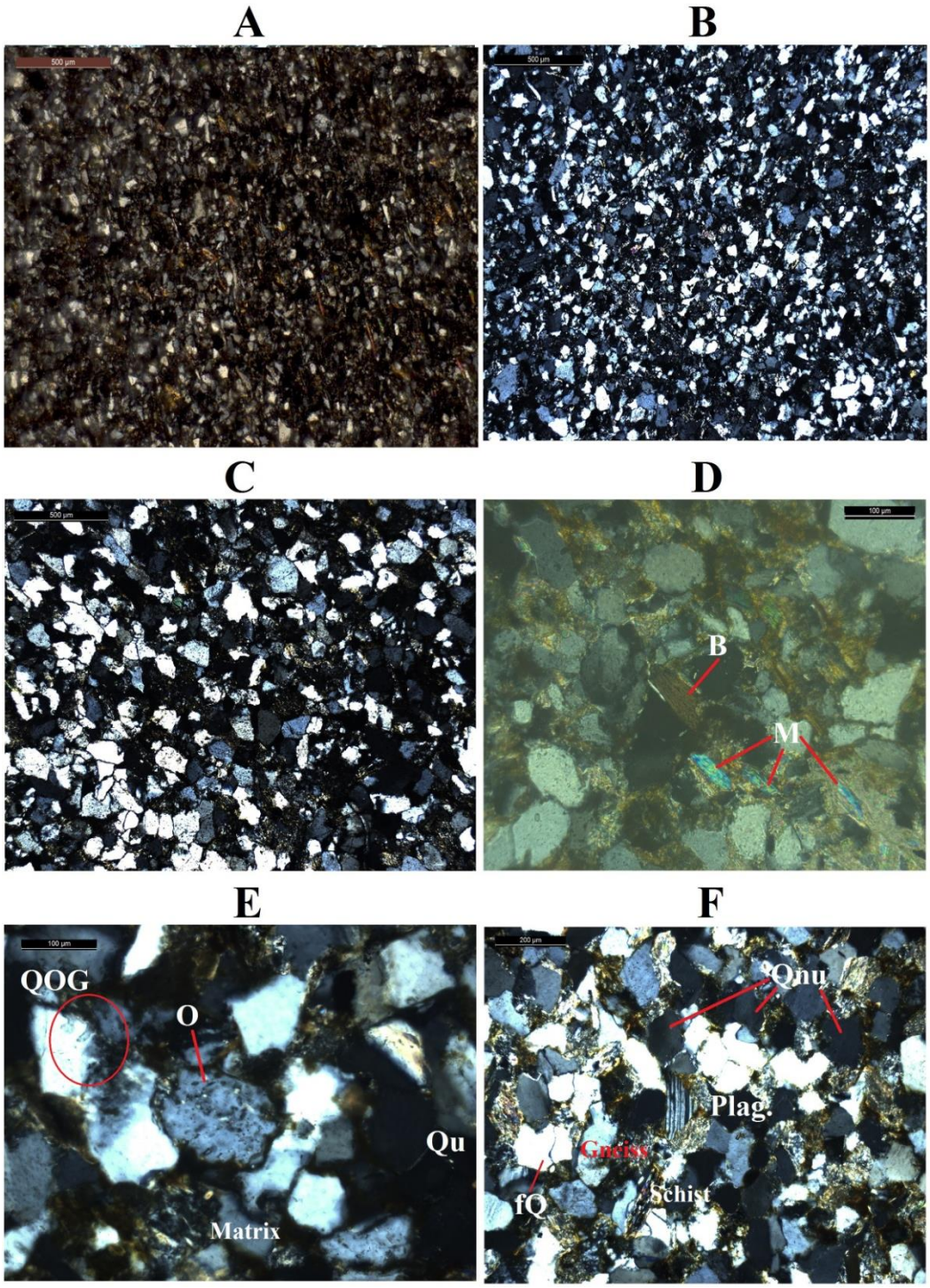

(A) Siltstone (B) Very fine grained sandstone (C) Fine grained Sandstone (D) Micas: B-Biotite, M-Muscovite (E) QOG – Quartz overgrowth (circle), O- Orthoclase, Qu-Undulatory Quartz (F) fQ- Fracturng Quartz, Qnu – Non undulatory Quartz, Plag. – Plagioclase.

PLATE 2

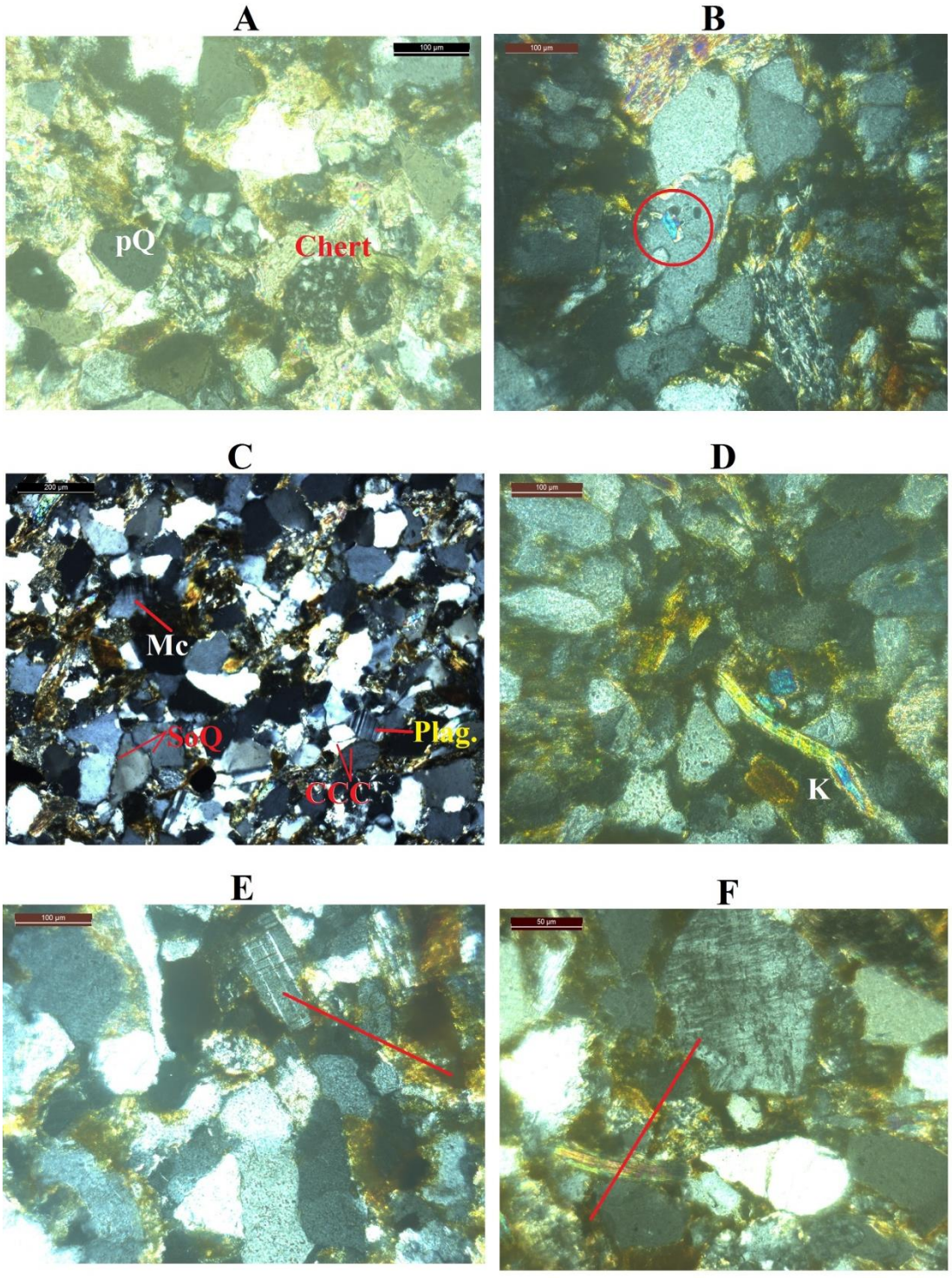

(A) pQ- Polycrystalline Quartz (B) Circle - Heavy mineral inclusion (C) SoC- Suturing of Quartz, Mc - Microcline, Plag. – Plagioclase, CCC – Concavo convex-contact (D) K - kink band of Mica (E) Antiperthite and (F) Perthite.

6.3. SANDSTONE MINERALOGICAL CLASSIFICATION

Although the relative abundance of matrix plays a role in some classification, descriptive classification of sandstone is based fundamentally on framework mineralogy. The classification of Barail sandstones is established through quantitative modal analysis of the rock thin sections (Pettijohn *et al.*, 1972; Folk, 1980 and McBride, 1963). Classification schemes, QFL ternary plot of Pettijohn *et al.* (1972), QFL plot after Folk (1980) and Pettijohn (1972) have been used to determine the Sandstone classification in the present study. Each sandstone rock sample has had its primary detrital framework grains, including quartz, feldspar, and lithic particles, enumerated. The modal count their recalculated percentile of the framework grains are display in Tables 6.1 & 6.2. Quartz, one of the framework grains, is the mineral that is most abundant, it constitutes 51.58 – 75.32% of the total framework grains. Lithic fragment, by contributing 9.95 – 23.83% of the total framework of grains is second abundant. Feldspar minerals, which make up just 1.96 - 11.52% of the three minerals found in Barail sandstones, are the least abundant. Based on sandstone classification after Pettijohn (1972), majority of the barail sandstones are Arkosic Wacke (55%), followed by Lith-Graywacke (20%) and 15% Sublith Arenite (Figure 6.3). According to the Sandstone classification diagram (QFL) constituting framework minerals, after Folk (1980) and Pettijohn *et al.* (1972), most of the the Barail sandstones fall in the field of Sublitharenite(93%), 3% of the samples falls in Litharenite and Felspathic each. So, the sandstone are classified as Sublithic arenite or Sublitharenite (Figure 6.1 and 6.2).

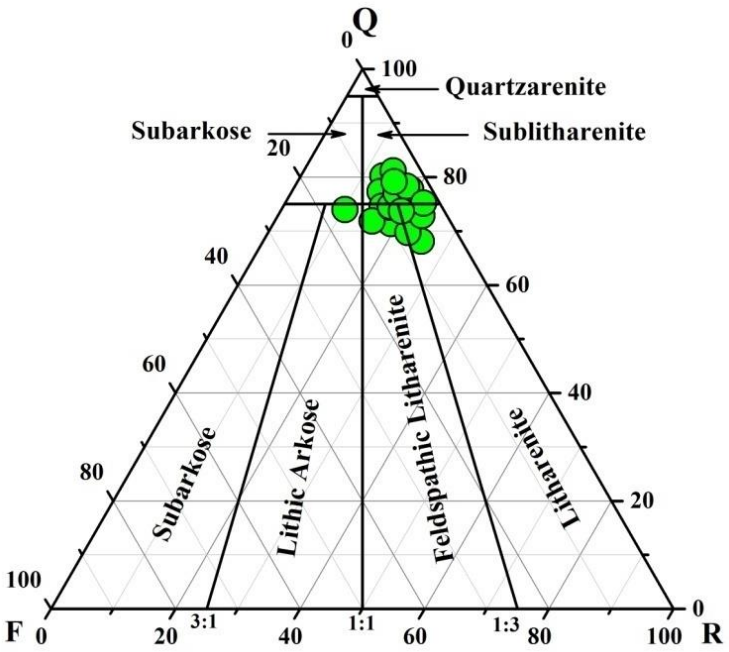

Figure 6.1. Triangular plot of QFR for mineralogical classification of Barail sandstones, Ngopa, Mizoram. (after Folk, 1980).

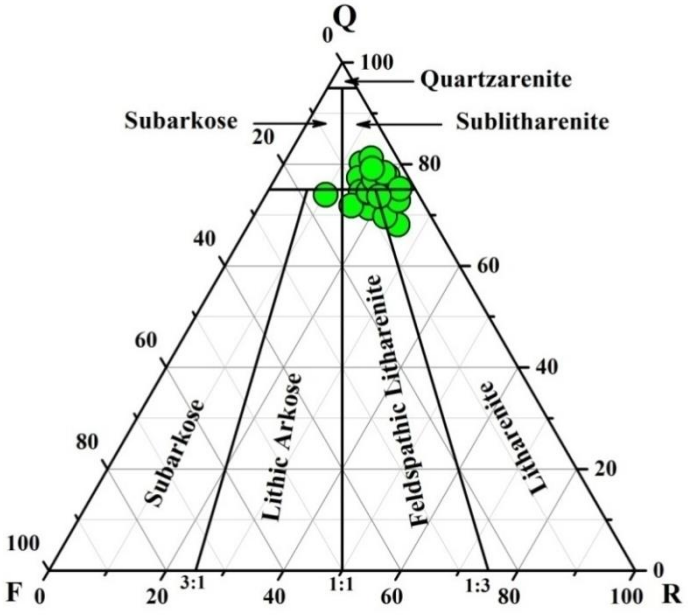

Figure 6.2. Triangular plot of QFR for mineralogical classification of Barail sandstones, Ngopa, Mizoram (after Pettijohn, 1972).

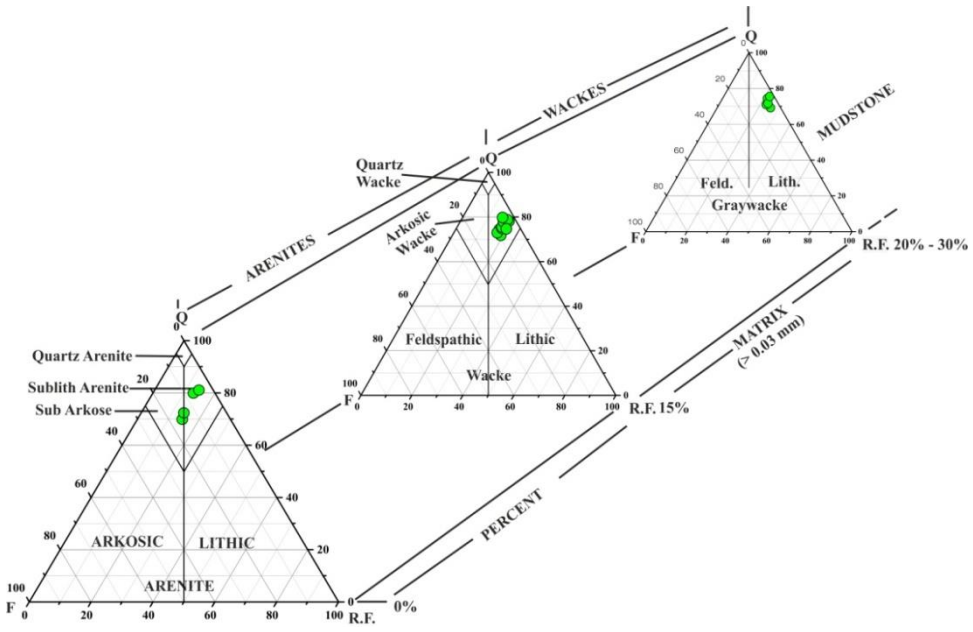

Figure 6.3 Petrographic classification of Barail sandstones, Ngopa, Mizoram After Pettijohn (1972)

5.4. PROVENANCE

Quartz species like Monocrystalline and polycrystalline quartz can be used to interpret the provenance of an area. The petrography of the studied samples shows that among Quartz detrital varieties, monocrystaline undulatory quartz (Qmu) have highest percentage 32.85 – 64.26% by constituting average of 53.13% second by monocrystalline non-undulatory quartz (5.13 – 16.29% having an average concentration 9.83%), Polycrystalline quartz >3 (0 - 7.26 - % having average of 2.87%) & polycrystalline quartz 2-3units (0 – 5.07% with an average of 2.08%). The high undulatory quartz amount (undulose extinction >5 degrees) indicates the metamorphic origin whereas the non-undulatory quartz represents an igneous source rock (Krynine, 1940 and Folk, 1974). Occurrence of Polycrystalline quartz has been considered as indicator of metamorphic origin. The undulatory quartz grains show strain effect due to compressive forces (wavy extinction) which represents the metamorphic source rock.

Basu *et al*. (1975) had proposed the diamond plot and had discriminated various rock sources such as- Plutonic, low, middle and upper rank metamorphic types to find out the provenance. The recalculated detrital Quartz varieties are quantified and plotted in a discriminant diamond diagram proposed by Basu *et al.*,(1975). According to Figure 6.3, all of the studied sandstone samples clustered within the region of low rank metamorphic rock and this also explained why majority of Quartz content are undulatory.

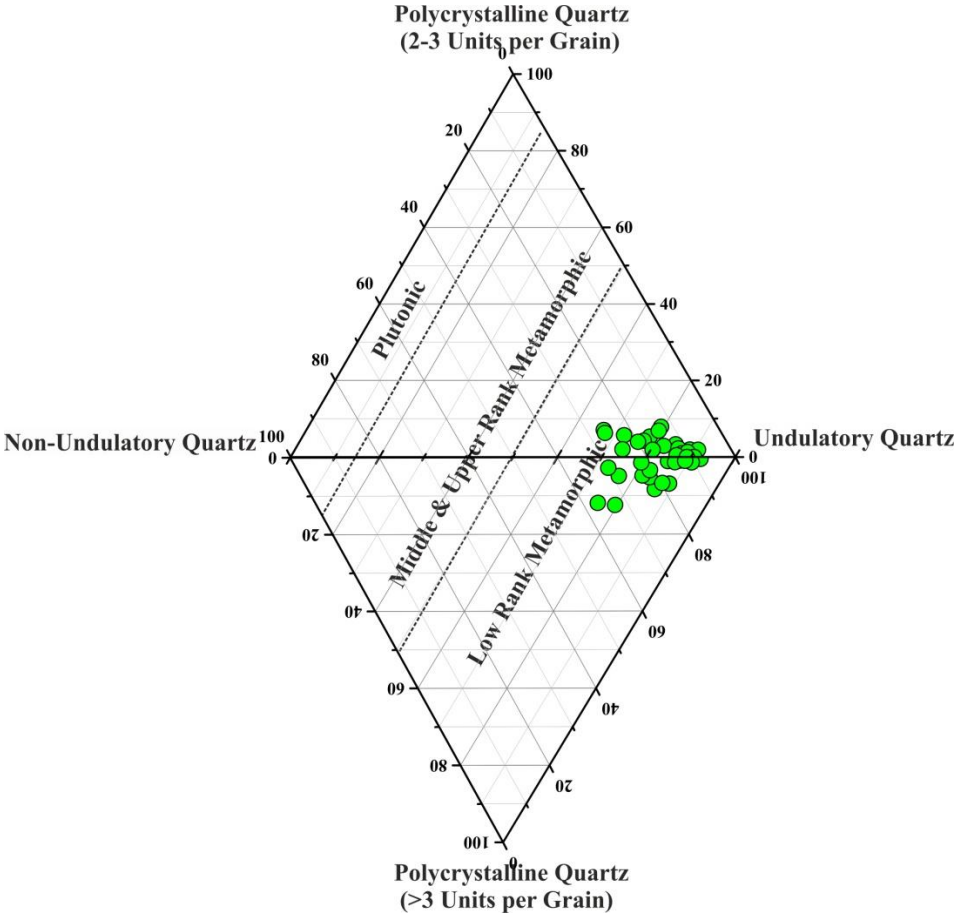

Figure 6.4. Diamond plot for interpretation of provenance of Barail sandstones, Ngopa, Mizoram (Basu *et al.*,1975).

Tortosa *et al.* (1991) had proposed a customized form of diamond diagram to fathom out the provenance. Their modified plot has the same distinguishing feature, but their field classification of the source rock were not the same. All of the Barail sandstones fall within Granite according to the plot suggesting an origin of granitic terrain (Figure 6.4). It can be suggested based on the two provenance discrimination that the anaysed sandstones have been derived from low rank metamorphic rocks and of granite.

The Feldspar concentration is lower when compared to other frameworks detrital grain. They accounts for only 1.96 – 11.52% with an average of 3.64%. This can suggests that the sediments undergo average distance of transportation and also from Heavy minerals analysis, the occurrence of rounded zircon in some samples imply rework sediments.

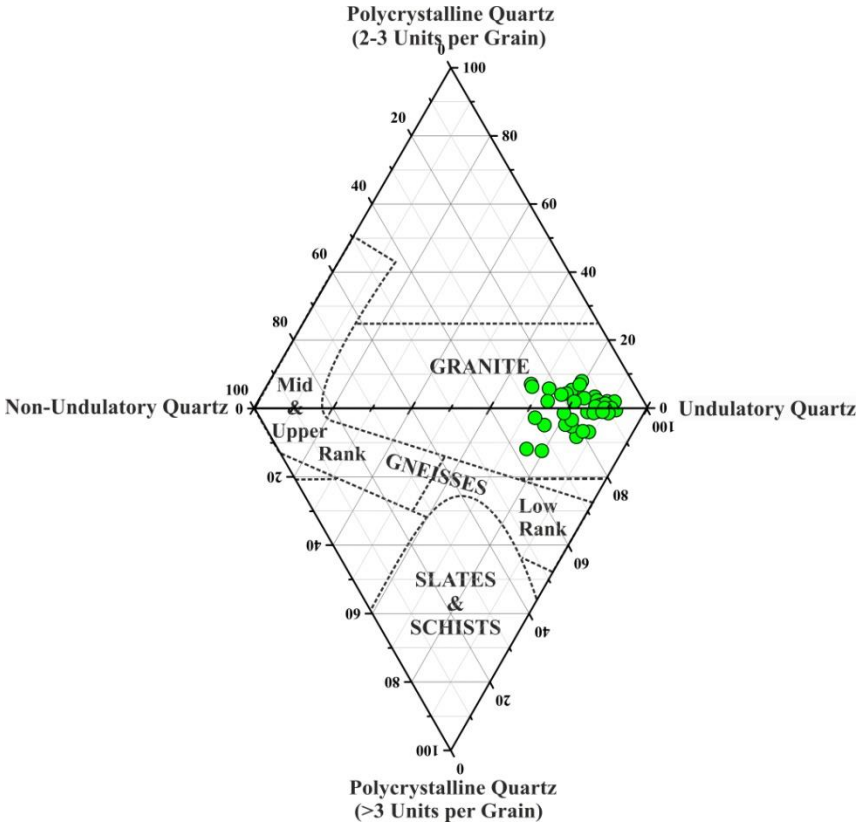

Figure 6.5. Diamond plot for interpretation of provenance of Barail sandstones, Ngopa, Mizoram (after Tortosa *et al.*, 1991).

6.5. TEXTURAL MATURITY

Pettijohn (1975) stated that "*Textural Maturity refers to the degree to which physical characteristics of grains and populations of grains approach the ultimate end product"*. In order to estimate the textural maturity, Folk (1951) suggested three textural properties and they are:-

i) The amount of clay-size sediment in the rock

ii) The sorting of the framework grains, and

iii) The rounding of the framework grains.

He then differentiates into four stages: immature, submature, mature, and supermature. Texturally immature sediments are characterized by a >5 % of clay, their poor sorting, and angular grain characteristics. "While texturally mature sandstone has low clay concentrations, good to moderate sorting, and rounded to sub-rounded grains, submature sediments have low clay concentration, moderate sorting, and sub-rounded grains". The devoid of clay content and its well-sorted, well-rounded nature are characteristics of a supermature stage. The analysed sediment samples of Ngopa area showed that they are texturally mature to immature sandstone.

6.6. MINERALOGICAL MATURITY

Pettijohn (1975) stated that "The mineralogical maturity of clastic sediment is the extent to which the sediments approached and reached the ultimate end product the formative processes that operates upon it". Quartz showed the most durable and most stable minerals among the framework detrital components and their mineralogical maturity is defined by their resistant to prolonged weathering erosion. "The high quartz content indicates the high degree of textural and mineralogical maturity, which is demonstrated by the well-sorted and rounded grains. But the decrease in feldspar content or the quartz/feldspar ratio indicates that the sediments are mature in terms of their mineralogical maturity". Therefore, according to the

petrography, the sandstone samples analyzed from Ngopa area are immature to submature.

6.7. DIAGENESIS

Von Gumbel coined the term "diagenesis" for the first time in 1888. It is a process that takes place when loose sediments go through physical and chemical changes as rocks are being formed. Diagenesis starts after deposition and it continues through the lithification process. The changes which sediments had gone through between deposition and lithification under normal pressure-temperature conditions are called diagenesis, Sengupta (1994). The different processes that occur during diagenesis are: compaction, recrystallization, dissolution, replacement, authigenesis and cementation (Tucker, 2012). Using Petrography the evidence of these processes can be studied. Over the course of the 1980s and 1990s, researchers discovered the significance of diagenesis.

“The metamorphic process starts with diagenesis, which can proceed when buried at a depth of 4 to 7 kilometers, where the temperature has reached 120 to 220 °C”. Sengupta (1994) classified diagenesis into three stages: Telegenetic - occur near the surface, Eogenetic which take place at a shallower depth and Mesogenetic which occur at deeper level.

The studied sandstones from the Ngopa region have underwent these three phases of diagenesis, based on a thorough examination of petrography. All of the samples exhibit bending of mica flakes, deformation, and breaking of ductile feldspar grains, which is the characteristic of mechanical compaction during diagenesis. The occurrence of fractures in ductile quartz and feldspar grains post deposition also indicates to tectonic disturbances. The presence of quartz overgrowth and dissolution of feldspar by cementing material indicatedthe Telegenetic stages of diagenesis (Sengupta, 1994). It has also been noticed that the ferric oxide that gives red color to ferruginous represents the Eogenetic phases of diagenesis. The presence of silica overgrowth, the point contact between quartz grain and alteration of K-feldspar represents the locomorphic stages of diagenesis (Plate 5.1 and 5.2) (Kichu and Srivastava, 2018; Dapple, 1967). The nature of long contact of quartz grains represents the moderate degree of compaction (Plate 5.1 and 5.2Porosity alters or

decreases as burial depth and compaction increase. Changes in the pressure solution result as a result (Sengupta, 1994). The suture grains contact, concavo convex, and lengthy contact of grains are examples of the pressure solution reflexes that characterise the burial stage of diagenesis. The late stage (mesogenetic) of diagenesis is characterised by the substitution of albite for microcline, the development of overgrowth in feldspar and quartz that are authigenic, and the breaking and wrapping of quartz in mica flakes.

5.8. PALEOCLIMATIC CONDITION

Sandstone's mineral compositions as well as their maturity were influenced by the climatic conditions that existed at the time of sediment deposition. The deposited sediments preserved climatic signatures and the detritus does not suffer any sedimentary due to their long distance transportation and high energy condition (Suttner *et al.*, 1981). According to Suttner *et al.*, (1981) The high abundance of quartz compared to fewer amounts of feldspar and rock fragments manifest their derivation from metamorphic source under a humid climatic condition. The framework grains of Barail sandstones are plotted in a ternary QFR diagram which has been proposed by Suttner *et al.* (1981). From the plot, we can see that all the samples analyzed fall inside the metamorphic humid region except for one sample, which is also lying just outside the region (Figure 6.5).

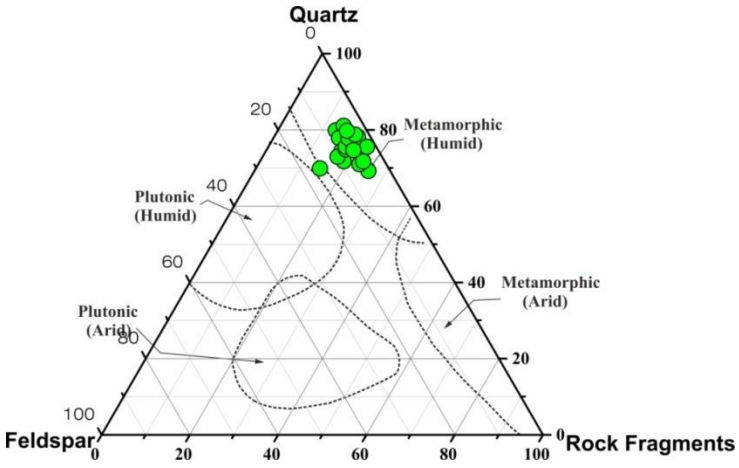

Figure 6.6 Triangular plots of QFR for climatic conditions of Barail sandstones, Ngopa, Mizoram (after Suttner *et al.*, 1981).

The discriminant plot of ratios of (Q_{Total}/F+RF) vs (Q_P/F+RF) proposed by Suttner and Dutta (1986) was again plotted so as to find out the climatic condition and according to the plot, most of the sandstone samples fall within the semi humid while two sample fall under the humid region and one sample falls just outside the semi humid border, within semi arid region (Figure 6.6). Analyzing the results of these two climatic condition diagrams, the Barail sandstones show metamorphic origin which has been deposited under semi-humid to humid climatic condition.

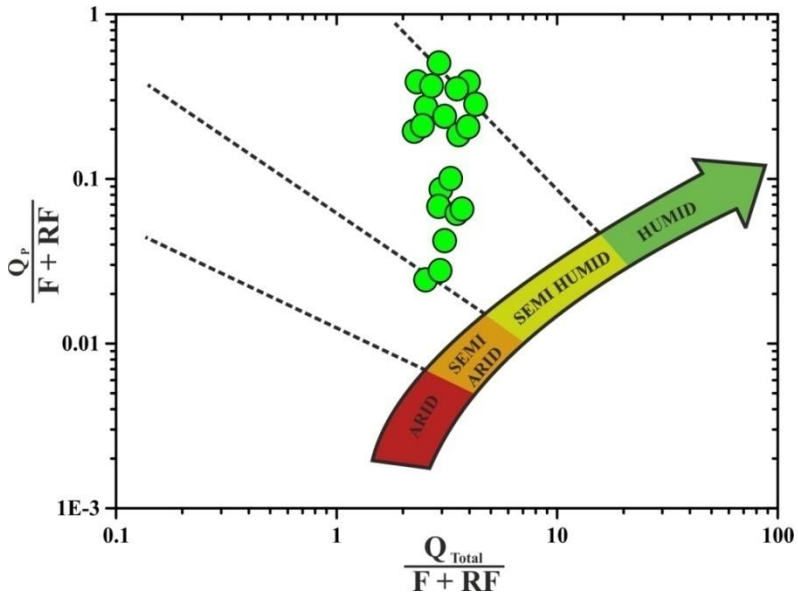

Figure 6.7. Bivariate for climatic conditions of Barail sandstones, Ngopa area, Mizoram (after Suttner and Dutta, 1986).

Grantham and Velbel (1988) also determined the nature of paleoclimatic condition by the weathering index, WI= C x R (WI-Weathering index, C-Climate and R-Relief) and the bivariate plot of ln(Q/R) vs ln(Q/F) (Weltje, 1994) according to the plot, the Barail sandstones represent a metamorphic source and these samples fall within the weathering indices at 1 which suggests a moderate (hill) relief under sub-humid climatic condition as observed in the plots.

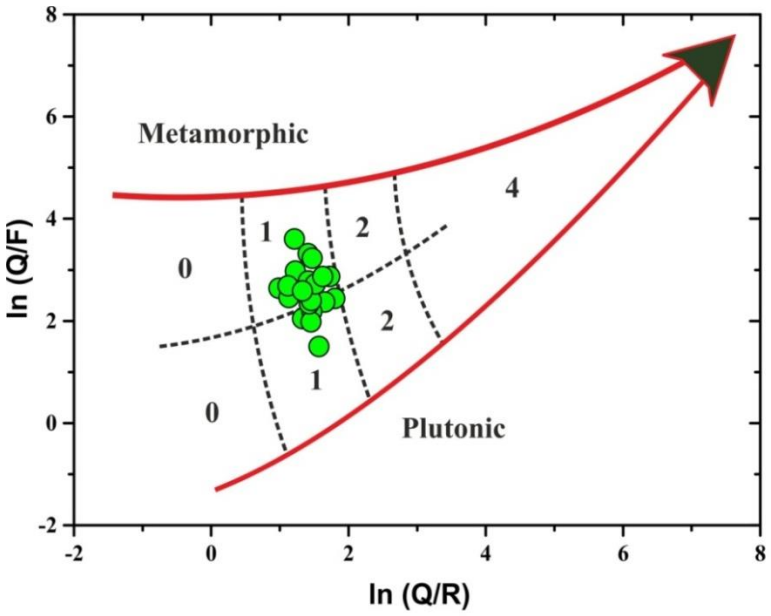

SEMI-QUANTITATIVE WEATHERING INDEX (Grantham and Velbel, 1988)			PHYSIOGRAPHY (Relief)		
			High (Mountain)	Moderate (Hills)	Low (Plains)
			0	1	2
CLIMATE (Precipitation)	(Semi-) Arid & Mediterranean	0	0	0	0
	Temperate Subhumid	1	0	1	2
	Tropical Humid	2	0	2	4

Figure 6.8. Semi Quantitative Weathering Index for Barail sandstones, Ngopa, Mizoram (after Weltje, 1994; Grantham & Velbel, 1988).

6.9. TECTONIC SETTINGS

The tectonic history of the source area can be uncovered by their sediment s' mineral compositions (Krynine, 1984). Dickinson and Suczek (1979) and Dickinson *et al.* (1983) had proposed a QFL and QmFL compositional diagram to interpret the tectonic setting of the source area. According to the QFL diagram (Figure 6.8) all of the analyzed sandstone samples are fall within the region of recycled orogen. QmFL compositional diagram also shows that the sandstones are obtained from a Quartzose recycled orogen (Figure 6.9).

The source rock, from which sediments were derived, can be revealed by the nature of their detrital grains. Monocrystalline quartz which have a wavy extinction (due to strain effect) suggests a derivation of metamorphic origin. Plutonic source rock is indicate by the presence of non-undulatory quartz and polycrystalline quartz.

Perthite has been observed in some of the samples that show an evidence of granite or pegmatite (Plate 6.2 E & F).

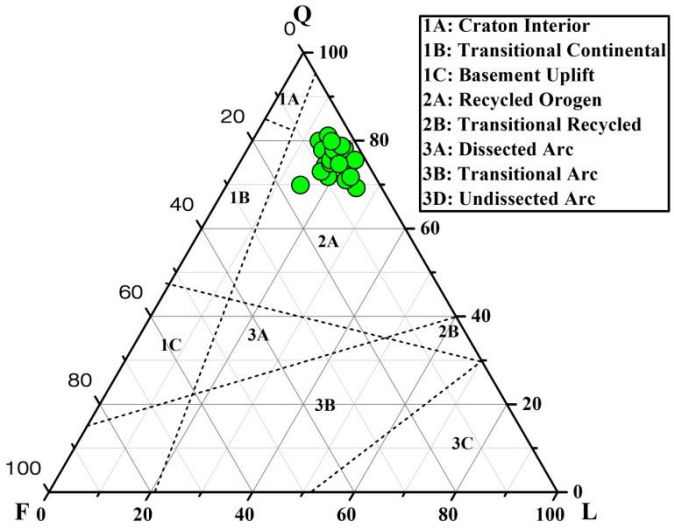

Figure 6.9. Q-F-L plot for tectonic settings of Barail sandstones, Ngopa, Mizoram (after Dickinson & Suczek, 1979).

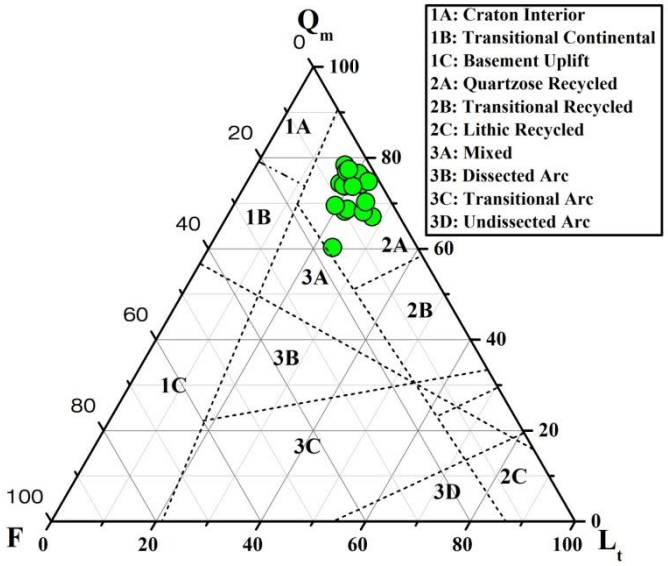

Figure 6.10. Qm-F-L triangular plot for tectonic settings of Barail sandstones, Ngopa, Mizoram (after Dickinson *et al.* 1983).

6.10. DISCUSSION

Quartz forms the most abundant minerals from the petrographic studies of Barail sandstones which constitutes an average concentrations of 67.34%, second being rock fragments with an average 67.34%, and then feldspar for having average concentrations 5.42%. The characteristics of different types of quartz serve as an important indicator of respective source rock. While less common grains like non-undulose monocrystalline quartz refer to a plutonic source, the existence of monocrystalline quartz with a wavy extinction implies a metamorphic provenance. polycrystalline Quartz is the main indicator of a metamorphic origin. Perthite were found, which revealed the presence of granitic or pegmatite sources. Additionally, remnants of gneiss and schist imply that analyzed Barail sandstones were formed from metamorphic protoliths.

Barail sandstones have been classified as litharenite and sublitharenite when plotting the data in classification diagrams after Pettijohn *et al*. (1972) and Folk (1980). The provenance diamond diagram plots like Basu *et al*. (1975) and the modified form of diamond diagram, Tortosa *et al.,* (1991) revealed that the Barail sandstones have been clustered within the provenance of low-rank metamorphic rock and granite field. From paleoclimatic plotting of the ternary QFR diagram proposed by Suttner *et al*. (1981), all the sandstones are put in the field of metamorphic (Humid) origin. The bivariant plot of (Q_{Total}/F+RF) vs (Q_P/F+RF) after Suttner *et al.* (1986) suggests a mixed of semi-humid as well as humid climatic condition. The weathering index (Grantham and Velbel, 1988): WI=C x R (WI-Weathering index, C-Climate and R-Relief) and the bivariate plot of ln(Q/R) vs ln(Q/F) after Weltje (1994) of the evaluated sandstones also suggested a moderate relief (hill) of metamorphic terrain which has been influenced by temperate subhumid climatic conditions. The QFL and QmFL ternary plots after Dickinson and Suczek (1979) and Dickinson *et al.* (1983) respectively showed that the sandstones of the study area are procured from Recycled Orogen.

CHAPTER 7
HEAVY MINERALS ANALYSIS

7.1. INTRODUCTION

Heavy minerals are those accessory minerals having a percentage less than 1% and specific gravity higher than 2.89 g/cm^3, and they are also volumetrically less than 1% by weight of terrigenous rocks (Folk, 1980). These detrital sediments contain accessory minerals which composed of many different mineral species for which they possess their own history. Because of their nature of deposition and transportation behaviour, sediments alter their physical and chemical character which could lead to modification in the provenance. The source rock, their diagenetic processes, and how they are transported can all be determined by their characteristics like stability, ability to withstand abrasion, and resistance toward chemical alterations.. The mineral assemblage can also infer the source rock whether they are from igneous, metamorphic or sedimentary origin (Sengupta, 1996). The heavy minerals assemblages influence grain particle size, specific gravity, erosion, weathering, post-depositional changes, and distance of transportation. Andel (1950) also suggested that nature of transportation controls the availability of heavy minerals.

The heavy mineral suites are not only controlled by provenance, but also affected by the source area weathering, process of transportation, deposition and post-depositional alteration (Morton, 1985). The stability of heavy mineral compositions determines their occurrence. Sengupta, 1996 stated that "The most stable among heavy minerals like tourmaline, zircon and rutile are found in older sandstone bed while those less stable minerals like olivine, amphibole and pyroxene are found in younger beds".

Several workers have put forth on heavy mineral analysis and their interpretation in association with the provenance (Mackie, 1923; Blatt, 1967; Hubert, 1962, 1971; Pettijohn *et al*., 1972; Morton, 1985; Garzanti, 2017).

7.2. HEAVY MINERALS DESCRIPTION

Their characteristics and assemblage of heavy minerals can interpret the source rock lithology. Samples collected from Barail sandstones of Ngopa area is consisting of numerous numbers of heavy minerals such as Zircon, Tourmaline, Rutile, Garnet, Apatite, Chlorite, Monazite, Epidote, Chloritoid, Enstatite, Diopsite, Augite, Kyanite, Clinozoisite, Hypersthene, Staurolite, Silliminite, Zoisite, Muscovite and non-opaque minerals. These Opaque heavy minerals are discussed below:

7.2.1 **Zircon**

Zircon is one of the most stable stable mineral and also the second most abundant heavy mineral in the studied Barail sandstones. It is present in every sample. They exhibits distinctive characteristics such as high relief, high order interference, parallel extinction they lack cleavage, and displayed zoning. They are prismatic, elongated grains and normally colourless or slightly greyish under plane polarised light. According to Krumbein and Pettijohn, (1938) sub-rounded edge of this mineral indicates long transportation with derivation from rework sediments. Zircon accounts for 5.85 – 14.77% of the heavy mineral assemblages with an average of 10.04%.

7.2.2 **Tourmaline**

Tourmaline display wide range of colours and colour zoning is frequent. They show high pleochroism from dark brown to light brown and yellowish brown to pale yellow colour which are indications of composition like Iron and magnesium bearing minerals (Mange and Maurer, 1992). They exhibit different shapes like prismatic, angular and also rounded. Long distance transport is evident by a well-rounded oval grain. Among the investigated Barail sandstones, Tourmalines are the most abundant heavy minerals. It constitutes about 6.76 – 20.99% with an average 14.36%. Krumbein and Pettijohn (1938) “The minerals are derived from pegmatites, pneumatolytic rocks, schist and gneiss”.

7.2.3 **Rutile**

Rutile is distinct from other heavy minerals as it is easily identified by its deep blood red, brownish red or yellowish brown color. They show high refractive index, cleavage absent and they exhibits euhedral and subhedral and even short prismatic form. The mineral varies from 3.03 – 11.35% with an average of 7.47% in the current studied samples.

7.2.4 **Garnet**

In sediment, detrital Garnets occur as euhedral, sharp irregular fragments and sub-rounded to rounded grains. They are generally colourless, light pale pink or pale brown. The mineral is easy to identify due to their high relief and isotropic nature. They constitutes about an average of 6.22% among the mineral assemblages.

7.2.5 **Apatite**

They are usually colourless, but due to impurities like manganese of ferric irons etc., they can show greyish-green or reddish brown colour. They are identified by their moderately high relief and weak birefringce. They constitute about average of 3.23%.

7.2.6 **Chlorite**

Detrital chlorite exhibits shades of green. They are thin flaky, oval or irregular shape. They lack pleochroism. They constitute for an average 2.10% of the mineral assemblages.

7.2.7 **Monazite**

Monazite occurs as pale yellow, pale amber, almost colourless and greenish pale yellow. It has high relief with resinous lustre. Dark rim surrounds the mineral outline. They are often spherical, egg-shaped, or well-rounded. They are readily distinguishable due to their high relief, color, and typically rounded shape.. The mineral constitute an average 0.56% of the mineral assemblages.

7.2.8 **Epidote**

Epidote are showing shades of green, yellowish green or grass green. Their distict character is high relief and their irregular shape. They have parallel or near parallel extinction. On average, they make up 3.86% of all mineral assemblages.

7.2.9 **Zoisite**

Typically, zoisites are colourless. They have a short prismatic habit, high relief, and can exhibit parallel to prism-outline extinction, although they can also exhibit undulatory or incomplete extinction. It makes up on average 0.34 percent of the heavy mineral assemblages.

7.2.10 **Clinozoisite**

Clinozoisite has a colourless, light yellow, or light green appearance. They can be found in either short or long prisms and are characterized by their high relief. They make up on average 0.77% of the total.

7.2.11 **Enstatite**

Enstatites are colourless. They exhibit long or short stumpy prism. They are easy to identify for their moderate relief, prismatic, cleavage and lamellar structure and also parallel extinction. The mineral constitutes for an average 6.23% of the heavy mineral assemblages.

7.2.12 **Diopside**

The minerals display colorless to pale green colour. They occur as prismatic habit, mineral edge are round or subrounded and they have well developed cleavages. The mineral exhibits bright interference color. Diopside contributes an average 3.93% of the total heavy mineral assemblages.

7.2.13 **Augite**

Augite display fairly high relief and obtain large extinction angle. They appear as pale green or sometomes, brown and yellowish brown and compositional zoning is common. Due to this compositional zoning, the mineral exhibits mottled extinction. Augite present in the studied sandstone contributes an average of 3.78%.

7.2.14 **Kyanite**

Kyanites typically have pronounced cleavages and are colourless. In cross nicol, they exhibit bluish colour and weak pleochroism. The minerals typically exhibit parallel extinction and prismatic texture. The minerals constitute an average of 4.75% of the heavy mineral assemblages.

7.2.15 **Hypersthene**

Hypersthenes show pale pink to pale reddish brown or green. They occurred as short prisms. The mineral exhibits pleochroism that ranges in colour from pale pink to pale green. The mineral makes up 0 to 14.09% of a heavy mineral assemblages, on average 3.21%.

7.2.16 **Staurolite**

Staurolites occurs in different forms, irregular, angular or platy. They have high relief and display bright yellow or shades of pale yellow colour. The mineral show pleochroism which depends upon the grain thickness. The minerals, if detectable, display parallel extinction. The mineral makes from 0 to 11.22% of heavy mineral assemblages, on average 4.76%.

7.2.17 **Sillimanite**

Sillimanite typically forms as a long, thin prismatic habit. The m ineral grains have no colors. They exhibit parallel extinction and a significantly high relief. The minerals make up 1.98 - 12.11% of the heavy mineral assemblages, on average 5.94%.

7.2.18 **Muscovite**

Muscovite are colourless or may show some stained colouration due to inclusion of magnetite/haematite or other accessory minerals. They appear as basal plates. They lack pleochroism but show perfect interference figure.

7.2.19 **Opaque Minerals**

Contrary to non-opaque minerals, opaque minerals do not permit light to flow through them; as a result, even when the stage is rotated, the grains remain black under plane polarised light and crossed nicol. The minerals make up 6.25 - 31.68% of all the heavy mineral assemblages, on average 16.35%.

The microphotographs of heavy minerals identified under petrographic microscope are displayed in **Plate 7.1, Plate 7.2 and Plate 7.3.**

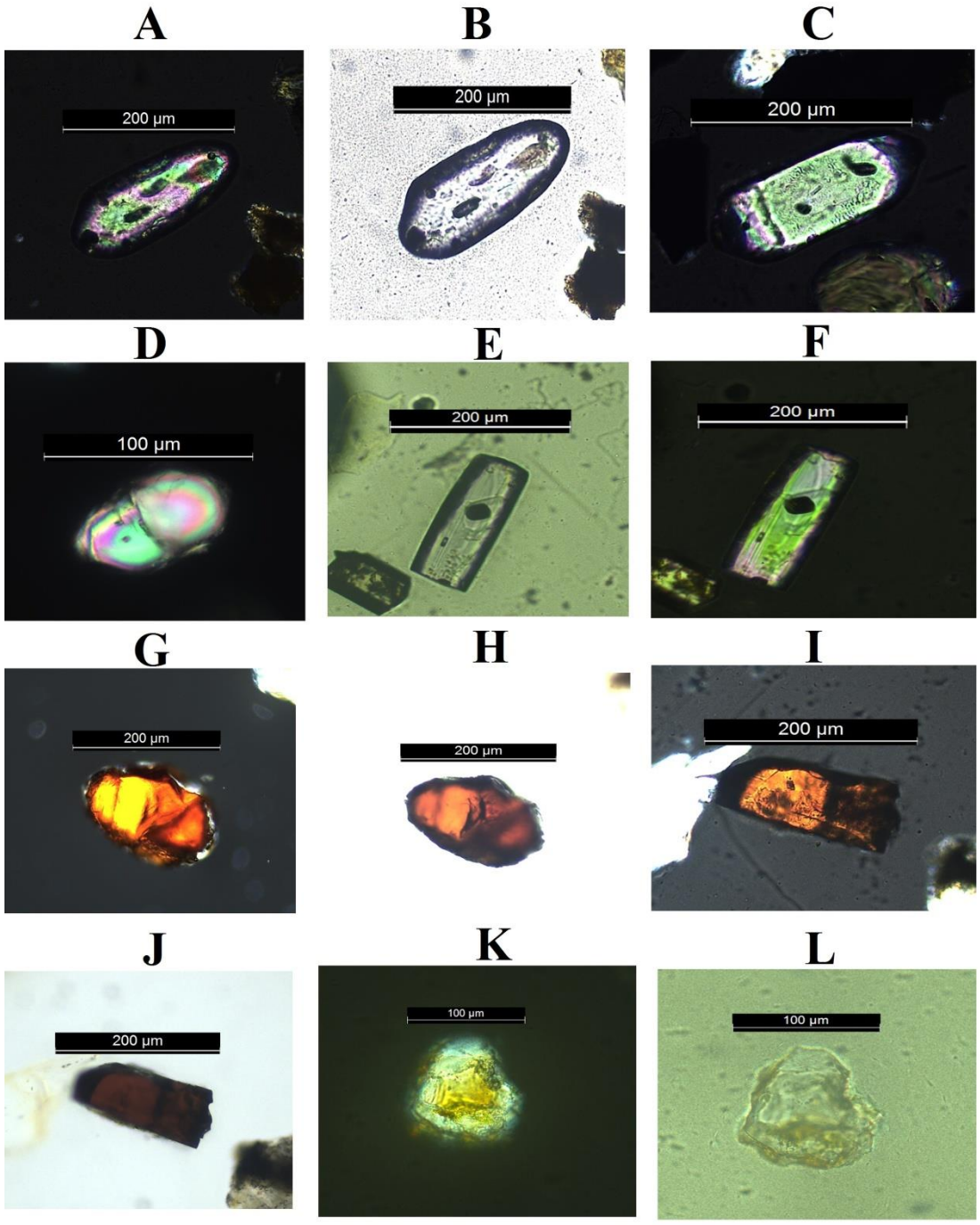

Plate 1: A-D: Zircon, E-F: Tourmaline, G-K: Rutile, K-L: Garnet

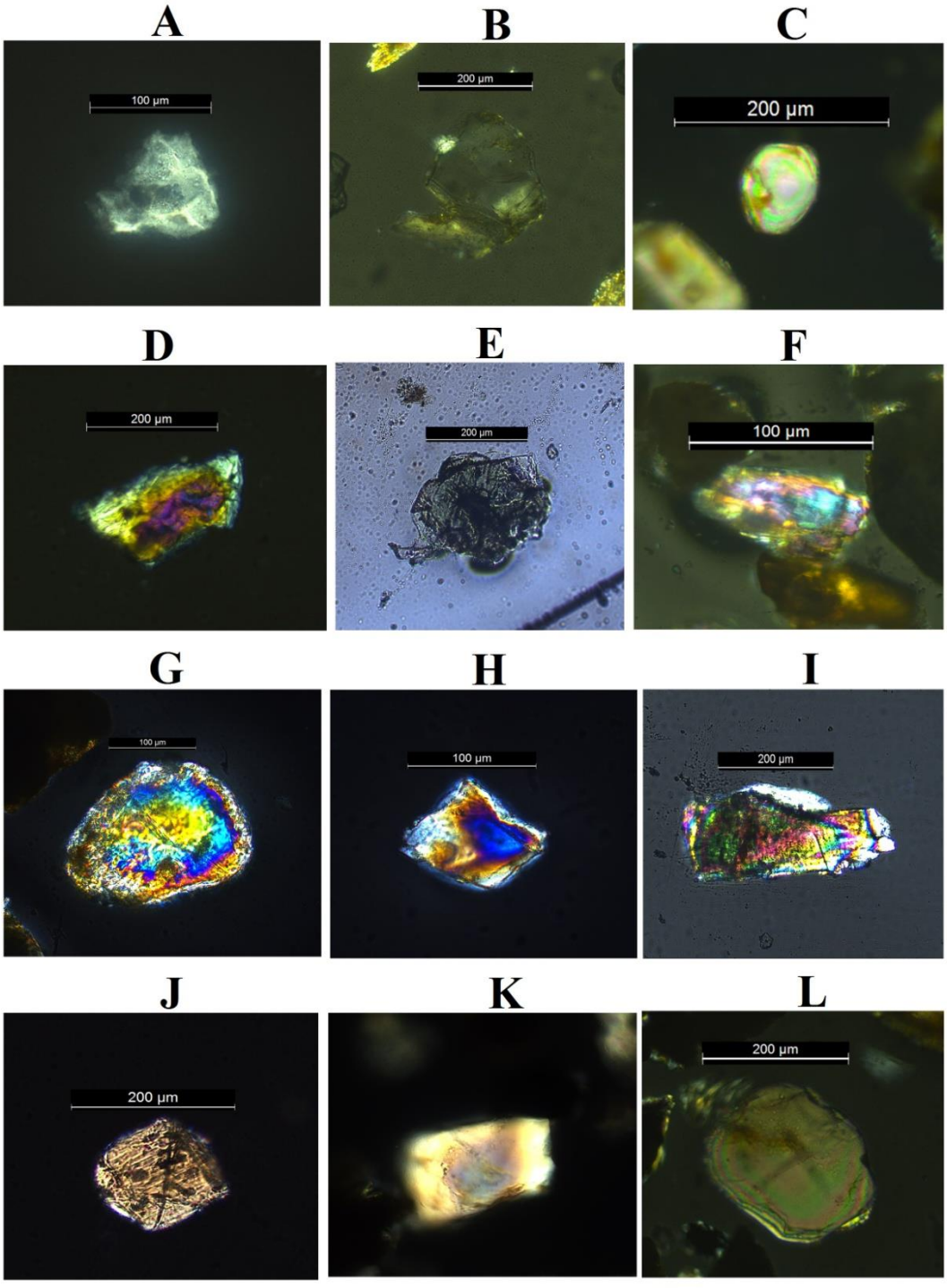

Plate 2: A- Apatite, B- Chlorite, C- Monazite, D- Epidote, E- Chloritoid, F- Enstatite, D- Diopsite, E- Augite, F- Kyanite, G- Diopsite, H- Augite, I- Kyanite, J- Clinozoisite, K- Hypersthene, L- Staurolite.

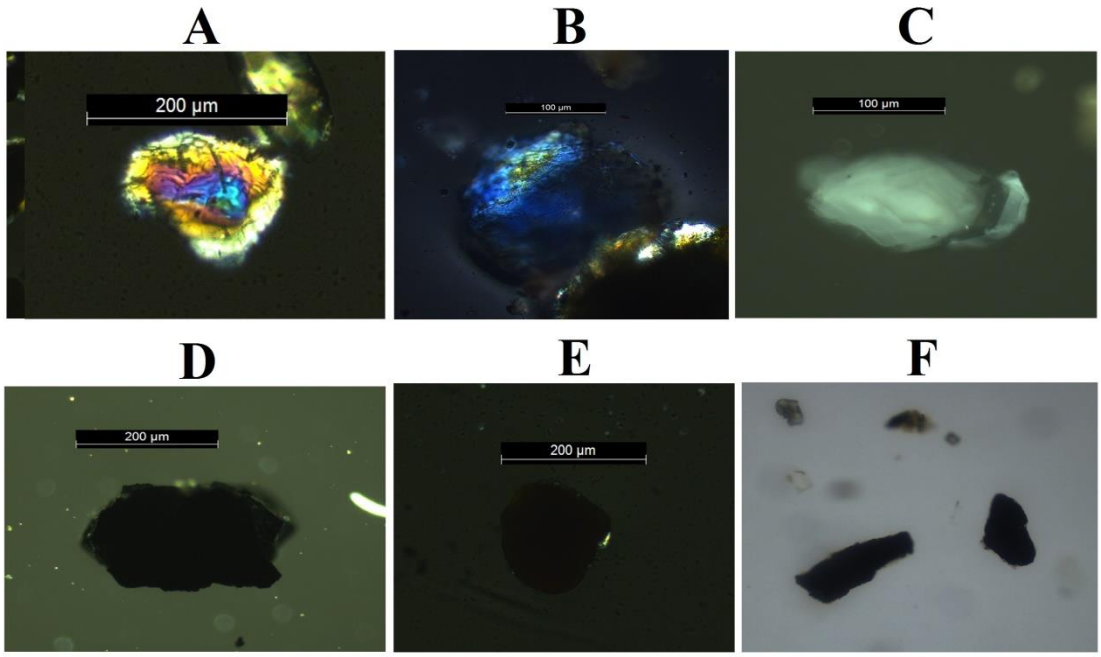

Plate 3: A: Silliminate, B: Zoisite, D: Muscovite, D-F: Opaque minerals.

DESCRIPTION OF PLATE [Scale = 100µm & 200µm]

Plate 7.1 (A - D) : Photomicrograph of Zircon
Plate 7.1 (E - F) : Photomicrograph of Tourmaline
Plate 7.1 (G - K) : Photomicrograph of Rutile
Plate 7.1 K - L : Photomicrograph of Garnet

Plate 7.2 A : Photomicrograph of Apatite
Plate 7.2 B : Photomicrograph of Chlorite
Plate 7.2 C : Photomicrograph of Monazite
Plate 7.2 D : Photomicrograph of Epidote
Plate 7.2 E : Photomicrograph of Chloritoid
Plate 7.2 F : Photomicrograph of Enstatite
Plate 7.2 G : Photomicrograph of Diopside
Plate 7.2 H : Photomicrograph of Augite
Plate 7.2 I : Photomicrograph of Kyanite
Plate 7.2 J : Photomicrograph of Clinozoisite
Plate 7.2 K : Photomicrograph of Hypersthene
Plate 7.2 L : Photomicrograph of Staurolite

Plate 7.3 A : Photomicrograph of Sillimanite
Plate 7.3 B : Photomicrograph of Zoisite
Plate 7.3 C : Photomicrograph of Muscovite
Plate 7.3 D - F : Photomicrograph of Haematite

Table 7.1. Heavy mineral percentage of Barail sandstones, Ngopa area, Mizoram (where Zr=Zircon, Tr=Tourmaline, Rt=Rutile, Gr=Garnet, Bt=Biotite, Zt=Zoisite, Ky=Kyanite, Si=Sillimanite, Ep=Epidote).

Sample No.	Zr	Tr	Rt	Gt	Ap	Cl	Mn	Ep	Clt	En
BNG-1	12.50	19.17	10.00	1.67	0.00	4.17	1.67	2.50	4.17	2.50
BNG-2	12.87	17.82	5.94	0.00	1.98	0.00	0.00	11.88	0.00	4.95
BNG-3	6.78	12.71	10.17	0.00	6.78	3.39	2.54	5.08	2.54	4.24
BNG-4	10.59	11.86	10.17	5.93	5.08	9.75	0.85	4.24	0.85	8.47
BNG-5	9.28	12.37	3.09	7.22	6.19	5.15	0.00	0.00	1.03	12.37
BNG-6	14.77	14.09	9.40	3.36	2.01	0.00	0.00	4.70	0.00	2.01
BNG-7	13.73	16.67	9.31	5.88	2.94	0.98	0.49	5.39	3.92	7.84
BNG-8	8.90	15.25	8.05	9.75	4.24	2.97	0.00	0.85	2.54	7.20
BNG-9	9.18	13.27	6.63	9.18	2.04	2.04	2.55	4.08	0.00	3.57
BNG-10	7.41	20.99	4.32	5.56	0.00	0.00	0.62	1.85	0.00	4.32
BNG-11	11.46	16.15	8.33	10.42	4.69	1.56	0.00	7.81	2.08	0.00
BNG-12	10.81	6.76	4.05	8.11	5.41	0.00	0.00	0.00	1.35	12.16
BNG-13	10.24	12.68	6.34	3.90	2.44	0.00	0.00	3.41	0.98	11.22
BNG-14	8.33	14.44	11.67	10.00	3.33	2.78	1.11	3.89	1.67	3.33
BNG-15	9.61	13.54	8.30	5.24	3.06	4.80	0.00	3.49	2.62	5.24
BNG-16	6.07	9.35	4.67	13.55	7.01	0.00	0.47	4.21	0.47	11.21
BNG-17	7.91	14.42	9.30	8.84	3.72	0.93	0.00	2.79	0.00	6.98
BNG-18	11.35	13.97	5.24	5.68	3.06	1.31	0.87	3.49	2.18	5.24
BNG-19	6.36	13.78	8.48	5.65	0.71	0.00	0.00	5.65	0.00	7.77
BNG-20	12.56	17.94	5.83	4.48	0.00	2.24	0.00	1.79	0.90	4.48
Average	10.10	14.19	7.50	6.35	3.55	2.21	0.62	3.87	1.47	6.27

Cont....

Cont. Table 7.1

Sample No.	Di	Au	Ky	Czt	Hy	St	Si	Zt	Ms	Opx
BNG-1	5.00	0.00	5.00	0.83	1.67	7.50	5.83	0.00	0.83	15.00
BNG-2	3.96	5.94	0.00	0.00	0.00	0.99	1.98	0.00	0.00	31.68
BNG-3	5.08	5.08	1.69	0.00	0.00	0.00	8.47	0.00	0.00	25.42
BNG-4	0.00	1.69	1.27	0.00	0.85	5.08	2.97	0.00	0.85	19.49
BNG-5	3.09	0.00	9.28	3.09	3.09	2.06	4.12	1.03	5.15	12.37
BNG-6	1.34	0.00	1.34	0.00	14.09	0.00	6.04	0.00	1.34	25.50
BNG-7	4.41	0.00	2.45	0.49	4.90	1.96	5.88	0.98	0.00	11.76
BNG-8	4.66	2.12	6.78	2.54	6.78	0.00	3.39	0.00	0.00	13.98
BNG-9	6.12	11.73	2.55	0.00	1.53	0.51	3.06	0.00	2.04	19.90
BNG-10	4.32	3.70	0.00	0.00	0.00	9.88	7.41	0.00	1.23	28.40
BNG-11	0.00	2.60	10.94	1.56	4.17	2.60	8.85	0.52	0.00	6.25
BNG-12	8.11	10.81	6.76	0.00	0.00	0.00	9.46	0.00	0.00	16.22
BNG-13	1.95	0.98	7.80	0.98	7.32	11.22	4.88	0.49	1.46	11.71
BNG-14	6.67	2.78	7.22	1.67	0.00	6.67	5.00	2.78	0.00	6.67
BNG-15	2.62	4.37	6.55	2.18	7.42	8.30	5.68	0.00	0.00	6.99
BNG-16	4.67	8.41	0.47	0.00	2.34	7.94	2.80	0.93	0.47	14.95
BNG-17	4.19	4.65	7.91	0.00	3.26	9.30	2.33	0.00	0.00	13.49
BNG-18	2.62	3.93	5.24	0.00	1.75	5.24	11.79	0.00	0.00	17.03
BNG-19	5.65	1.77	6.36	1.06	4.95	8.83	6.71	0.00	0.00	16.25
BNG-20	4.04	4.93	5.38	0.90	0.00	7.17	12.11	0.00	1.35	13.90
Average	3.93	3.78	4.75	0.77	3.21	4.76	5.94	0.34	0.74	16.35

Table 7.2. Table containing averages of heavy minerals of Barail sandstones, Ngopa area, Mizoram.

Sl.No	Minerals	Average
1	Zircon	10.04
2	Tourmaline	14.36
3	Rutile	7.47
4	Garnet	6.22
5	Apatite	3.23
6	Chlorite	2.10
7	Monazite	0.56
8	Epidote	3.86
9	Chloritoid	1.36
10	Enstatite	6.26
11	Diopsite	3.93
12	Augite	3.78
13	Kyanite	4.75
14	Clinozoisite	0.77
15	Hypersthene	3.21
16	Staurolite	4.76
17	Silliminate	5.94
18	Zoisite	0.34
19	Muscovite	0.74
20	Opaque minerals	16.35

Table 7.3: Table of ZTR calculated values of Barail sandstones, Ngopa area, Mizoram.

Sample No.	Z+T+R	Total N.O	ZTR values
BNG-1	50	102	49.02
BNG-2	37	69	53.62
BNG-3	35	88	39.77
BNG-4	77	190	40.53
BNG-5	24	85	28.24
BNG-6	57	111	51.35
BNG-7	81	180	45.00
BNG-8	76	203	37.44
BNG-9	57	157	36.31
BNG-10	53	116	45.69
BNG-11	69	180	38.33
BNG-12	16	62	25.81
BNG-13	60	181	33.15
BNG-14	62	168	36.90
BNG-15	72	213	33.80
BNG-16	43	182	23.63
BNG-17	68	186	36.56
BNG-18	70	190	36.84
BNG-19	81	237	34.18
BNG-20	81	192	42.19
Average			38.42

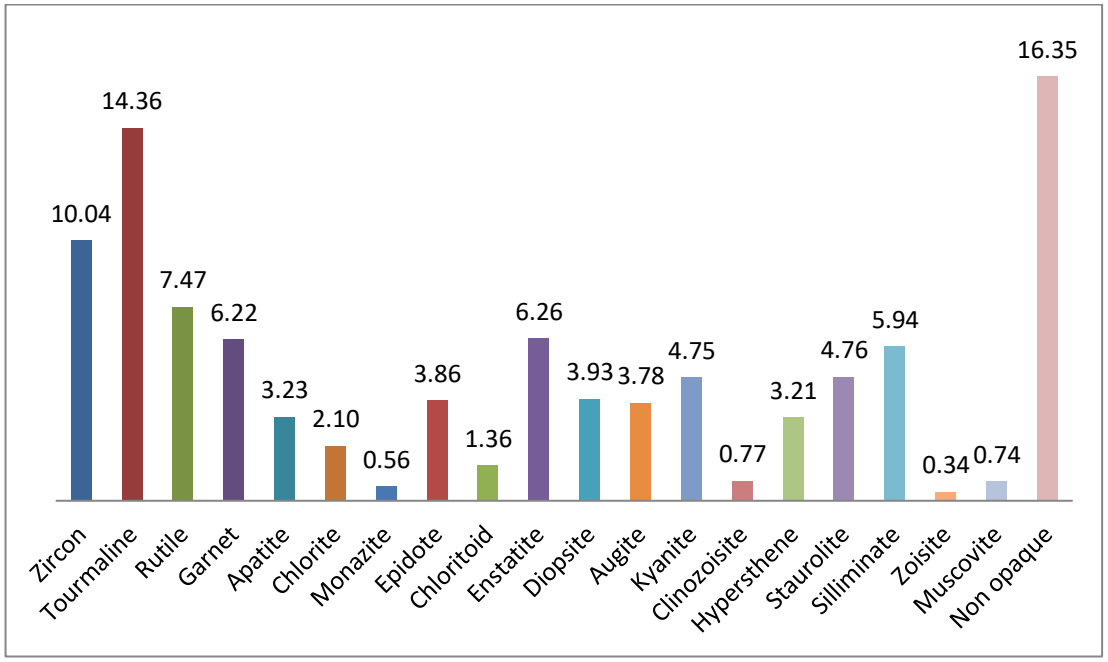

Figure 7.1: Histogram of average values of the heavy minerals of Barail sandstones, Ngopa area.

7.3. ZTR MATURITY INDEX

Zircon, Tourmaline and Rutile, three of the most stable heavy minerals are employed to determine the maturity of the Sandstone samples (ZTR index, Hubert 1962). According to Hubert, "It is the percentage of the combined zircon, tourmaline and rutile grains among the transparent, non micaceous and detrital heavy mineral". These minerals are highly resistant to mechanical and chemical weathering, and thus help in determining the source rock condition of the sediments (Pettijohn *et al.*, 1972).

The formula/equation proposed by Hubert (1962) is used to calculate the ZTR maturity of Barail sandstones collected from Ngopa area, Mizoram:

$$\text{ZTR} = \frac{Z + T + R}{tot.no.of\ N.O} \text{x}100$$

Where, N.O is non-opaque minerals, Z is Zircon, T is Tourmaline and R is Rutile.

Table 7.3 lists the calculated ZTR maturity index values for Barail sandstones. When the average value of the ZTR Maturity Index is greater than 75%, sediments are said to be mature; when it is lower than 75%, sediments are said to be immature to sub-mature. ZTR values for the Barail sandstones range from 23.63 to 53.62%, with an average of 38.42%. The average ZTR Maturity Index value is <75, indicating that the Barail sandstones are thought to have been formed from sub-mature sediments.

To assess their abundance, the percentile concentrations of zircon, tourmaline, and rutile have been recalculated (Table 7.4) and are displayed in the ZTR maturity triangular diagram (modified after Hazarika, 1984). The individual abundance of zircon varies from 22.22 – 50.00%, and tourmaline mineral varies from 31.25 – 64.15% and rutile also varies from 12.50 – 34.29% with an average of 23.33%. From the ternary diagram (Figure 7.2), Most of the sample (14 samples) falls within the C1 region. C1 tier implies that the proportion of Tourmaline is highest, followed by Zircon and then Rutile. The plot also indicates a moderate maturity and predominant of metamorphic provenance. So, according to the plot, Sediments from the the study area are moderately matured and are derived from metamorphic source rock.

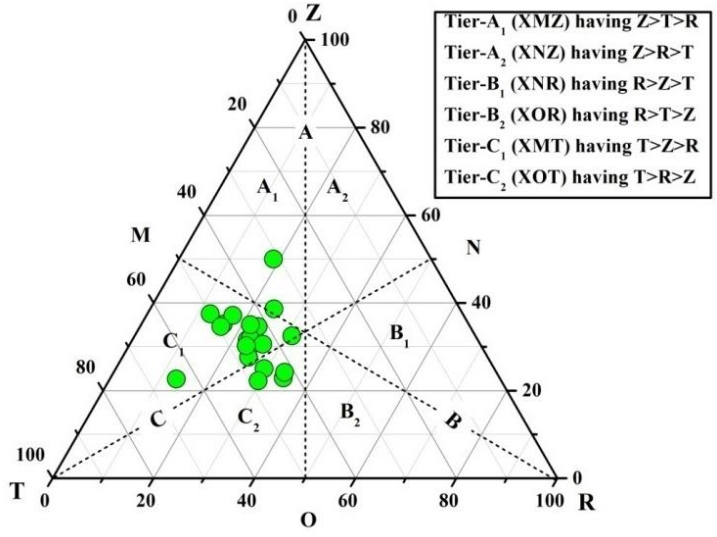

Figure 7.2. Ternary plot of ZTR Maturity of Sandstone samples from Ngopa area, Mizoram (Hazarika, 1984).

7.4. DISCUSSION

The Barail sandstones of the Ngopa area contain opaque and non-opaque heavy mineral assemblages. Non opaque minerals like zircon, tourmaline, rutile, garnet, Apatite, Chlorite, Monazite, Epidote, Chloritoid, Enstatite, Diopsite, Augite, Kyanite, Clinozoisite, Hypersthene, Staurolite, Silliminite, Zoisite and Muscovite are present. The abundance of tourmaline, zircon, rutile, and opaque minerals indicates that the sediments are derived from acidic igneous source (Feo-Codecido, 1956). Prismatic and elongated grains of some zircon and tourmaline minerals observed in the sample suggest derivations from igneous source rock. Zircon and tourmaline grains that are euhedral indicate short-distance travel. However, rounded zircons, tourmalines, and rutile are also often found, which shows that sedimentary rock may have been recycled and transported over a considerable distance. Zircon fragments observed suggest short to moderate transportation as well.

Minerals like Zircon, Tourmaline, Apatite, Enstatite, Diopsite, Augite, Hypersthen and Monazite suggests that the studied sediments are derived from basic and acidic Igneous rocks. Minerals like Rutile, Chlorite, Garnet, Epidote, Kyanite, Chloritoid, Clinozoisite, Staurolite, Sillimanite, Zoisite and Muscovite suggests derivation fromLow to medium, intermediate to high grade Metamorphic rocks.

The Barail sandstones of the Ngopa area are derived from mixed sources and are originated from sub-mature sediments, according to the mineral assemblages and the ZTR maturity index. The majority of the sediments revealed igneous and metamorphic origins as their sources. The heavy minerals' rounded to subrounded shapes suggested that the sediments had been reworked.

CHAPTER 8
GEOCHEMISTRY

8.1. INTRODUCTION

"Sediments endured several processes during the clastic rock formation or evolution, including pedogenesis, erosion, transport, deposition, and burial. However, these sediments are altered by a variety of processes, including as burial diagenesis, chemical weathering, physical breakdown, abrasion, hydrodynamic sorting, and alteration by authigenic inputs. The traces of these processes are maintained in the detrital components of the sediments". 1993 (Johnsson). This offers critical insight into the sediments' tectonic settings, paleo weathering conditions, depositional environment, and provenance interpretation. Suttner (1974) proposes a number of variables, such as provenance, transportation, deposition, depositional environment, and diagenesis, which regulate the composition of clastic deposits. The chemical alterations that take place during deposition are therefore determined by the environment of deposition, which is primarily controlled by subsidence rate.

When determining sedimentary provenance in relation to tectonic settings, sandstone type and composition offer hints. Using petrographic information on sedimentary terrain, Dickinson and Suczek (1979) investigated the relationship between tectonic environment and sandstone composition. The tectonic environment was divided into three categories: (i) continental block (ii) magmatic arc (iii) recycled orogen. Geochemical composition of sedimentary rocks provides accurate information about sedimentation, origin, and tectonic settings. (McLennan *et al.*, 1993). McLennan *et al*. (1993) established the provenance classes such as Old Upper Continental Crust, Recycled Sedimentary Rocks, Young Undifferentiated Arc, Young Differentiated Arc, and various Exotic Components, such as ophiolites, based on the examination of entire rock chemistry and Nd-isotope composition. Understanding the bulk geochemistry of sedimentary rocks can help identify the tectonic setting where the source sediments formed (Bhatia, 1983, 1985; Bhatia and Crook, 1986; Roser and Korsch, 1986, 1988). The chemical composition of sandstone and its primary structural components have also been extensively studied by a variety of researchers to deduce the source rock and tectonic settings of the

sediments (Bhatia, 1983, 1985; Bhatia and Crook, 1986; Roser and Korsch, 1986). Since they are static and can preserve the parent rock even in the presence of weathering and diagenesis, rare earth elements are particularly useful for evaluating provenance. (Nesbitt, 1979; Nesbitt *et al*., 1980; Johnsson,1993).

The alteration in the chemical makeup of sediments can be used to infer weathering signals. Chemical weathering results in the loss of unstable minerals, which elevates the concentration of stable minerals in the sediments. According to McLennan *et al*. (1993), "Intensity of weathering appears to be primarily controlled by climate (precipitation and temperature) and vegetation (particularly the nature and activity of organic acids) and duration of weathering is controlled by many factors, including relief, slope, and sediment storage prior to ultimate deposition and sedimentation rate."The abundance and nature of REE concentration in sediments has been provide significant information in interpreting the nature of the source rock (Taylor and McLennan, 1985; McLennan *et al*., 1993). Evaluation of the sedimentary processes is aided by the high concentration of trace elements and REE in fine-grained, clay-rich sediments and their stationary character (Nesbitt, 1979; Nesbitt *et al*., 1980, Johnsson 1993, Cullers *et al*., 1987). The concentration of REE and several trace elements, such as Th, Sc, Cr, and Co, is higher in terrigeous sedimentary rocks than it is in sea and rivers, and these concentrations are typically unaltered by the processes of diagenesis and metamorphism (Rollingson, 1993; Johnsson, 1993). "Terrigenous sediments may reflect the features of their source rocks on the assumption that some elements (particularly rare earth elements, Th, Zr, Hf, and Sc) are transformed from the site of weathering to the terrigenous components of the sediments, and their abundances are not significantly modified during weathering, sediment transport, diagenesis, or metamorphism," wrote Taylor and McLennan in 1985.

Nesbitt (1979) demonstrated that REE chemistry, which is impacted by extreme weathering, can be used to gauge the degree of weathering or weathering condition of source sediments. Various multi-element ratios, such as La/Sc, Th/Sc, La/Co, Th/Co, Eu/Sm, and La/Lu, offer hints for figuring out the provenance (Cullers, 1988). Large cations (Cs, Rb, and Ba) are fixed in the weathering profile,

but smaller cations (Na, Ca, and Sr) are more easily leached, as demonstrated by Wronkiewicz and Condie in 1987.

8.2. GEOCHEMICAL DATA AND INTERPRETATION

Table 8.1 contains major elements in terms of weight percentage of oxides, trace, and REE in terms of parts per million (ppm) (GSR-4: Chinese Sandstone Standard from Xenjing *et al*., 2007 and UCC: Upper Continental Crust from Rudnick and Gao, 2003, 2005). This studies the entire rock geochemistry of Barail sandstones from Ngopa area, Saitual Distric, Mizoram.

8.2.1. **Major Oxides**

Major oxide concentrations are examined to determine the area's provenance, tectonic settings, and depositional environment. The geochemical investigation of the Barail sandstones in the Ngopa area led to the tabulation of the Major oxide concentrations in Table 8.1. Highest concentration is of SiO_2 (which ranges from 64.79-74.56% with an average of 71.46%) followed by Al_2O_3 (7.98-13.82% with an average of 10.14%). Al_2O_3 concentration exhibits a positive correlation with Fe_2O_3, K_2O, Na_2O, MnO, and CaO, according to the correlation graph plots (Figure 8.1). Al_2O_3 does, however, it shows negative correlations with SiO_2 (-0.86). SiO2 is found in substantial amounts as quartz grains, indicating quartz dilution. The concentration of SiO_2 exhibits a high negative connection with Al_2O_3 (r = -0.86) (Omotoso *et al*., 2017; Babeesh *et al*., 2018). Al_2O_3/SiO_2 ratios are considerably high (4.69-9.14%, average=7.20%), which suggests that quartz is enriched in sandstone (Table 8.1). Al_2O_3 and K_2O have a very strong positive correlation (r = 0.84), indicating that K-bearing minerals have a big influence on Al distribution. The clay mineral is principally responsible for the significant amounts of Al and K. (McLennan *et al*., 1983). Only SiO_2, Fe_2O_3 and TiO_2 have larger concentrations than UCC when compared to other oxides (Rudnick and Gao, 2003). Al_2O_3 and MgO (r = 0.74) and TiO_2 (r = 0.08) showed weak positive correlation, suggesting the presence of micaceous clay minerals. TiO_2 is present, but in modest concentrations (0.54-1.11%, average = 0.73), indicating the existence of phyllosilicates (Condie *et. al*., 1992).

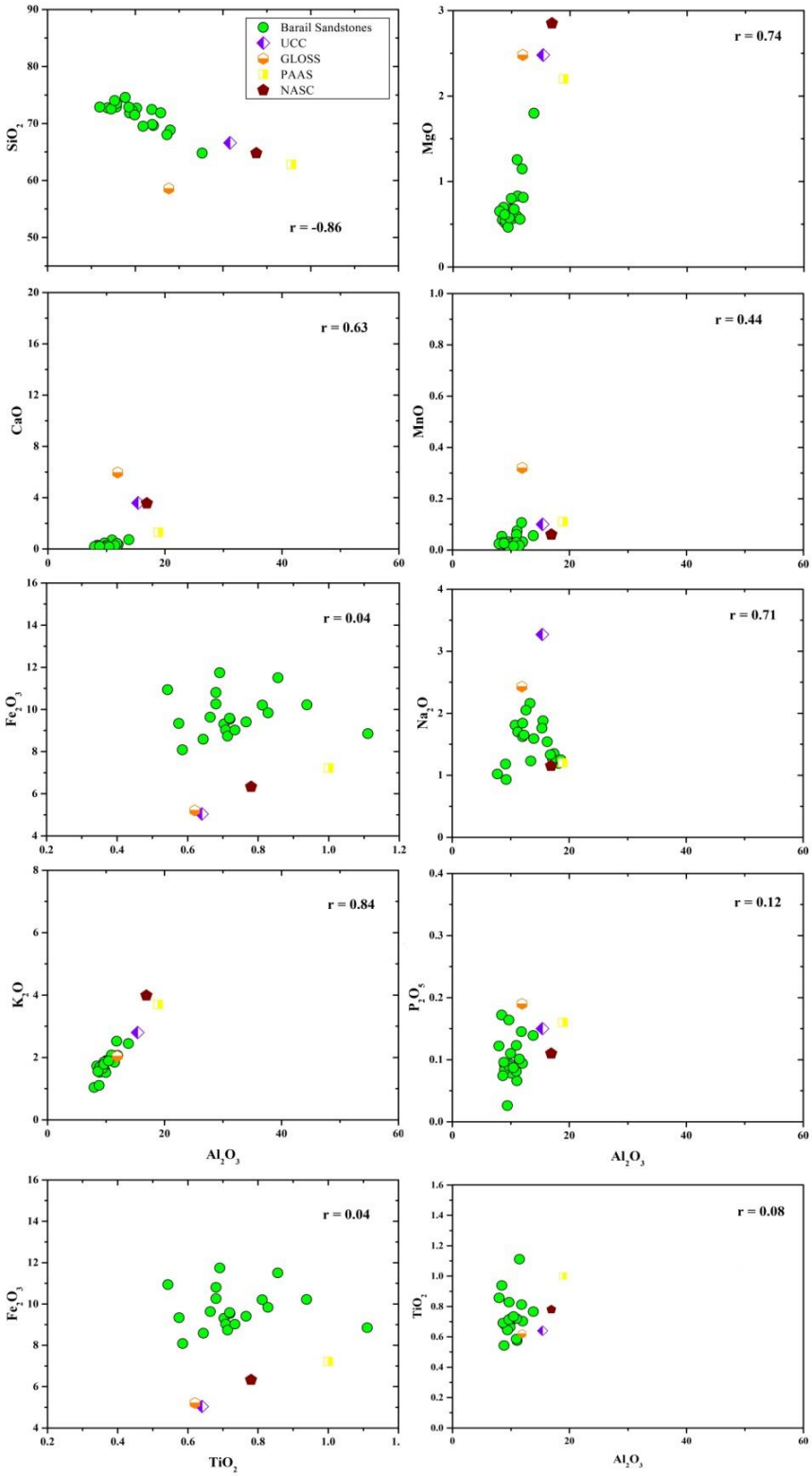

Figure 8.1 Major oxides correlation of Barail sandstones from Ngopa area, Mizoram.

Probability of Fe_2O_3 precipitation during diagenesis was suggested by the enrichment of Fe_2O_3 content (8.09-11.74%, average = 9.73%). Na-rich Plagioclase is associated with a concentration of Na_2O that ranges from 0.72 to 1.76 percent, with an average of 1.07%. K-feldspar is slightly more common than plagioclase due to the modest Na_2O/K_2O ratio (avg = 1.72), which is more than 1 (Na_2O/K_2O) (Al-Juboury, 2012). This is similar composition to the petrographic result. The origin of the detrital materials from a continental source is indicated by the ratio of Al_2O_3/TiO_2, which is rather mild (8.98-19.19% with an average = 14.17%), (Fyffe and Pickerill, 1993) (Table 7.1). The enriched SiO_2, Al_2O_3, Fe_2O_3, and TiO2 can be observed in the UCC normalised pattern (Figure 7.2). The decrease in CaO (on average 0.29), shows that calcic plagioclase was removed during sedimentation.

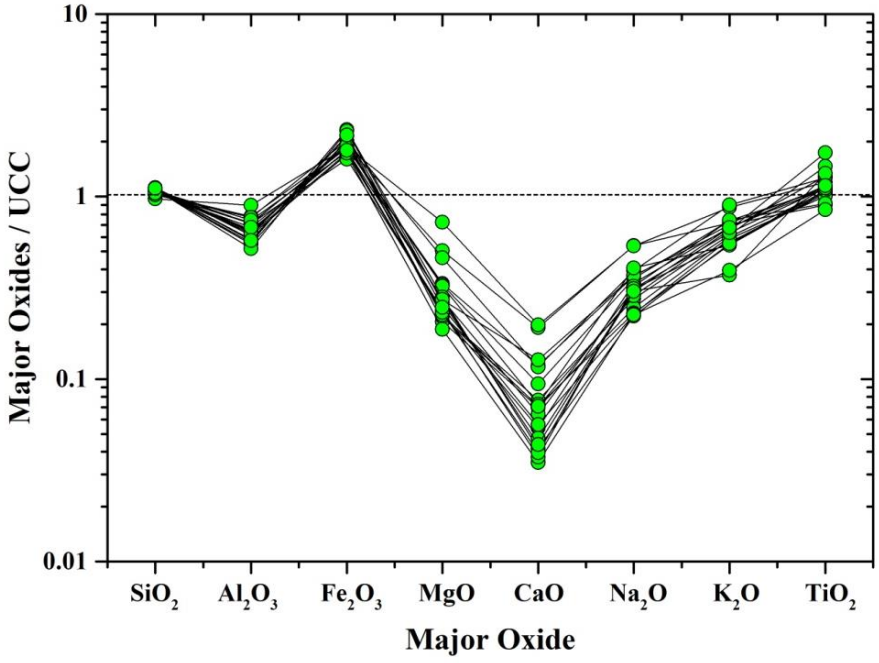

Figure 8.2: UCC normalized major elemental spider diagram of Barail sandstones, Ngopa area, Mizoram (UCC values after Taylor and McLennan 1993).

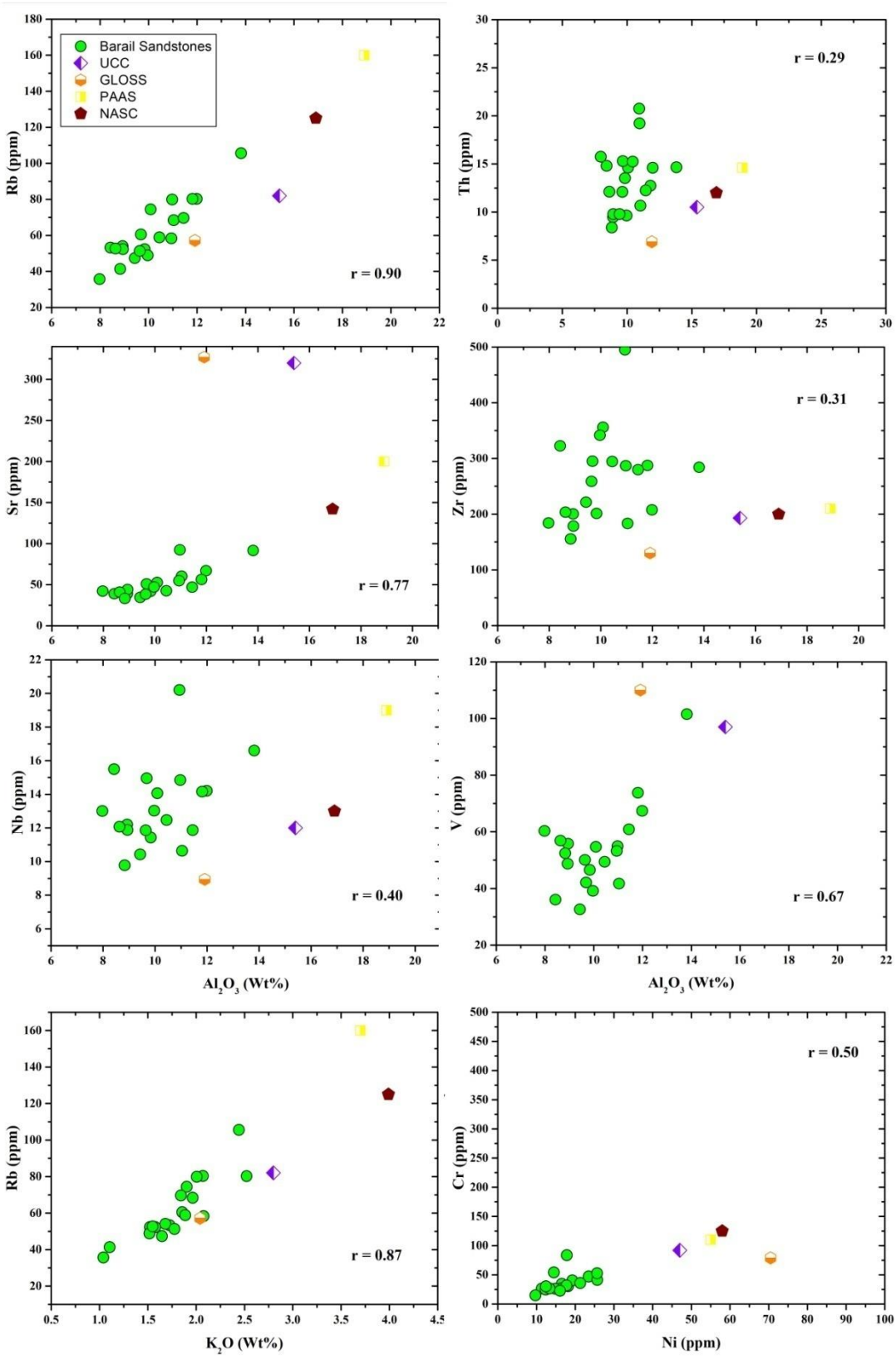

Figure 8.3. Correlation of Al_2O_3 w.r.t various trace elements of Barail sandstones from Ngopa area, Mizoram. (Pearson, 1895).

8.2.2**. Trace Elements**

The concentration of large ion lithophile elements (LILE) relative to UCC (Rudnick and Gao, 2003) and GSR-4 (Chinese Sandstone Standard from Xeujing *et al*., 2007) are shown in Table 8.3. Among these elements, Y (average 21), Zr (avgerage 261.86), Nb (average 12), Pb (average 17), Ba (average 142.88) and Th has higher concentration than UCC (average 10.5). Al_2O_3 showed positive correlation with all the elements as shown in Figure 8.3.

When compared to UCC, the sandstones of the study area have higher concentration of Zr (average = 261.86). This denotes Zr enrichment which is supported by the high population Zircon among the heavy mineral assemblages in the sandstones. The high positive correlation between K_2O and Rb (r = 0.87) indicates the likelihood of the presence of K-bearing rock forming minerals like K-feldspar, biotite, etc., in the rock samples (McLennan *et al*., 1983, Feng and Kerich, 1990). Ni/Cr ratio (r = 0.50) shows a fairly good positive correlation. It is possible that secondary minerals have formed and that organic matter is present (Ali *et al*., 2014). Low levels of Sc (average = 7.74) and Ni (average =16.84) are observed in the sandstones. The UCC normalization of Barail sandstones of the study area is shown in Figure 8.4.

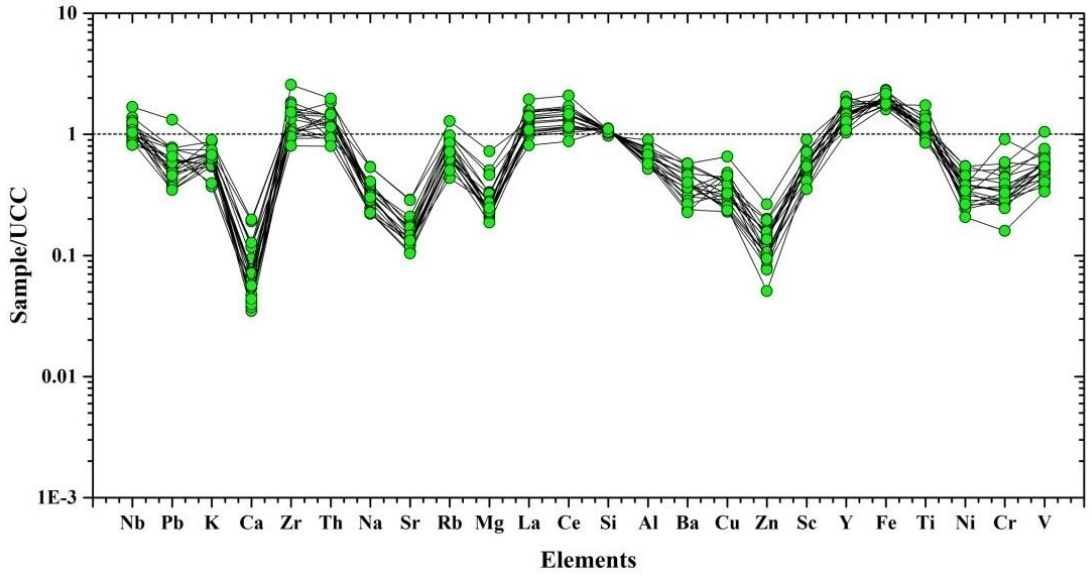

Figure 8.4: UCC normalized multi-element pattern of Barail sandstones, Ngopa area, Mizoram.

8.2.3. **Rare Earth Elements (REE)**

The analytical results of REE concentrations and the subsequent calculations on the ratios of selected elements are shown in Table 8.2. The patterns of heavy rare earth elements (HREE: Gd-Lu) was slightly enrichmed whereas the pattern of light rare earth elements (LREE: La-Sm) was characterised by slightly depleted as shown in Figure 8.5. The elements display a pattern which is remarkably similar to UCC. The negative Eu anomaly of the chondrite-normalized REE of Barail sandstones behave similar to that of the UCC standard and ranges from 0.99-2.10 with an average of 1.42 percent. The ratios of (La/Sm) N which ranged from 3.01-3.96 (avg = 3.47) and the value of (Gd/Yb)N which vary from 1.43-1.98 (average 1.66) are quite similar to the characteristics of the UCC and GSR standards.

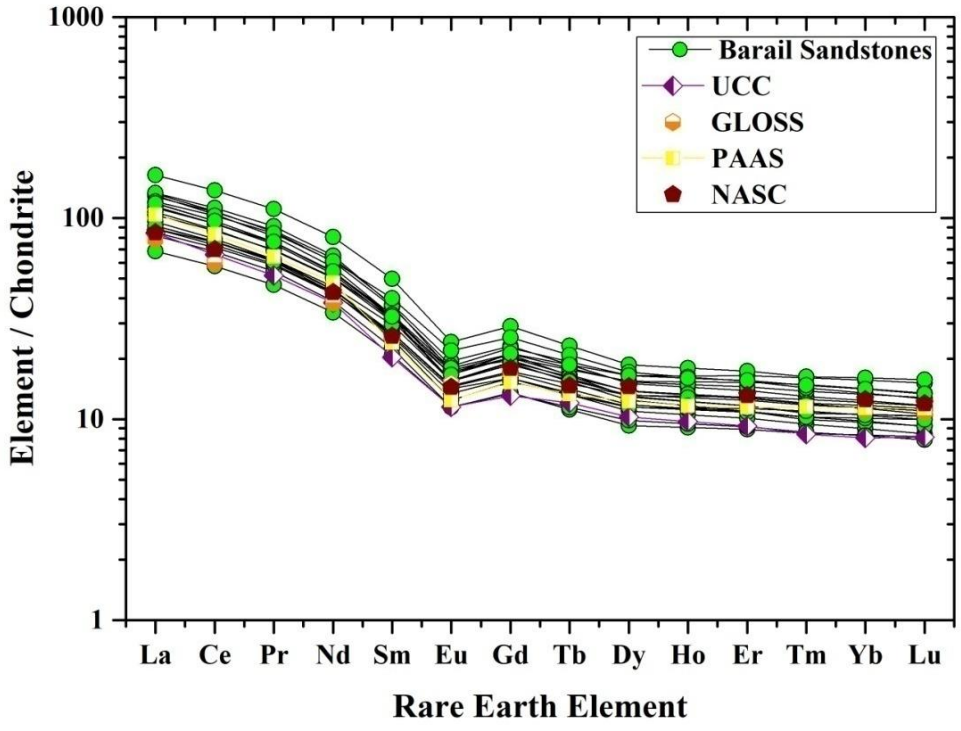

Figure 8.5: Chondrite normalised REE elemental ratio of Barail sandstones, Ngopa, Mizoram, (Chondrite values after Taylor and McLennan., 1985).

The value of (La/Yb)N is ranging from 7.56 to 12.62 (avg=9.40) which is lower than the referred standard. According to the HREE pattern, ratio of (Gd/Yb) N ranges between 1.43-1.98 (on average 1.66) which indicates a depleted source. The ratio of LREE/HREE or (La/Lu)N spans between 7.98 to 12.91 (avg. = 9.80), exhibiting a higher ratio as compared to UCC values, which suggested that there is significant fractionation in the studied sandstone. This led us to believe that, based on the REE ratio and chondrite normalised pattern, the investigated sandstone is primarily generated from fractionated felsic to intermediate source rock such as granitoids, (Slack and Stevens., 1994).

8.3. CLASSIFICATION

The categorization of a certain area's sandstone is established by geochemical analyses utilising the main oxide content. Pettijohn et al. (1972), Blatt *et al.* (1980), and Herron (1988) are only a few of the researchers who developed several geochemical classification schemes for sandstone utilising key elements. In order to categorise sandstone into six types, Pettijohn *et al*. (1972) used the logarithm values of the ratio of SiO_2/Al_2O_3 against logarithm value of Na_2O/K_2O. These types included quartz arenite, sublitharenite, arkose, litharenite, and greywacke. The majority of the samples on this plot fall into the Arkose & litharenite classifications. (Figure 8.6). Herron (1988) modify Pettijohn's classification approach by substituting the log ratios of SiO_2/Al_2O_3 and Fe_2O_3/K_2O for Na_2O/K_2O.

The samples of sandstone that came from this classification plot were dispersed throughout litharenite and arkose. Figure 8.7 also demonstrates how majority of the sandstones are found in Herron's Fe-sandstone (1988). The geochemical data, namely the weight percentages of Na_2O, (Fe_2O_3+ MgO), and K_2O, were once more used in Blatt *et al* (1980)'s classification system. He divided sandstone into three types: lithic, arkose, and greywacke. The plot pattern reveals that all of the analysed samples are contained in “lithic sandstone” classification region. (Figure 8.8).

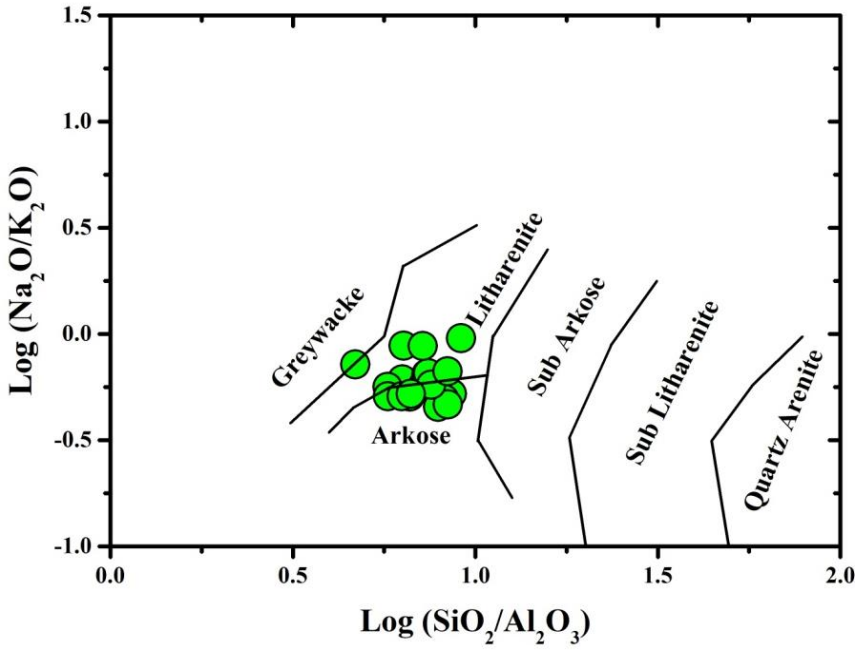

Figure 8.6: Log(SiO_2/ Al_2O_3) vs Log(Na_2O_3/K_2O) classification of Barail sandstones, Ngopa area, Mizoram (Pettijohn *et al.*,1972).

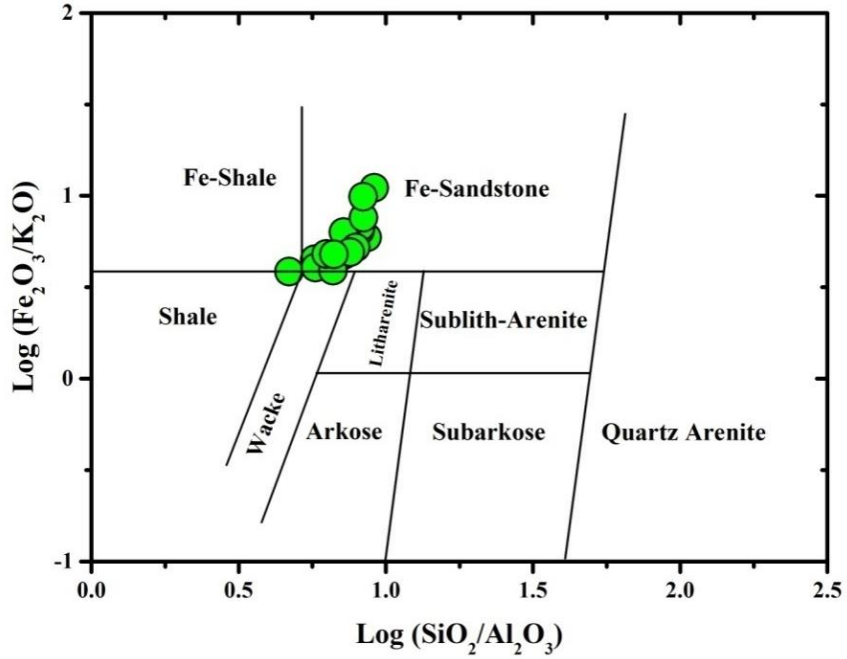

Figure 8.7: Log(SiO_2/Al_2O_3) vs Log(Fe_2O_3/K_2O) classification scheme of Barail sandstones, Ngopa, Mizoram (after Herron, 1988).

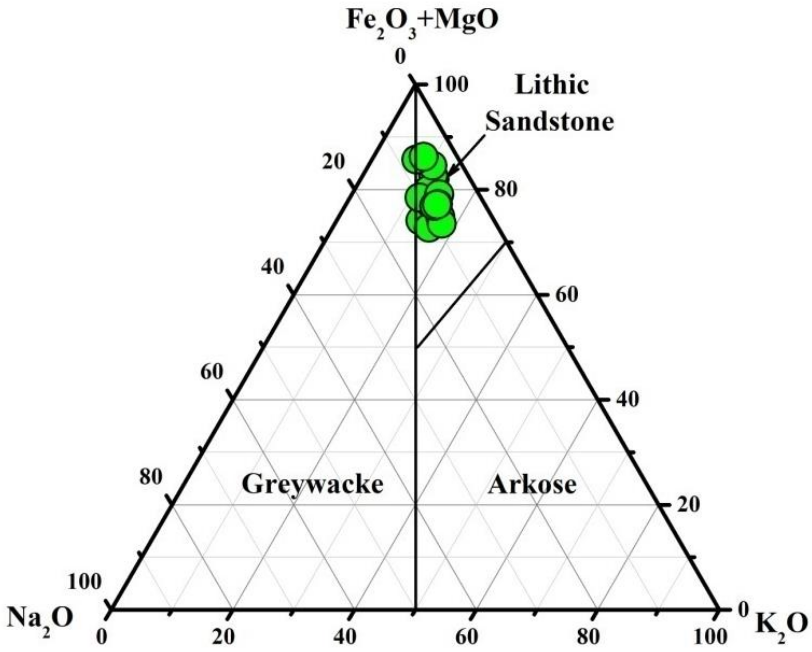

Figure 8.8: Na_2O - (Fe_2O_3+ MgO) - K_2O classification scheme of Barail sandstones, Ngopa, Mizoram (after Blatt *et al.*, 1980).

8.4. PROVENANCE STUDY

The geochemical composition of clastic sedimentary rock is controlled by the source rock's characteristics, transportation, the depositional environment, and the post-depositional environment (such as diagenesis and hydrothermal alteration). Therefore, geochemical analyses offer the most precise method for identifying the type of source rock. Due to their chemical and mineralogical makeup, provenance investigations based on geochemical composition have lately gained popularity in addition to petrographic research. Major oxide concentrations are used to deduce provenance, although, due to their mobility during weathering and alteration, they sometimes don't generate the precise outcomes that are expected. In order to determine the provenance and tectonic settings, the most immobile components, such as trace elements and REE, are therefore used (Bhatia, 1983; Taylor and McLennan, 1985; McLennan *et al*., 1993).

To assess provenance and weathering condition, incompatible elements including Cr, Co, Ni, and V are typically employed (Feng and Kerrich., 1990). The immobility of the high field strength elements Zr, Nb, Th, U, and Y acts as a marker for the composition of the source rock (Taylor and McLennan, 1985). Additionally, the nature of the research area's source rock can be deduced from the elemental ratios of compatible and incompatible elements like Zr/Sc, La/Sc, Th/Sc, and Th/Co.

The various geochemical data are graphically represented in this study using various geochemical plots developed by various researchers, including Bhatia (1983), Roser and Korsch (1988), Floyd *et al*. (1989), Hayashi *et al*. (1997), Bracciali *et al*. (2007), Jinliang and Xin (2008), Schoenborn and Fedo (2011), Mongelli *et al*. (2006), and McLennan *et al*. (1993).

Major oxides including CaO, Na_2O, and K_2O were used in a ternary plot created by Bhatia (1983) to determine the origin of the sediments under study. Different fields on the Na_2O-CaO-K_2O ternary plot denote diverse source rocks, including andesite, dacite, granodiorite, and granite. The majority of the samples from the examined sandstones were scattered throughout the Granite field, according to plotting results, indicating that they originated from granitic sources. (Figure 8.9). This can be the result of CaO concentration in Barail sediments being reduced or less abundance.

To determine the provenance, Roser and Korsch (1988) suggested a discriminant function diagram that was used to plot the major oxide concentration of Barail sandstones. They divided the binary plot into four categories: quartzose sedimentary provenance, intermediate igneous, felsic igneous, and mafic igneous. Most of the Barail sandstones found on the site are of Mafic igneous origin (Figure 8.11). The provenance of clastic deposits has been determined using incompatible and stationary elements like Ni, V, and Th. A provenance system was proposed by Bracialli *et al*. The V-Ni-Th x 10 ternary plot and the several source fields were arranged in various areas based on their abundances. While Th elements are typically prevalent in felsic rock and V elements are commonly found in mafic rocks, ultra mafic rocks tend to have a comparatively high concentration of Ni elements. According to the discriminant V-Ni-Th x10 plot, the studied samples are particularly rich in Th, while the other two elements, V and Ni, are rather low.

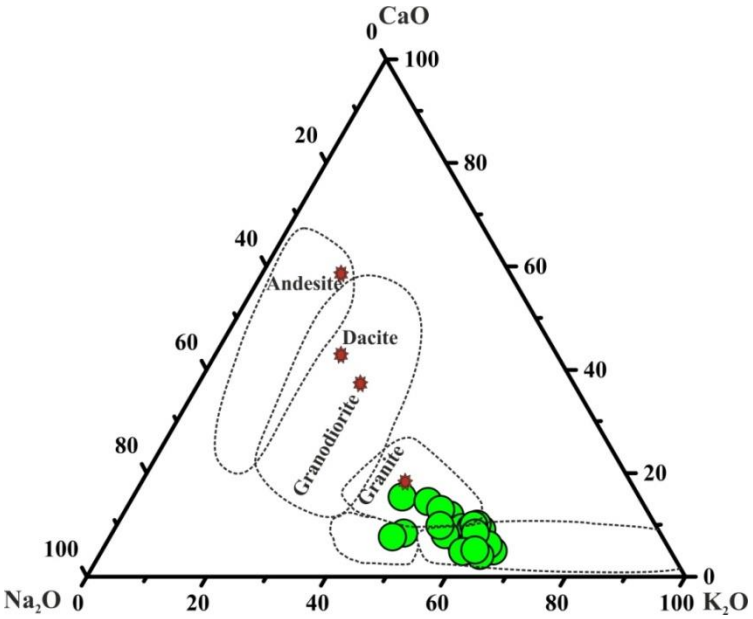

Figure 8.9. Na_2O-CaO-K_2O ternary provenance plot of Barail sandstones, Ngopa area, Mizoram (after Bhatia, 1983).

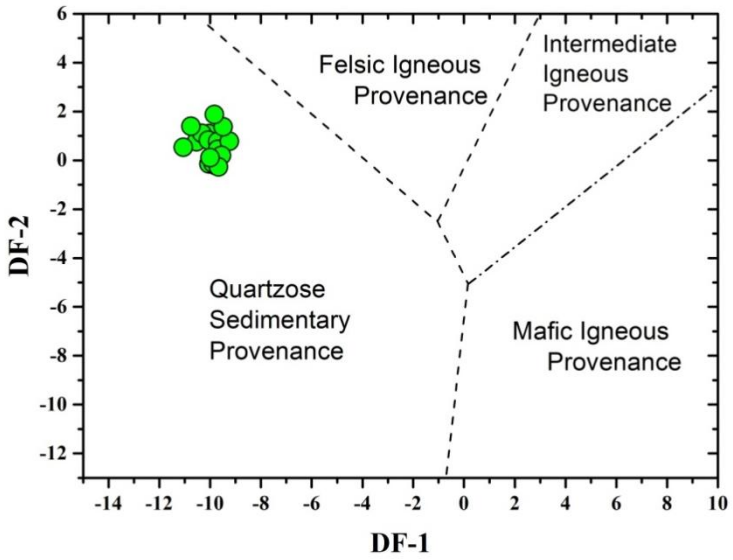

Figure 8.10: Discriminant function diagram for the provenance signatures of Barail sandstones, Ngopa, Mizoram (after Roser and Korsch, 1988).

To ascertain the origin of the investigated Barail sandstones, Floyd *et al*. (1989's binary TiO_2 vs. Ni plot) was also used. Although some of the sample is spread out outside of the region, the majority of it falls in the field of the acidic

source. The plot, however, suggests that the studied samples were derived from felsic source was derived in connection to a characteristic of the magmatogenic greywacke. (Figure 8.12).

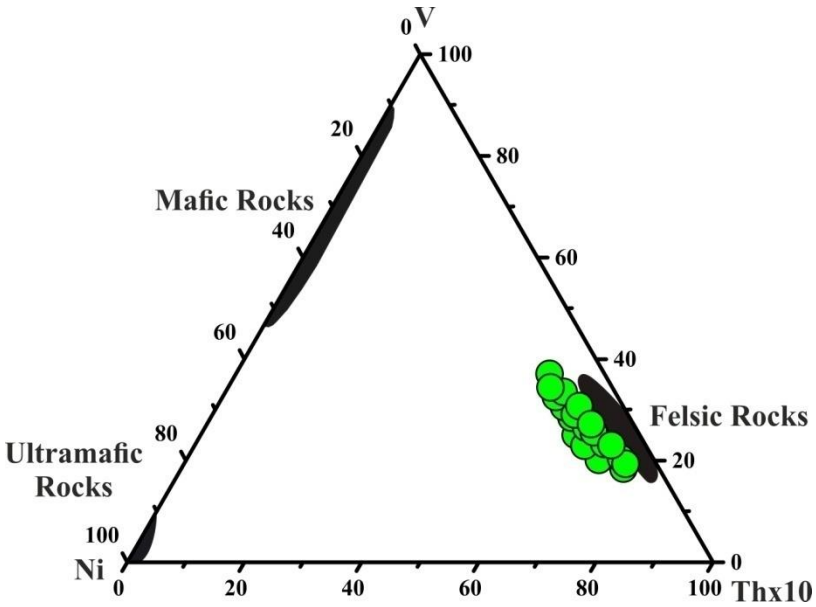

Figure 8.11: Ternary diagram of V-Ni-Th*10 for provenance determination of Barail sandstones, Ngopa, Mizoram (after Bracciali *et al.*, 2007).

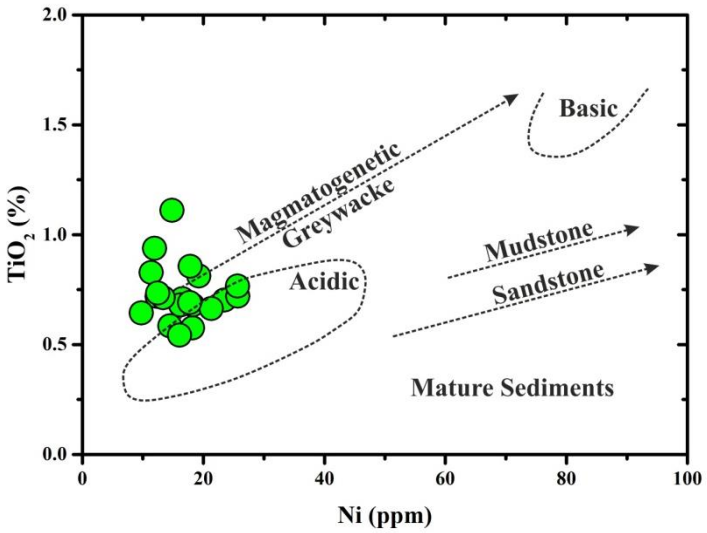

Figure 8.12: Binary diagram of Ni vs TiO_2 for provenance determination of Barail sandstones, Ngopa area, Mizorm (after Floyd *et al.*, 1989).

A provenance binary diagram is represented by Hayashi *et al*. (1997) using the main oxide TiO_2 and the trace element Zr. The ratio of TiO_2/Zr falls as SiO_2 concentration rises, and it should be noted that mafic source rock has a ratio of > 200, intermediate source rock has a ratio of 195-55, and felsic source rock has a ratio of 55. In general, Barail sandstones have very low TiO_2/Zr ratios (avg= 0.003). As a result, the plot shows that the sandstone is entirely concentrated inside the field of Felsic/Acidic igneous rocks (except for one sample which falls just inside Intermediate igneous rock) indicating that the Barail sandstones' origin is felsic igneous (Figure 8.13).

Jinliang and Xin (2008) presented a provenance ternary diagram of La-Th-Sc using data on trace elements, where the two main source rocks are the intermixing of granite (with Eu/Eu*: 0.5 and Th/Sc: 1.18) and granodiorite (with Eu/Eu*: 0.7 and Th/Sc: 0.5). Following the ternary plot, the sandstones samples clustered up toward the region of granite from granodiorite as a result of La's enrichment (Figure 8.14). We can draw the conclusion that the analysed sandstones from Ngopa area are likely to have originated from granitic source rock based on their average Eu/Eu* and Th/Sc values of 0.64 and 0.75 respectively.

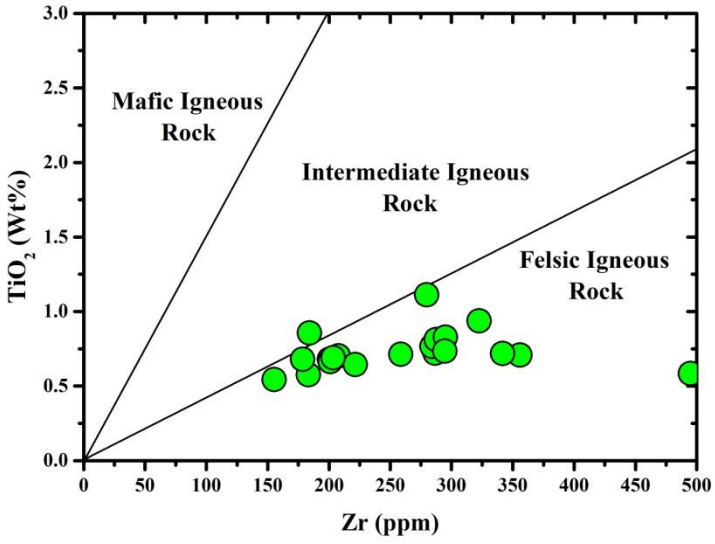

Figure 8.13: Zr vs TiO_2 binary plot for Barail sandstones, Ngopa area, Mizoram (after Hayashi *et al.*, 1997).

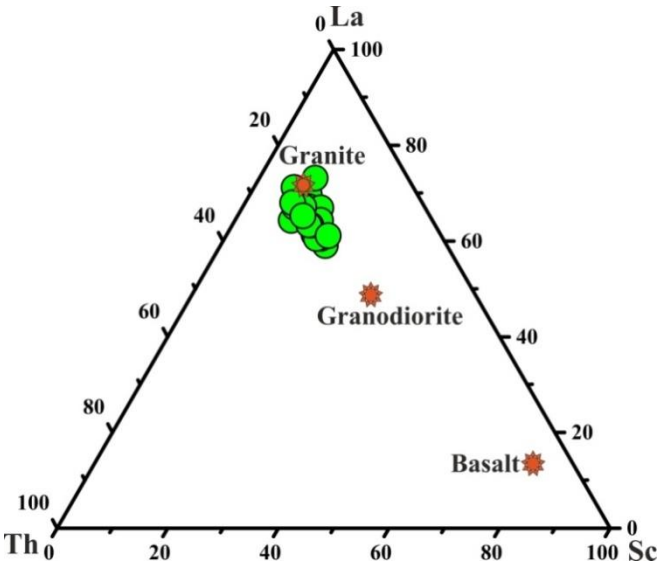

Figure 8.14. Triangular diagram of La-Th-Sc indicating the mixing of various source sediments for Barail sandstones, Ngopa area, Mizoram (after Jinliang and Xin, 2008).

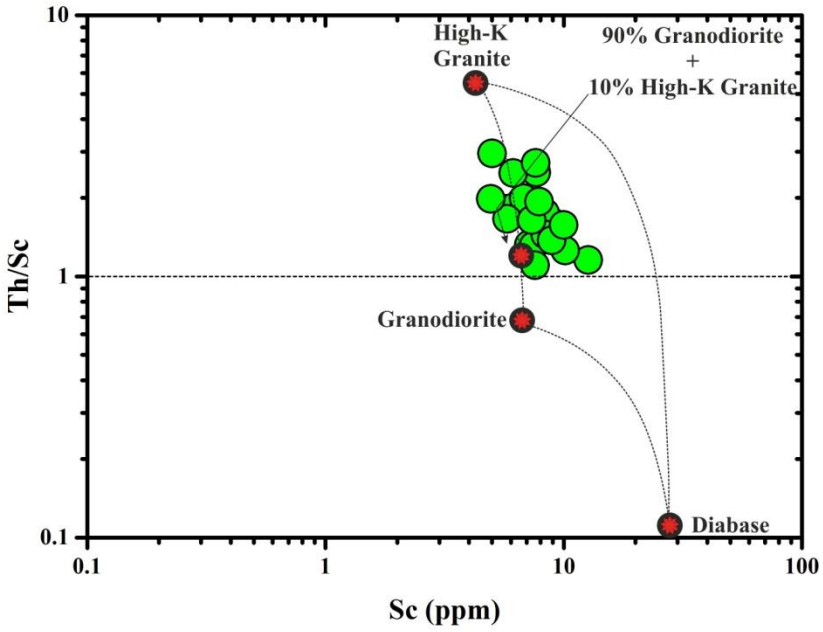

Figure 8.15: Binary diagram of Sc vs Th/Sc for Barail sandstones fom Ngopa area, representing mixing of source rocks (after Schoenborn and Fedo, 2011).

The binary plot of Sc vs Th/Sc following Schoenborn and Fedo (2011) is frequently used to quantify the source rock estimation. Figure 8.15 depicts the plotted samples of Barail sandstones, all of which are dispersed throughout the designated source area. The samples gathered close to a field of 90% granodiorite and 10% High-K granite. It suggests that the sandstones of the study area are derived from granodiorite and granite source rocks. It proves that K-feldspar has undergone higher enrichment than plagioclase feldspar, which is also corroborated by petrography.

Mongelli *et al*. (2006) proposed a binary mixing model curve between granite and ultramafic end member using the ratio of Y/Ni versus Cr/V to represent a mixing source of an area. The source rock was derived from granitic terrain as indicated by the ratio of Cr/V, which is quite low (average = 1.39). The binary mixing curve figure reveals that portion of the ultramafic source area's sandstone fallout was concentrated towards the granite's apex (Figure 8.16).

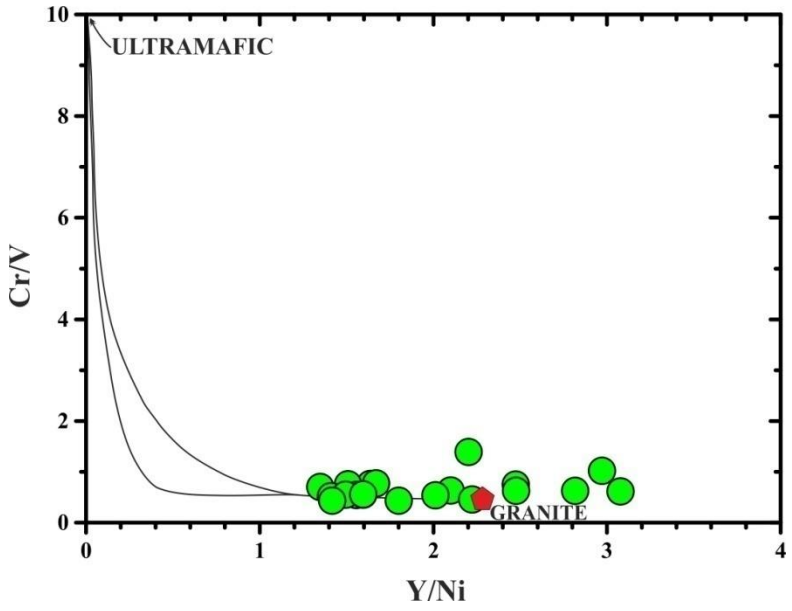

Figure 8.16. Granite-Ultramafic end member mixing binary plot of Y/Ni vs Cr/V (after Mongelli *et al.,* 2006).

To ascertain the compositional variation of the source rock and sedimentation processes, McLennan *et al*. (1993) proposed a binary plot of a trace element, specifically Th/Sc and Zr/Sc ratio. Two lines make up the discriminant binary plot of Th/Sc versus Zr/Sc, with the straight line representing the original source rock's composition and the skewed line indicating the effects of the source due to sedimentary processes, like sediment recycling, which show an enrichment of heavy minerals like zircon. According to the plot created, every sediment sample followed the pattern of compositional variation, with the majority of the samples deviating in favour of the sediment recycling trend. (Fig. 8.17). This implies that the sandstone was formed from felsic parent rock as a result of sediment recycling activities. Mobile alkali elements leaching and a concentration of heavy minerals like zircon cause sediments to change during movement. Additionally, zircon is the second-most prevalent heavy mineral according to the ZTR index from the Heavy minerals study and has a considerably high geochemical concentration (average 494.96). Based on the binary diagram, concentration of detrital zircon, as well as heavy mineral studies, it is assumed that the studied sandstones originated from sediment recycling provenance.

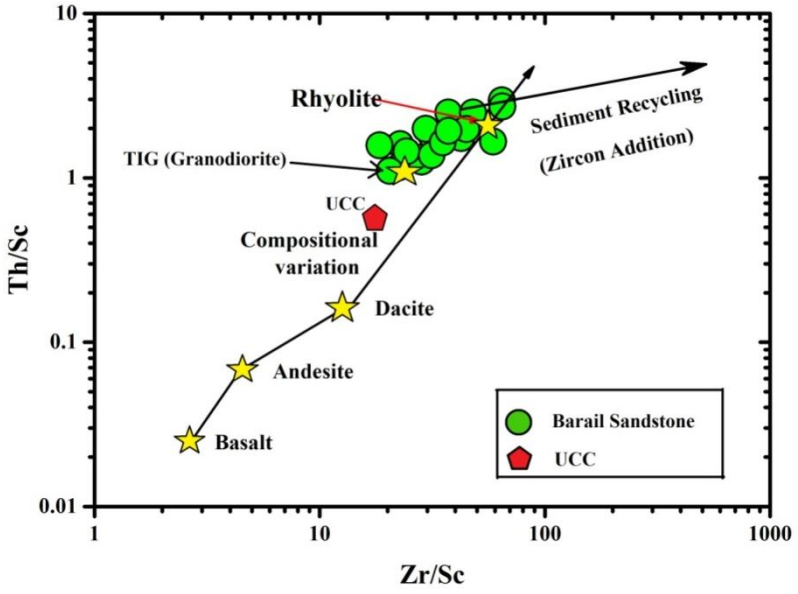

Figure 8.17. Binary plot Zr/Sc vs Th/Sc representing the original source composition along with extent of sediment recycling (after McLennan *et al.,* 1993).

Trace elements and REE are frequently employed to establish the provenance of clastic sedimentary rocks due to their resistance to sedimentation. Many researchers try to predict the source rock by evaluating the elemental ratios in a specific area to the average value of the trace and REE ratio. Table 8.4 shows the value of different standard elemental ratio proposed by Cullers (1994, 2000) and Cullers and Podkovyrov (2000) which is the elemental ratio of trace and REE for comparison. The elemental ratio ranges of the analysed sandstones (La/Lu: 7.98-12.91, La/Sc: 3.11-9.78, La/Co: 2.68-6.64, Th/Sc: 1.78-1.10, Th/Co: 1.00-2.19, and Cr/Th: 1.50-2.66) show sediments derived mostly from felsic source rocks. A basic igneous source rocks are suggested by the predominance of incompatible ferromagnesian elements as Ni, Cr, V, and Sc. Basic igneous source rocks are indicated by the prevalence of incompatible ferromagnesian elements such as Ni, Cr, V, and Sc.

A mafic source is indicated by an Al_2O_3/TiO_2 ratio greater than 8, an Al_2O_3/TiO_2 ratio between 8 and 21 indicates an intermediate igneous source rock, and an $Al2O_3/TiO_2$ ratio greater than 21 indicates a felsic igneous source rock, according to Hayashi *et al*. (1997). As a result, the Barail sandstones have an average Al_2O_3/TiO_2 ratio of 14.56, which points to an intermediate igneous parent rock.

A clue for determining the nature and sorts of source rocks is provided by the chondrite normalised REE pattern and Eu anomaly (Basu *et al*., 1975; Armstrong-Altrin, 2009). According to Cullers (1994, 2000), greater LREE/HREE ratios with negative Eu anomalies are indicative of felsic source rock, whereas lower LREE/HREE ratios are indicative of mafic source rock. The Barail sandstones' comparatively high LREE/HREE ratio, which displays a negative anomaly and indicates to a felsic source rock, indicates this. The Chondrite normalised REE plot reveals a higher concentration of LREE and a lower concentration of HREE. As a result, the high LREE/HREE ratio points to granitoids as the source of the Barail sandstones. The K enrichment is consistent with the negative Eu anomaly's post-Archaean source. The ratio of (La/Lu)N, which varies from 7.98 to 12.91 (average 9.80), represents the fractionation of the sediments that results in the enrichment of K. Reduced Sr composition implies that fractionation of Ca-rich plagioclase is the reason of the negative Eu anomaly (avgerage 50.76).

The sediments were primarily transported from the uplifted and worn (eroded) Himalayan crystalline felsic terrain, with some sediments (deposition) from the Indo-Burmese Arc, according to the plotting and observations indicated above.

8.5. PALEOWEATHERING

The nature of alkali and alkaline earth elements, such as Ca^{2+}, Na^{+}, and K^{+}, can be used to determine the weathering condition of siliciclastic deposits (Nesbitt and Young, 1982). Weathering causes the chemical composition or components to degrade or change, which leads to the creation of clay minerals. Thus, a key tool for assessing the weathering state of the original source location is the geochemical signature that leaves an imprint in every sediment cycle (Nesbitt and Young, 1982; McLennan *et al*., 1993; Fedo *et al*., 1995). Using geochemical data, the weathering indices provided by various researchers are used to assess the paleoclimatic condition. The chosen chemical indices are Weathering Index of Parker (WIP, Parker 1970), Chemical Index of Alteration (CIA, Nesbitt and Young, 1982), Plagioclase Index of Alteration (PIA, Fedo *et al*., 1995), Chemical Index of Weathering (CIW, Harnois, 1988), and Index of Chemical Variation. These indices are based on the molecular proportion of mobile and immobile elements (Na_2O, CaO, K_2O (ICV, Cox *et al*., 1995). Following is the mathematical derivation, where CaO* denotes the amount of calcium integrated into the silicate-bearing material, # denotes using molecular proportions.

$$\text{“}\mathbf{CIA}^{\#} = \left[\frac{\mathbf{Al_2O_3}}{\mathbf{Al_2O_3 + CaO^{*} + Na_2O + K_2O}}\right] \times 100$$

$$\mathbf{PIA}^{\#} = \left[\frac{\mathbf{Al_2O_3 - K_2O}}{\mathbf{Al_2O_3 + CaO^{*} + Na_2O - K_2O}}\right] \times 100$$

$$\mathbf{CIW}^{\#} = \left[\frac{\mathbf{Al_2O_3}}{\mathbf{Al_2O_3 + CaO^{*} + Na_2O}}\right] \times 100$$

$$\mathbf{CIW}^{\#} = \left[\left(\mathbf{2}\,\frac{\mathbf{Na_2O}}{\mathbf{0.35}}\right) + \left(\frac{\mathbf{MgO}}{\mathbf{0.9}}\right) + \left(\mathbf{2}\,\frac{\mathbf{K_2O}}{\mathbf{0.25}}\right) + \left(\frac{\mathbf{CaO^{*}}}{\mathbf{0.7}}\right)\right] \times 100$$

$$\mathbf{ICV}^{\#} = \left[\frac{\mathbf{Fe_2O_3 + K_2O + Na_2O + CaO^{*} + MgO + MnO + TiO_2}}{\mathbf{Al_2O_3}}\right] \times 100\text{”}$$

Table 8.5 compares the calculated values of several weathering indices with the standard GSR (GSR 4-Chinese Sandstone Standard from Xeujing *et al*., 2007) and UCC. These indices include CIA, PIA, CIW, WIP, and ICV (Upper continental crust from Rudnick and Gao, 2003). Since CIA values between 76 and 100 indicate a strong and intense degree of weathering, while values below 50 indicate almost no chemical alterations and reflect the source area's unweather condition (Nesbitt and Young, 1982; Fedo *et al*., 1995). Table 8.5 shows that the chemical index of alteration for the Barail sandstones from Ngopa area ranges from 63.45 to 76.08, with average of 70.87 that is more than the UCC value (50.17). This suggests that the source location has undergone moderate weathering. Additionally, the moderate CIA value and the negative Eu anomaly point to the possible presence of some nearby source sediment that has undergone moderate to rapid mechanical weathering and lower concentrations of alkali-bearing minerals. Additionally, it shows quick sedimentation with limited transit and poor source sediment sorting (Camire *et al*., 1993). The Barail sandstones are thought to have originated in the Himalayan mountains and were transported by the paleo-Brahmaputra with juvenile contributions from the Indo-Burmese arc, Naga Hills, etc (Najman *et al*., 2008; Bracciali *et al*., 2015; Govin *et al*., 2018; Hussain and Bharali, 2019). According to Nesbitt and Young (1982), a ternary diagram of the CIA vs. A-CN-K diagram utilising Al_2O_3-(CaO+Na_2O) -K_2O is used to represent the weight percentage of main elements such as Na_2O, CaO, K_2O, and Al_2O_3. The observation shows that the samples were dispersed along the trend of the A-CN line and dropped very high, reaching over 70% Al_2O_3 (CIA avg = 70.87), which implied moderate chemical weathering. When components like CaO and Na_2O completely leach, there is intense weathering and the trend shifts toward the A-K line, suggesting K enrichment.

As the leaching of alkali elements increased, the majority of the sandstone samples aligned themselves closer to the A-K line in the A-CN-K diagram (Figure 8.18). K is still being removed, and trends are still pointing in the direction of the intense weathering zone of Al_2O_3 (CIA =70.87). Extreme weathering, on the other hand, resulted in the complete loss of K, and the trend was in the direction of the Al_2O_3 apex. The elimination of potassium may take place because K-metasomatism reflects the concentration of K. Additionally, K-rich pore fluids may be the cause of

the enrichment, and as K is added, the trend will go toward the K apex. Plagioclase may turn into K-feldspar or clay minerals as a result of K enrichment that might happen during the metasomatism process.

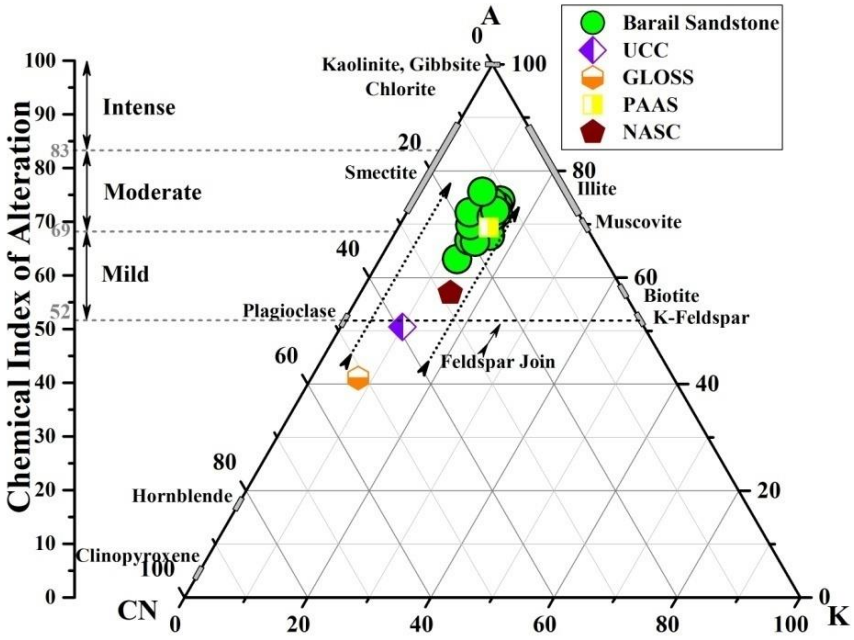

Figure 8.18. A ternary A-CN-K diagram of Barail sandstones from Ngopa area representing a moderate to intense weathering of source rocks (after Nesbitt and Young, 1984, 1989)

Remobilization of K during sedimentary and metamorphic processes is considered and plotted by the CIA. The Chemical Index of Weathering (CIW), which uses weight percentage of alkalis other than K_2O to prevent K-metasomatism, has been utilised to reduce this significant shortage. During sedimentation, K is frequently enriched or leached from the weathering products. Furthermore, the interaction of K+ ions with pore solution may be the cause of the creation of minerals containing K. Clay minerals instead of Na+ and Ca+ are formed as a result of this high exchange capability (Kroonenberg, 1992; Harnois, 1988). The removal of Na

and Ca increases the value of CIW for Al. The Barail sandstones exhibit high CIW, higher than UCC (average = 81.85) (Table 8.5).

The PIA (Plagioclase index of Alteration), developed by Fedo *et al*., is another geochemical weathering indicator used to gauge the degree of source rock weathering (1995). The ternary diagram of AK-C-N following Fedo *et al*. (1995) was plotted using the weight percentage of alkalis (Figure 8.19). The maximum value of PIA represents the total weathering of gibbsite, kaolinite, etc., and increases as the degree of weathering increases (i.e 100). Additionally, the unweathered plagioclase is represented by the PIA values of 50. The Barail sandstones in the study area have PIA values that are greater than UCC values, ranging from 67.96-84.02 (average 78.53). It implies that there has been significant weathering of plagioclase in the research area.

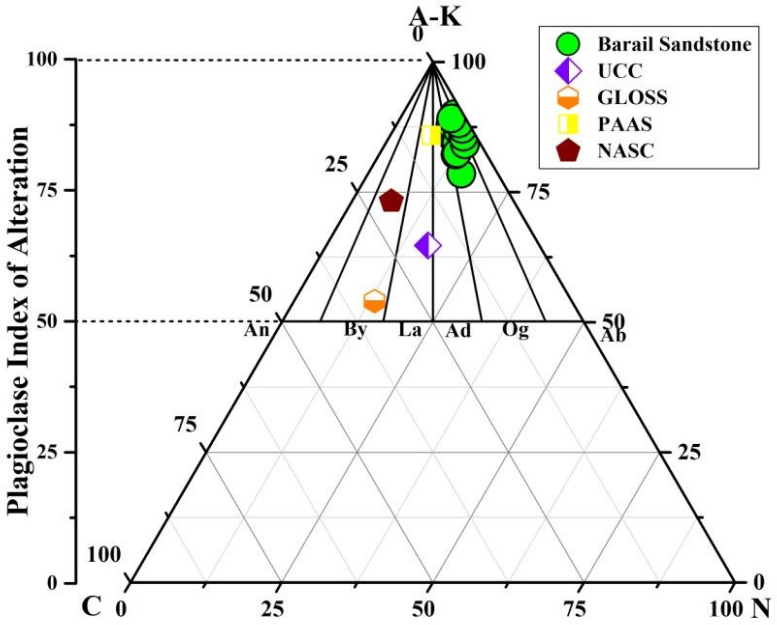

Figure 8.19. Ternary AK-C-N plot of Barail sandstones, Ngopa, Mizoram (Fedo *et al.*, 1995).

The first Chemical Weathering Index was proposed by Parker in 1930 (WIP-Weathering Index of Parker). Instead of Si, he used most mobile alkali and alkaline earth metals such as Ca, K, Mg and Na. But, while Si tends to be mobile, these elements were removed during hydrolysis. Due to irregular movement, amount of leaching decreases. Also, Due to the mobile alkaline earth elements as well as alkali

present, they will generally produce WIP values greater than zero. So, it shows that these elements play vital role in determining the values of WIP. The WIP value of the analysed Barail sandstones ranges from 18.38-43.68, with an average of 27.87, indicating a low weathered source rock (Table 8.5)

Based on the amount of Al_2O_3, the Index of Chemical Variation (ICV) developed by Cox *et al*. (1995) is used to distinguish between clay and non-clay minerals. The abundance of alumina in relation to other main cations is determined by this parameter. The low amount of Al_2O_3 in the non-clay minerals suggests an increase in ICV value. This demonstrates that minerals other than clay have high ICV values. As a result, sandstone samples with ICV values greater than 1 are indicative of immature sediments that contain a significant amount of non-clay minerals. It suggests that tectonically active environments experience sediment recycling. Additionally, strata with lesser ICV values suggest mature sediments with a significant concentration of clay minerals, which then suggests an environmentally calm and stable craton. The transformation of feldspar into clay minerals containing aluminium is mostly to blame for the decline in ICV value. According to Cox *et al*. (1995), feldspar, muscovite, and illite are represented by an ICV range between 0.6 and 1.0. The Barail sandstones from Ngopa area, which represent compositionally mature sediments, have ICV values ranging from 1.15 to 1.91, with an average of 1.44. (Table 8.5). The high values of the SiO_2/Al_2O_3 ratio suggested that sandstones were mature mineralogically (Potter, 1978). The investigated sandstone's SiO_2/Al_2O_3 ratio ranges from 4.69 to 9.14 (average = 7.20), indicating that it is immature or gradually becoming mature (Roser *et al*., 1996). Feldspar is represented by a K_2O/Al_2O ratio of 0.3 to 1.0, while clay minerals are indicated by a range of 0.0 to 0.3. The research area's Barail sandstones have a K_2O/Al_2O_3 ratio that varies from 0.13 to 0.21 having an average value 0.18. Due to this, there is less feldspar, muscovite, and glauconite concentration in the investigated sandstone, which is also supported by petrographic studies.

Long *et al*. (2012) developed a binary plot of CIA vs ICV to assess the maturity and type of weathering of clastic sedimentary rocks (Figure 8.20). According to the binary plot of CIA vs ICV, all of the samples fall into the category of Immature - weak to moderate weathering conditions and all of them have an ICV

value more than 1 and a high CIA value (average 70.87), which show that the sediments are chemically immature.

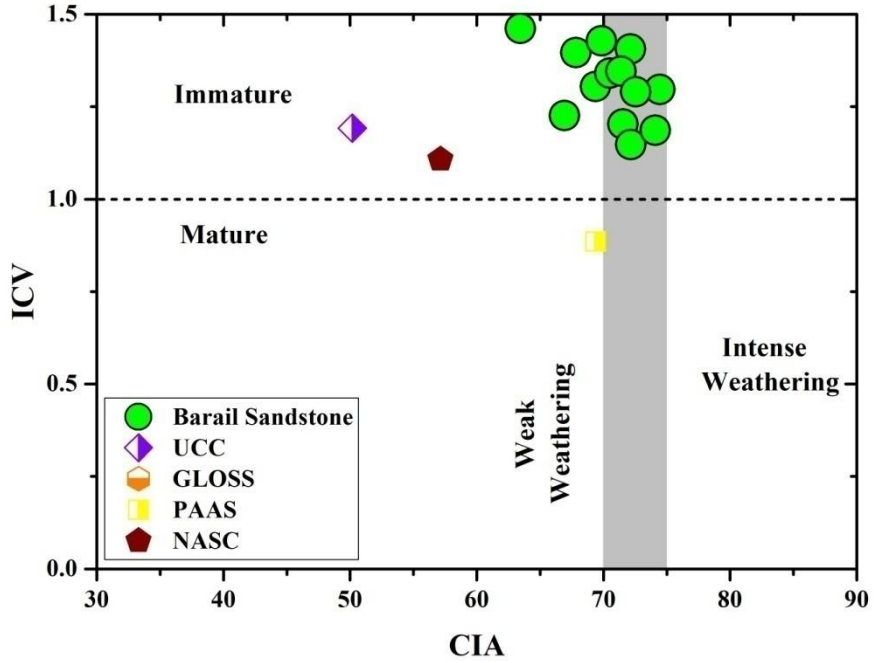

Figure 8.20: CIA vs ICV binary plot of Barail sandstones, Ngopa area, Mizoram representing maturity and intensity of weathering of the source rock (after Long *et al*., 2012).

A binary plot of Th vs Th/U was proposed by Mc Lennan *et al*. (1993) to illustrate the degree of weathering that occurs in sediments. The Th/U ratio in the upper crust sediments ranges from 3.5 to 4.0, and exceeding this number will indicate a weathering tendency (Mc Lennan *et al*., 1993). The average Th/U ratio for Barail sandstones is 6.82, which is greater than the UCC value (3.89). The samples' proximity to the upper crust region and the fact that they are all above it show that the studied sediments have weathered at moderate rate. (Figure 8.21).

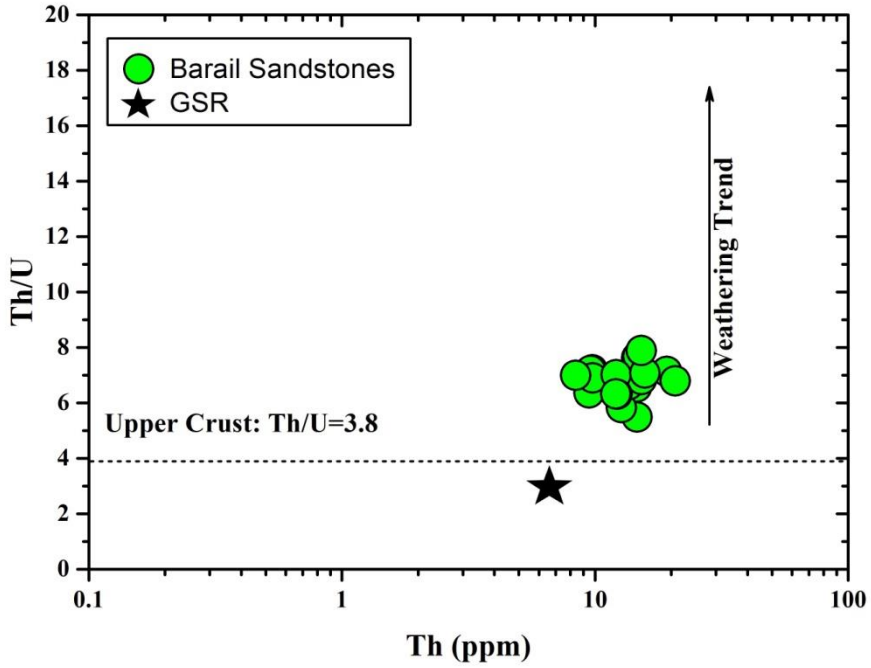

Figure 8.21. Discriminant binary diagram of Th vs Th/U plot of Barail sandstones from Ngopa area, Mizoram (McLennan *et al.*, 1993).

Additionally, compared to Rb components, the Sr element leaches more during diagenesis and weathering. As a result, a rock's weathering condition is significantly influenced by the Rb/Sr ratio. The high weathering is shown by the high Rb/Sr ratio. The average Rb/Sr ratio of the Barail sandstones is 1.23, which is greater than the UCC standard (0.26). According to the results of several weathering indices and element abundances, the removal of significant oxides, such as CaO followed by Na_2O, MgO, and K_2O has been observed. Barail sandstones have undergone moderate to severe weathering, according to the Th/U and Rb/Sr value ratios. Therefore, it can be said that the analysed sandstone from the research region has endured moderate to intense conditions of weathering..

8.6. TECTONIC SETTINGS

One of the most important factors in understanding the tectonic setting of siliciclastic sedimentary rocks is the geochemical investigation. Several researchers have presented a variety of theories to infer ancient tectonic settings based on the geochemical composition of clastic deposits. The selected major elemental

discrimination plots employed in this research study are (Fe_2O_3+MgO) Vs Al_2O_3/SiO_2 proposed by Bhatia (1983), (Fe_2O_3+MgO) Vs TiO_2 (Bhatia, 1983) and the binary discriminant function plot of DF1 Vs DF2 after Bhatia (1983), where:

DF-1: (0.0447× SiO_2)-(0.972× TiO_2)+ (0.008× Al_2O_3)-(0.267× Fe_2O_3)+(0.208×FeO)
(3.082×MnO) + (0.14×MgO)+ (0.195×CaO)+(0.719×Na_2O)
(0.032×K_2O) + (7.51×P_2O_5)+ 0.303

DF-2: (-0.421× SiO_2) + (1.988× TiO_2)(0.526× Al_2O_3)-(0.551× Fe_2O_3)
(1.61×FeO)+ (2.72×MnO)+ (0.881×MgO)
(0.907×CaO)- (0.177×Na_2O)- (1.84× K_2O)+(7.244× P_2O_5)+43.57]

Also, a tectonic setting discrimination plot makes use of some immobile trace components. La/Sc Vs Ti/Zr after Bhatia and Crook (1986) and the Ternary plot of La-Th-Sc after Bhatia (1983) were chosen as the discrimination diagrams for the current study.

The major elemental discrimination plots of (Fe_2O_3+MgO) vs. Al_2O_3/SiO_2, according to Bhatia (1983), are connected to a variety of tectonic fields, including the Continental Island Arc (CIA), Active Continental Margin (ACM), Passive Margin (PM), and Oceanic Island Arc (OIA). He proposed that "The active continental margin sandstone deposits have lower values of Fe_2O_3+MgO (2-5 wt%), and higher value of K_2O/Na_2O (≈1), suggesting that the sediments in are originated from felsic sources (granite, gneisses etc.)". From the observations, the Barail sandstones from the study area shows Fe_2O_3+MgO (avg. 10.48 wt%), Al_2O_3/SiO_2 (average 0.14), and K_2O/Na_2O (Average 2.11) they are almost identical to those proposed by Bhatia. Almost all of the samples are clustered outside of the Continental Island Arc & Oceanic Island Arc, and only a small number of samples fall within the OIA and CIA region, as per the binary diagram plot of "Fe_2O_3+MgO with Al_2O_3/SiO_2 and TiO_2". This may be related to an increase in Fe_2O_3+MgO value (Figure 8.22 & 8.23). This suggests that the Barail sediments contain remnants of basement mafic components.

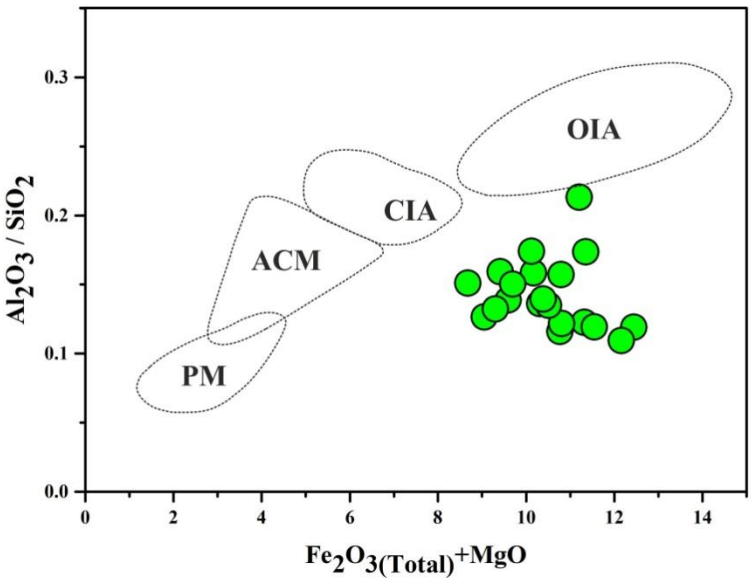

Figure 8.22. Fe_2O_3+MgO vs Al_2O_3/SiO_2 tectonic discrimination diagram of Barail sandstones, Ngopa area, Mizoram (after Bhatia, 1983).

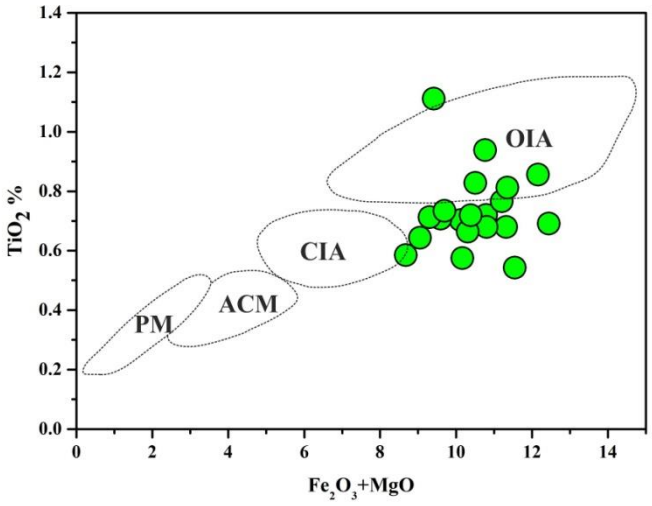

Figure 8.23. Tectonic discrimination diagram of Fe_2O_3+MgO vs TiO_2 of Barail sandstones, Ngopa area, Mizoram (after Bhatia, 1983).

When the computed discriminant functions, DF1 and DF2 established by Bhatia (1983). (Figure 8.24) is employed to plot the binary discriminant function diagram, itsuggests that the examined Barail sandstones scattered inside the field of

Oceanic Active Continental margin which reveal that they are derived from the Active Continental Margin.

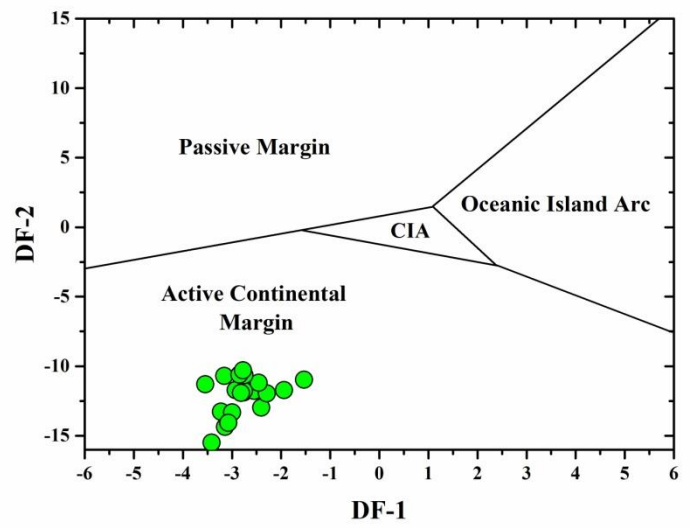

Figure 8.24. Tectonic discrimination plot of Barail sandstones, Ngopa area, Mizoram. (Bhatia, 1983).

In accordance with the La-Th-Sc ternary diagram (Figure 8.25) all of the sandstone samples gathered around the Active Continental Margin (C) and Continental Island Arc (B). Bhatia and Crook (1986) proposed that the sandstone deposited at the Continental margin should have a La/Sc ratio of 4, and that it should be settled towards the peak of La. The Barail sandstones from Ngopa area have nearly the same value as that predicted by Bhatia and Crook, indicating that they originated from the Continental Island Arc and Active Continental Margin (Figure 8.25). Another parameter to infer the tectonic setting can be seen in the binary plot of La/Sc vs. Ti/Zr (Bhatia and Crook, 1986). Many of the Barail samples are found either in the Active Continental Margin or just outside its margin , whereas only a small number of samples are concentrated in or near the Passive Margin regions (Figure 8.26). We can infer from the geochemical analyses that the Barail sandstones' deposits are found in the Active Continental Margin and Continental Island arc. This statement is also support by Petrography results.

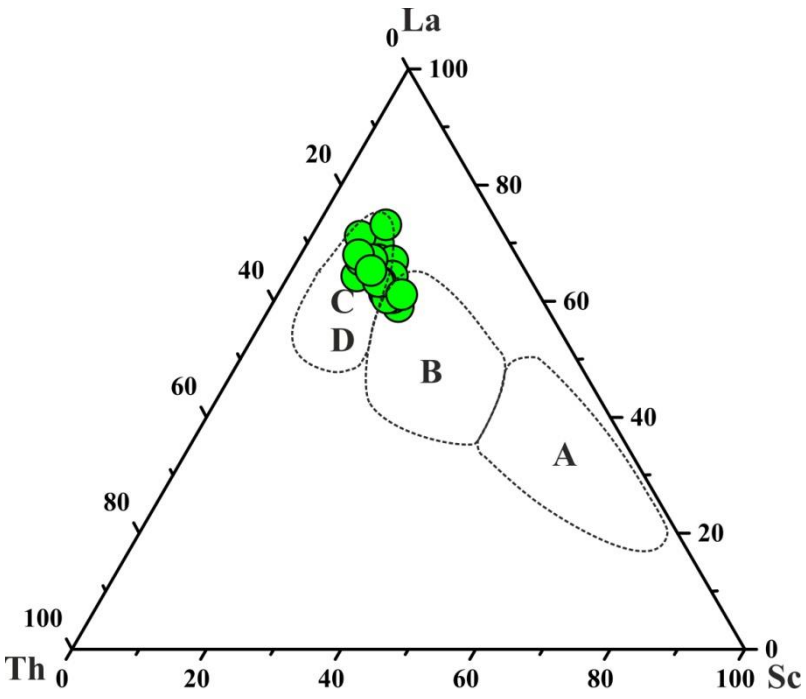

Figure 8.25. La-Th-Sc ternary diagram of Barail sandstones, Ngopa area, Mizoram (after Bhatia and Crook, 1986)

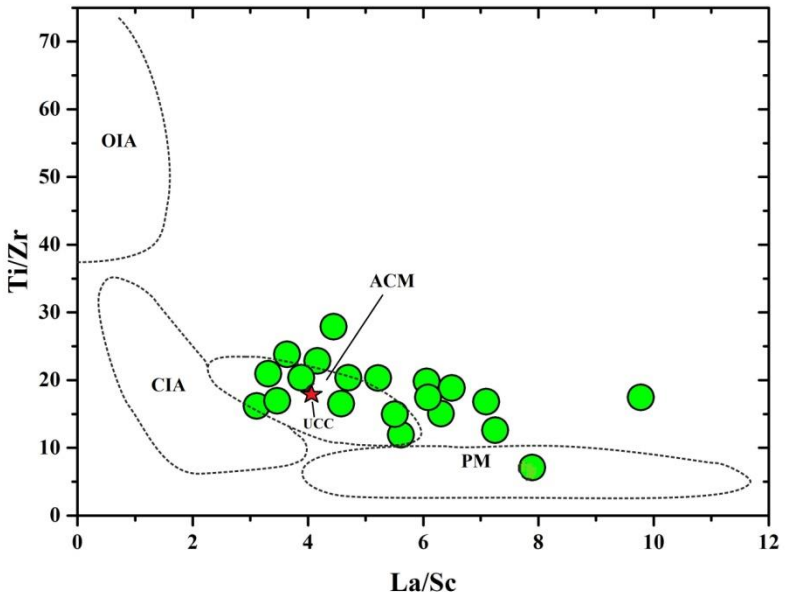

Figure 8.26. La/Sc vs Ti/Zr binary diagram of Barail sandstones, Ngopa area, Mizoram (after Bhatia and Crook, 1986).

8.7 DISCUSSION AND CONCLUSION

According to geochemical analysis, the main oxides concentration in Barail sandstones include SiO_2, which is the highest concentration (64.79-74.56% with an average 71.46%) which is higher than the UCC standard, followed by Al_2O_3 (7.98-13.82%, average 10.14%),Fe_2O (8.09-11.74%, average 9.73) and other minor oxides (Rudnick and Gao, 2003, 2005). The low Al_2O_3/SiO_2 ratio (0.11-0.21%, average = 9.73%) suggests that quartz is enriched in the sandstone (Table 8.1). Al2O3 and K2O have a very strong positive connection (r = 0.84), which points to the occurence of K-bearing minerals. The likelihood of Fe_2O_3 precipitation during diagenesis is demonstrated by the enrichment of Fe_2O_3 concentration (avg = 9.73%).

K-feldspar is somewhat more abundant than plagioclase due to the moderate Na2O value (1.07), and the ratio of Na_2O/K_2O (avg = 0.66) that is less than 1 (i.e $Na_2O/K_2O<1$) (Al-Juboury, 2012). This demonstrates a slightly more abundance of K-feldspar than plagioclase (Al-Juboury 2012). This is also supported by comparable composition to the petrographic finding. The less prevalent CaO value (average 0.29) indicates that Calcic plagioclase was removed considerably during the sedimentation process.

The high concentration of Zircon (average 261.86) indicates an enrichment of zircon grains which statement is also consistent with the heavy mineral assemblages. The existence of clay minerals (kaolinite, illite and biotite) containing K is suggested by the high positive association between K_2O and Rb (r = 87. The presence of organic materials and subsequent mineral production are suggested by the high concentrations of Cr and V.

Light rare earth elements (LREE:La-Sm) are slightly enriched, while heavy rare earth elements (HREE:Gd-Lu) are somewhat depleted, with a little negative Eu anomaly (average of 0.64%) in the REE chondrite normalised pattern. The fractionation HREE of the examined sandstone is represented by the ratio of LREE/HREE, that is, (La/Lu)N, which ranges from 7.98-12.91 having average of 9.80. The Barail sandstones are thought to have originated from a fractionated felsic to intermediate source rock (granitoid) based on the evidence presented above (Slack and Stevens., 1994).

The sandstone of the Barail formation is classified as Litharenite 92%), ar kose (7%) and Greywacke (1%) based on the discrimination plotting of geochemical classification schemes of sandstone developed by Pettijohn *et al*. (1972), Blatt *et al*. (1980), and Herron (1988) using major oxide concentration. The Barail sandstones are thought to have been formed from granitic source rock based on the ternary plot of the three main oxides, Na_2O-CaO- K_2O. According to Roser and Korsch's (1988) discrimination function diagram, the examined sandstone is of Quartzose Sedimentary provenance. According to Bracialli *et al.,* (2007)'s provenance ternary diagram (V-Ni-Thx10), Barail sandstones originated from Felsic source rock. Another bivariant plot of TiO_2 vs. Ni suggests the origin of the examined sediments as Acidic and their connection to the signature of the magmatic source rock. According to the provenance binary diagram plotted by Hayashi *et al*. (1997) utilising the principal oxide TiO_2 and trace elements Zr, almost all of the investigated sandstone clusters in the category of acidic igneous rocks.

The trace element, La-Th-Sc diagram of Barail sandatone using the ternary diagram of Jinliang and Jin (2008) reveals granitic source rock with an average value of Eu/Eu* = 0.64 and Th/Sc = 0.75. The binary plot of Sc vs Th/Sc represents the origin of the intermixed Granodiorite and Granite parent rock of the sediments under study (Schoenborn & Fedo 2011).

When compared to UCC (Rudnick & Gao, 2003, 2005), the various geochemical weathering indices, including Chemical Index of Alteration (CIA) after Nesbitt and Young (1982), Plagioclase Index of Alteration (PIA) after Fedo *et al*., (1995), Chemical Index of Weathering (CIW) after Harnois (1988), and Index of Chemical Variation (ICV) after Cox *et al*., (1995), revealed mild to moderate, immature and weak weathering. As a result, it suggests that the sediments came from a nearby source and were sorted poorly which is a characteristic of short and rapid sedimentation.

The tectonic settings of the Barail sandstones are Active Continental Margin associated with Continental Island Arc setting, according to the various tectonic discrimination diagrams produced by various researchers, such as Fe_2O_3+MgO) Vs Al_2O_3/SiO_2 after Bhatia (1983), (Fe_2O_3+MgO) Vs TiO_2 after Bhatia (1983), Binary Discriminant Function plot after Bhatia (1983),

Table 8.1. Major oxides of Barail Sandstones in terms of wt% and their corresponding elemental ratios (where, GSR-4: Chinese Sandstone Standard from Xenjing *et al*., 2007 and UCC: Upper continental crust from Rudnick and Gao, 2003, 2005).

Litho-Unit	Sample	SiO_2	TiO_2	Al_2O_3	Fe_2O_3	MnO	MgO	CaO	Na_2O	K_2O	P_2O_5
BARAIL SANDSTONES	BNG-1	69.65	0.58	11.04	9.34	0.07	0.83	0.43	1.2	1.96	0.07
	BNG-2	68.86	0.7	11.99	9.31	0.03	0.81	0.34	1.16	2.07	0.09
	BNG-3	72.68	0.71	10.08	9.03	0.03	0.56	0.19	1.1	1.9	0.08
	BNG-4	69.83	0.72	10.97	9.54	0.06	1.25	0.69	1.76	2.01	0.12
	BNG-5	64.79	0.77	13.82	9.41	0.06	1.8	0.71	1.75	2.44	0.14
	BNG-6	72.74	0.94	8.43	10.22	0.05	0.55	0.28	0.9	1.73	0.17
	BNG-7	72.9	0.68	8.93	10.81	0.02	0.51	0.25	0.81	1.68	0.09
	BNG-8	73.51	0.68	8.94	10.26	0.02	0.54	0.26	0.75	1.52	0.08
	BNG-9	68.03	0.81	11.81	10.2	0.11	1.15	0.42	1.28	2.52	0.15
	BNG-10	72.24	0.66	9.84	9.64	0.02	0.68	0.23	1.02	1.58	0.09
	BNG-11	71.83	0.83	9.68	9.84	0.03	0.67	0.46	1.21	1.86	0.16
	BNG-12	71.49	0.72	9.97	9.58	0.02	0.8	0.26	1.33	1.52	0.11
	BNG-13	74.56	0.64	9.43	8.58	0.02	0.47	0.13	0.75	1.65	0.03
	BNG-14	72.52	0.69	8.63	11.74	0.03	0.7	0.15	0.72	1.55	0.07
	BNG-15	72.46	0.59	10.94	8.09	0.03	0.59	0.13	1.05	2.08	0.08
	BNG-16	71.85	1.11	11.44	8.85	0.02	0.56	0.26	0.94	1.84	0.1
	BNG-17	72.88	0.86	7.98	11.51	0.02	0.65	0.17	0.99	1.04	0.12
	BNG-18	72.88	0.71	9.64	8.73	0.01	0.57	0.14	1.02	1.78	0.09
	BNG-19	69.52	0.73	10.44	9.02	0.02	0.68	0.16	0.99	1.89	0.09
	BNG-20	74.01	0.54	8.83	10.94	0.03	0.61	0.2	0.74	1.11	0.1
	GSR-4*	90.33	0.27	3.49	3.21	0.02	0.08	0.38	0.06	0.64	0.25
	UCC	66.6	0.64	15.4	5.04	0.1	2.48	3.59	3.27	2.8	0.15

Cont...

Sample	SiO_2/Al_2O_3	Al_2O_3/TiO_2	K_2O/Al_2O_3	K_2O/Na_2O
BNG-1	35.05	19.19	0.18	1.64
BNG-2	33.78	17.05	0.17	1.78
BNG-3	37.95	14.24	0.19	1.74
BNG-4	35.36	15.24	0.18	1.14
BNG-5	26.05	18.04	0.18	1.39
BNG-6	43.14	8.98	0.2	1.92
BNG-7	42.97	13.13	0.19	2.09
BNG-8	48.37	13.15	0.17	2.03
BNG-9	27.43	14.54	0.21	1.97
BNG-10	45.88	14.81	0.16	1.55
BNG-11	39.06	11.69	0.19	1.53
BNG-12	47.80	13.86	0.15	1.14
BNG-13	46.51	14.64	0.17	2.21
BNG-14	46.68	12.49	0.18	2.15
BNG-15	34.86	18.7	0.19	1.97
BNG-16	39.25	10.3	0.16	1.97
BNG-17	70.25	9.32	0.13	1.05
BNG-18	42.00	13.52	0.18	1.74
BNG-19	36.99	14.23	0.18	1.91
BNG-20	64.47	16.26	0.13	1.5
GSR-4*	143.79	12.88	0.18	9.95
UCC	24.03	24.06	0.18	0.86

Table 8.2. Rare Earth Elements of Barail sandstones from Ngopa areain terms of ppm and their corresponding elemental ratios (where, GSR 4: Chinese Sandstone Standard from Xuejing *et al*., 2007 and UCC: Upper Continental Crust from Rudnick and Gao, 2003, 2005).

Oxides/ Elements	BNG-1	BNG-2	BNG-3	BNG-4	BNG-5	BNG-6	BNG-7	BNG-8	BNG-9	BNG-10	BNG-11
La	38.09	47.60	46.93	48.50	39.38	48.95	33.60	31.11	35.16	41.20	43.54
Ce	82.88	100.11	102.82	103.70	84.03	107.56	73.17	68.49	75.30	90.05	92.74
Pr	9.52	11.13	11.89	11.72	9.47	12.47	8.41	7.95	8.52	10.39	10.44
Nd	36.14	40.57	44.95	43.18	35.72	46.26	31.14	29.88	31.29	38.23	38.27
Sm	7.32	7.57	8.60	8.36	7.08	8.50	6.04	6.20	6.22	7.66	7.34
Eu	1.53	1.49	1.69	1.59	1.45	1.52	1.24	1.26	1.27	1.56	1.35
Gd	6.02	6.18	7.05	6.93	6.20	6.41	4.89	5.20	5.29	6.45	5.88
Tb	0.93	0.96	1.08	1.12	1.02	0.95	0.77	0.82	0.87	1.04	0.94
Dy	4.95	5.24	5.74	6.28	5.87	4.91	4.18	4.49	5.00	5.84	5.28
Ho	1.05	1.12	1.23	1.40	1.30	1.04	0.89	0.96	1.10	1.27	1.13
Er	2.90	3.16	3.46	4.10	3.80	2.89	2.52	2.72	3.21	3.61	3.19
Tm	0.38	0.42	0.46	0.57	0.53	0.38	0.34	0.37	0.45	0.49	0.43
Yb	2.62	2.80	3.07	3.88	3.52	2.62	2.23	2.42	3.00	3.30	2.90
Lu	0.40	0.40	0.45	0.58	0.51	0.39	0.32	0.35	0.44	0.49	0.43
(La/Yb)N	9.81	11.50	10.33	8.45	7.56	12.62	10.20	8.68	7.91	8.43	10.15
(La/Sm)N	3.28	3.96	3.44	3.65	3.50	3.63	3.50	3.16	3.56	3.39	3.73
(Gd/Yb)N	1.86	1.79	1.86	1.45	1.43	1.98	1.78	1.74	1.43	1.58	1.64
Eu/Eu*	0.69	0.65	0.65	0.62	0.65	0.60	0.67	0.66	0.66	0.66	0.61
(La/Lu)N	9.98	12.25	10.93	8.75	7.98	12.91	10.84	9.20	8.23	8.79	10.48

Conti....

Cont. Table 8.2.

Oxides/ Elements	BNG-12	BNG-13	BNG-14	BNG-15	BNG-16	BNG-17	BNG-18	BNG-19	BNG-20	GSR-4 (OV)	UCC
La	42.03	30.07	32.47	60.21	32.41	44.42	33.62	43.43	25.12	20.25	31
Ce	89.95	65.14	72.60	131.77	70.57	98.52	72.80	92.69	55.11	46.44	63
Pr	10.17	7.45	8.55	15.22	8.11	11.52	8.32	10.45	6.38	5.21	7.1
Nd	37.43	27.48	32.47	57.15	30.13	43.43	30.37	38.54	24.13	20.28	27
Sm	7.18	5.23	6.80	11.52	5.97	9.24	5.79	7.48	4.81	4.65	4.7
Eu	1.34	0.99	1.35	2.10	1.17	1.91	1.08	1.45	1.00	0.97	1
Gd	5.71	4.13	5.82	8.86	4.88	7.79	4.70	6.50	4.11	4.50	4
Tb	0.91	0.65	0.89	1.35	0.78	1.21	0.77	1.08	0.67	0.78	0.7
Dy	5.03	3.54	4.74	7.10	4.39	6.53	4.37	6.29	3.76	4.05	3.9
Ho	1.09	0.77	0.99	1.53	0.95	1.38	0.97	1.36	0.81	0.74	0.83
Er	3.09	2.22	2.72	4.31	2.70	3.84	2.82	3.88	2.28	1.96	2.3
Tm	0.42	0.30	0.35	0.58	0.37	0.51	0.39	0.53	0.31	0.32	0.3
Yb	2.83	2.07	2.39	3.98	2.51	3.34	2.60	3.50	2.05	1.96	2
Lu	0.42	0.31	0.35	0.60	0.38	0.48	0.38	0.51	0.30	0.31	0.31
(La/Yb)N	10.04	9.81	9.19	10.23	8.73	8.98	8.75	8.39	8.28	6.99	10.47
(La/Sm)N	3.69	3.62	3.01	3.29	3.42	3.03	3.66	3.66	3.28	2.74	4.15
(Gd/Yb)N	1.64	1.62	1.98	1.81	1.58	1.89	1.47	1.51	1.62	1.86	1.62
Eu/Eu*	0.62	0.63	0.64	0.61	0.64	0.67	0.62	0.62	0.67	0.64	0.69
(La/Lu)N	10.42	10.03	9.56	10.45	8.89	9.59	9.23	8.86	8.68	6.73	10.38

Table 8.3. Trace elements of Barail sandstones, Ngopa area, in terms of ppm with their corresponding elemental ratios (where, GSR-4: Chinese Sandstone Standard from Xeujing *et al*., 2007 and UCC: Upper continental crust from Rudnick and Gao, 2003, 2005)

Oxides/ Elements	BNG-1	BNG-2	BNG-3	BNG-4	BNG-5	BNG-6	BNG-7	BNG-8	BNG-9	BNG-10	BNG-11
Sc	5.86	9.12	8.36	7.69	12.67	5.01	7.15	7.47	10.14	6.80	6.14
V	41.71	67.35	54.67	54.92	101.49	36.06	48.74	55.83	73.80	46.57	42.11
Cr	31.67	47.18	34.36	41.24	52.71	26.96	26.41	30.45	40.49	35.98	26.28
Co	6.15	8.18	6.30	7.42	14.70	4.75	6.57	8.47	11.10	6.97	5.27
Ni	18.19	23.49	16.56	25.68	25.64	11.95	16.24	18.19	19.24	21.30	11.36
Cu	11.10	11.02	8.96	6.77	18.34	13.32	8.19	9.71	12.34	8.99	6.92
Zn	9.74	13.49	9.00	6.78	17.76	6.92	10.74	13.15	9.26	10.27	3.40
Ga	10.43	11.86	10.67	13.50	16.45	9.44	9.17	9.34	13.56	9.22	11.39
Rb	68.39	80.30	74.38	79.87	105.59	53.23	54.06	52.29	80.27	52.28	60.50
Sr	60.35	67.00	52.56	92.37	91.57	38.89	38.90	43.96	56.26	41.88	50.84
Y	29.80	31.69	34.77	38.76	36.18	29.57	25.29	27.20	30.71	35.58	31.99
Zr	183.16	207.74	355.97	286.79	284.13	322.56	200.43	178.54	287.48	201.15	295.06
Nb	10.64	14.21	14.07	14.85	16.61	15.49	12.20	11.88	14.16	11.43	14.96
Cs	3.59	3.28	3.76	4.04	6.01	2.58	2.65	2.27	4.24	3.13	2.82
Ba	361.54	348.76	289.43	317.04	360.41	223.54	242.63	194.37	297.52	289.15	237.21
Hf	5.90	6.42	10.58	9.21	8.91	10.25	6.26	5.51	9.37	9.58	9.83
Ta	0.98	1.40	1.18	1.44	1.53	1.49	1.26	1.04	1.18	1.37	1.38
Pb	9.41	12.77	8.44	9.52	13.11	7.61	6.69	8.34	8.26	10.31	6.20
Th	10.65	14.60	14.61	19.21	14.65	14.80	9.47	9.77	12.73	13.53	15.29
U	1.60	1.91	2.22	2.70	2.67	1.93	1.49	1.36	2.18	2.04	2.24

Cont...

Oxides/ Elements	BNG-12	BNG-13	BNG-14	BNG-15	BNG-16	BNG-17	BNG-18	BNG-19	BNG-20	GSR-4 (OV)	UCC
Sc	5.79	4.94	8.36	7.63	8.91	9.99	7.35	7.89	7.59	5.51	14
V	39.16	32.64	56.90	53.22	60.85	60.27	50.08	49.41	52.42	30.25	97
Cr	24.50	14.71	31.60	54.19	26.17	83.56	26.65	30.23	22.61	18.78	92
Co	5.14	2.92	9.92	4.47	5.54	7.48	4.40	4.39	7.75	5.90	17.3
Ni	12.37	9.73	17.75	14.49	14.84	17.84	13.37	12.43	16.07	15.04	47
Cu	8.04	6.42	13.50	7.10	8.78	10.83	9.09	6.59	12.72	18.61	28
Zn	6.51	5.34	10.47	6.93	9.09	5.12	7.16	6.13	6.31	19.48	67
Ga	10.95	8.90	10.39	11.74	11.33	9.67	9.67	11.17	9.15	6.43	-
Rb	48.90	47.37	52.69	58.35	69.66	35.67	51.30	58.87	41.35	26.88	82
Sr	47.05	34.44	41.09	54.66	46.95	42.15	38.42	42.58	33.18	54.37	320
Y	30.63	21.63	28.35	43.07	26.72	39.29	26.91	38.28	22.80	20.08	21
Zr	341.67	221.49	203.49	494.96	279.86	184.13	258.64	294.56	155.34	199.88	193
Nb	13.03	10.43	12.07	20.21	11.87	13.01	11.86	12.47	9.78	5.47	12
Cs	2.47	2.10	2.54	2.35	2.90	2.52	2.19	2.51	2.01	1.83	
Ba	192.15	150.49	177.57	236.60	231.58	226.78	167.26	251.61	142.96	142.88	628
Hf	10.96	7.23	6.50	15.70	8.58	8.67	8.36	9.38	4.93	6.63	
Ta	1.19	0.89	1.06	1.88	1.01	1.78	1.09	1.18	0.90	0.42	
Pb	5.91	5.91	10.67	22.43	7.76	13.24	12.85	9.92	11.20	7.98	17
Th	9.63	9.79	12.11	20.74	12.24	15.75	12.08	15.25	8.38	7.01	10.5
U	1.34	1.42	1.73	3.06	1.94	2.23	1.91	1.93	1.20	2.14	2.7

Cont.....

Oxides/ Elements	BNG-1	BNG-2	BNG-3	BNG-4	BNG-5	BNG-6	BNG-7	BNG-8	BNG-9	BNG-10	BNG-11
Rb/Sr	1.13	1.20	1.42	0.86	1.15	1.37	1.39	1.19	1.43	1.25	1.19
Y/Ni	1.64	1.35	2.10	1.51	1.41	2.48	1.56	1.50	1.60	1.67	2.82
Co/Th	0.58	0.56	0.43	0.39	1.00	0.32	0.69	0.87	0.87	0.52	0.34
Th/Co	1.73	1.78	2.32	2.59	1.00	3.12	1.44	1.15	1.15	1.94	2.90
Cr/Th	2.97	3.23	2.35	2.15	3.60	1.82	2.79	3.12	3.18	2.66	1.72
Cr/Ni	1.74	2.01	2.08	1.61	2.06	2.26	1.63	1.67	2.10	1.69	2.31
Th/Cr	0.34	0.31	0.43	0.47	0.28	0.55	0.36	0.32	0.31	0.38	0.58
Zr/Cr	5.78	4.40	10.36	6.95	5.39	11.96	7.59	5.86	7.10	5.59	11.23
Th/Sc	1.82	1.60	1.75	2.50	1.16	2.96	1.32	1.31	1.26	1.99	2.49
Zr/Sc	31.25	22.77	42.57	37.31	22.43	64.44	28.04	23.89	28.35	29.59	48.07
Cr/V	0.76	0.70	0.63	0.75	0.52	0.75	0.54	0.55	0.55	0.77	0.62
Cr/Zr	0.17	0.23	0.10	0.14	0.19	0.08	0.13	0.17	0.14	0.18	0.09
Th/U	6.66	7.62	6.57	7.13	5.48	7.69	6.36	7.18	5.83	6.64	6.84

Cont...

Oxides/ Elements	BNG-12	BNG-13	BNG-14	BNG-15	BNG-16	BNG-17	BNG-18	BNG-19	BNG-20	GSR-4 (OV)	UCC
Rb/Sr	1.04	1.38	1.28	1.07	1.48	0.85	1.34	1.38	1.25	0.49	0.26
Y/Ni	2.48	2.22	1.60	2.97	1.80	2.20	2.01	3.08	1.42	1.33	0.45
Co/Th	0.53	0.30	0.82	0.22	0.45	0.47	0.36	0.29	0.93	0.84	1.65
Th/Co	1.87	3.35	1.22	4.64	2.21	2.11	2.75	3.47	1.08	1.19	0.61
Cr/Th	2.55	1.50	2.61	2.61	2.14	5.31	2.21	1.98	2.70	2.68	8.76
Cr/Ni	1.98	1.51	1.78	3.74	1.76	4.69	1.99	2.43	1.41	1.25	1.96
Th/Cr	0.39	0.67	0.38	0.38	0.47	0.19	0.45	0.50	0.37	0.37	0.11
Zr/Cr	13.94	15.05	6.44	9.13	10.69	2.20	9.70	9.74	6.87	10.64	2.10
Th/Sc	1.66	1.98	1.45	2.72	1.37	1.58	1.64	1.93	1.10	1.27	0.75
Zr/Sc	58.96	44.83	24.33	64.87	31.42	18.42	35.19	37.34	20.46	36.30	13.79
Cr/V	0.63	0.45	0.56	1.02	0.43	1.39	0.53	0.61	0.43	0.62	0.95
Cr/Zr	0.07	0.07	0.16	0.11	0.09	0.45	0.10	0.10	0.15	0.09	0.48
Th/U	7.17	6.89	7.01	6.78	6.30	7.07	6.31	7.88	6.99	3.28	3.89

Table 8.4. Trace and REE elemental ratios of Barail sandstones, Ngopa area, Mizoram showing provenance.

Elemental Ratio	Range of Barail Sandstone	Felsic Sources	Mafic Sources	UCC	GLOSS	PAAS	NASC
Eu/Eu*	0.60-0.69	0.32-0.83	0.70-1.02	0.69	0.71	0.63	0.65
La/Lu	6.72-12.91	3.00-27.0	1.10-7.00	10.38	7.24	9.22	7.08
La/Sc	3.11-9.78	0.70-27.7	0.40-1.1	2.21	2.2	2.39	2.09
La/Co	2.68-13.47	1.4-22.4	0.14-0.38	1.79	1.31	1.66	1.21
Th/Sc	1.10-2.96	0.64-18.1	0.05-0.4	0.75	0.53	0.91	0.8
Th/Co	0.99-4.64	0.30-7.5	0.04-1.40	0.6	0.31	0.63	0.46
Cr/Th	1.50-5.30	4.00-15.0	25-500	8.76	11.42	7.53	10.41
Th/Cr	0.19-0.66	0.06-4.0	0.002-0.045	0.11	0.09	0.13	0.1

Index of Table 8.4

Felsic Sources	Cullers (1994, 2000); Cullers & Podkovyrov (2000)
Mafic Sources	
UCC	Upper continental crust from Rudnick and Gao, 2003, 2005*
GLOSS	Global Subducting Sediment from Plank and Langmuir, 1998
PAAS	Post-Archean Australian Shales, from Taylor and McLennan, 1985
NASC	North American Shale Composite from Gromet *et al*., 1984

Table 8.5. Geochemical weathering parameters of Barail sandstones, Ngopa area, Mizoram.

Sample No.	CIA[1]	PIA[2]	CIW[3]	WIP[4]	ICV[5]
BNG-1	69.39	76.46	80.09	31.08	1.30
BNG-2	71.55	79.42	82.59	31.38	1.20
BNG-3	70.52	78.82	82.39	28.31	1.34
BNG-4	63.45	67.96	72.56	38.50	1.46
BNG-5	66.94	72.78	76.78	43.68	1.23
BNG-6	68.64	76.79	80.96	25.18	1.74
BNG-7	71.27	79.98	83.38	23.76	1.65
BNG-8	72.76	81.09	84.02	21.99	1.57
BNG-9	67.83	75.98	80.45	37.47	1.40
BNG-10	72.13	79.52	82.45	25.24	1.41
BNG-11	66.70	73.10	77.42	29.95	1.54
BNG-12	69.84	75.77	78.92	28.01	1.43
BNG-13	74.45	84.02	86.63	22.46	1.30
BNG-14	73.36	82.66	85.54	22.11	1.80
BNG-15	72.16	81.50	84.72	29.30	1.15
BNG-16	74.11	82.50	85.09	26.47	1.19
BNG-17	72.24	77.94	80.44	20.19	1.91
BNG-18	71.39	79.90	83.24	26.46	1.35
BNG-19	72.54	81.48	84.54	27.40	1.29
BNG-20	76.08	82.86	84.83	18.38	1.60
Average	70.87	78.53	81.85	27.87	1.44
[6]GSR-4	73.26	82.58	85.48	6.83	1.28
[7]UCC	50.17	50.22	55.81	69.91	1.19

Index:

[1]Chemical Index of Alteration after Nesbitt and Young, 1982

[2]Physical Index of Alteration after Fedo *et al.*, 1995

[3]Chemical Index of Weathering after Harnois, 1988

[4]Weathering Index of Parker after Parker, 1970

[5]Index of Chemical Variability after Cox *et al.*, 1995

CHAPTER 9
SUMMARY

Sedimentological research is an emerging geological research since recent years in Mizoram. This is due to the fact that Mizoram remains geologically unexplored for long time. The first important work covering the entire region was published by the Geological Survey of India in its Miscellaneous Publication No. 30 in which Mizoram is part of that report. However, that publication is generalized in the sense that no detail work was reported in terms of detailed local geology and the sedimentological aspects on origin of the entire sedimentary profiles.

The study area of Ngopa and its surrounding villages are located in the north eastern part of Mizoram in Saitual District bordering Manipur to the north and Burma to the east. The entire study area constitutes part of the Oligocene Barail Group of rocks found in Mizoram. The purpose of the study is to understand "the depositional history, tectonic setting and provenance and the paleo-weathering history of Barail sandstones exposed in the study area". The selected sites of study are located between Tuiphal river to Kawlbem village which traverse through Ngopa village. The areas fall in Survey of India Toposheet No.84E/1 and No.84E/2 which are geographically situated between 23°80'90''N, 93°16'09''E and 23°87'18''N, 93º16'09''E.

During field work, it was observed that the areas are constituted by varying thicknesses of "sandstone, siltstone and shale". The shales are hard but brittle, fragile and crumpled type whereas the sandstones are tough and highly compact with buff colour. The sandstones are "very fine to fine-grained". The thin section studies reealed that the buff colourations are caused by "ferruginous matrix and cementation" as well as high content of biotite and Fe-oxide detrital grains which may induce high leaching of iron into Fe-rich fluids and matrixes giving reddish-brown colour to the rocks. The rocks are most fossil barren except common preservation of burrows in some of the sandstone beds which in return suggested shallow depositional environment. Sedimentary

structures like “sandstone lenses, ball and pillow structures, load structures, rain drop structures, ripped-up clasts and ripple marks” are observed.

The petrographic studies indicate high concentrations of Quartz and Rock fragments in the sandstone samples. Based on the microscopic analysis, majority of the Barail sandstones are classified into Sublitharenite (93%). The geochemistry based classification also indicates the sandstones to be mainly of Litharenite (92%) and a few as Fe-Sandstone and Lithic sandstones. Based on petrography, the analysed Barail sandstones from Ngopa and its adjoining areas are found to be derived from Quartzose Recycled Orogen, Active Continental Margin, Island Arcs or Continental Island Arcs. The qualitative and quantitative data of the sandstones like the nature and characteristics of detrital grains present are utilized for provenance analysis. The useful tools for such inferences include undulatory and non-undulatory quartz, monocrystalline and polcrystalline quartz. The common occurrence of these grains in the studied rocks suggested that they might be derived from “plutonic and “metamorphic source”. Another useful tool is the common occurrence of perthite in the rocks which suggest the source to be likely of granite or pegmatite. The provenance analysis using diamond diagram plots of different polycrystallinity of quartz which confirmed that the Barail sandstones were derived from low-rank metamorphic rocks and granitic rocks.

The investigated Barail sandstones are also rich in heavy mineral populations. The indentified minerals include “Zircon, Tourmaline, Rutile, Garnet, Apatite, Chlorite, Monazite, Epidote, Chloritoid, Enstatite, Diopsite, Augite, Kyanite, Clinozoisite, Hypersthene, Staurolite, Silliminite, Zoisite, Muscovite and Opaque minerals”. Occurrence of Tourmaline, Zircon and Rutile indicates that the sediments are originated from “acidic igneous source”. While the occurrence of “rounded zircon, tourmaline, and rutile support long transportation or derivation from recycled sedimentary rock, and euhedral zircon and tourmaline grains indicate short distance of transportation”. The presence of heavy minerals like “Zircon, Tourmaline, Apatite, Enstatite, Diopsite, Augite, Hypersthene and Monazite” also suggested that they are derived from “basic and

acidic igneous rocks". The heavy minerals like Rutile, Chlorite, Garnet, Epidote, Kyanite, Chloritoid, Clinozoisite, Staurolite, Sillimanite, Zoisite and Muscovite suggested derivation from "low to medium and intermediate to high grade metamorphic rocks".

Based on the general petrographic analysis, heavy mineral assemblages and the ZTR maturity index, it was found that the Barail sandstones of Ngopa area are derived from mixed sources and they are derived from sub-mature sediments. Majority of the sample showed derivation from "metamorphic and igneous sources".

The degree of weathering in the source area has a significant impact on the diversity and amount of alkali and alkaline earth elements in terrigenous rocks. Weathering Index of Parker (WIP) after Parker (1970), Chemical Index of Alteration (CIA) after Nesbitt and Young (1982), Plagioclase Index of Alteration (PIA) after Fedo *et al.,* (1995), Chemical Index of Weathering (CIW) aftern Harnois (1998) and Index of Chemical Variability (ICV) after Cox *et al.* (1995) are employed for the chemical weathering indices of the investigated sandstones. Based on CIA values, the sandstone samples from Ngopa areas show moderate intensity of source area weathering. Moreover, the moderate CIA value and the negative Eu anomaly suggest to the likely presence of nearby source sediment that has experienced moderate weathering and rapid sedimentation which results in poor sorting and lesser amounts of alkali-bearing materials. The Barail sandstones from the study area show high CIW value (average = 81.85), higher than that of UCC value. The high CIW value shows a "moderate to high nature of paleoweathering condition". The PIA value of the samples are higher than that of UCC value (average = 78.53) which indicated that there was significant intensity of Plagioclase weathering in the source area. The WIP values are also indicating average value of 27.87, which was indication of low weathering of the source rock. A binary plot "Th versus Th/U" (Fig. 8.21) shows that the samples were falling just above the margin of UCC boundary which indicated low to moderate weathering. From petrography, a triangular plots of QFR for climatic conditions (Fig. 6.5) showed provenance of metamorphic (humid) and binary plot of (Q_{Total}/F+RF) versus (Q_P/F+RF) (Fig. 6.6)

indicated semi-humid climatic condition. A Weathering Index after Weltje, Grantham and Velbel (Fig. 6.7) suggested "moderate (hill) relief under sub-humid climatic condition".

A provenance diamond plot of monocrystalline and polycrystalline Quartz showed that the Barail sandstones are derived from "low rank metamorphic and Granitic source rocks". Both the undulatory Monocrystalline and non-undulatory quartz observed in the sample indicated metamorphic and plutonic source respectively. The occurrence of perthite also indicated granitic or pragmatic sources.

The light rare earth elements (LREE: La-Sm) were somewhat enriched whereas heavy rare earth elements (HREE: minimal Eu anomaly) were slightly depleted in the chondrite-normalized REE pattern (HREE: Gd-Lu). The (La/Lu)N ratio, also known as the LREE/HREE ratio indicated an average value of 9.80 (Table 8.4). This led us to believe that the studied sandstones were primarily derived from fractionated felsic to intermediate source rock such as granitoids (Slack and Stevens, 1994). The Barail sandstones were thought to have come from a variety of sources, ranging from "recycled sedimentary terrain to Granitic felsic sources (acidic region)", as indicated by various plots of geochemical data on provenance.

Grain size analysis was also employed to assess the size distribution and depositional environment of Barail sandstones in the study area. It can be interpreted from the Histogram and frequency distribution curves that the analyzed Barail sandstones were derived from "mixed environment of marine and fluvial environment where marine processes dominate the fluvial processes". It can be concluded from the log-probability curve that sorting was good in saltation population, fair in rolling and sliding population and poor in suspension populations. Statistical parameters of Grain size such as "inclusive graphic mean, inclusive graphic standard deviation, inclusive graphic skewness and kurtosis" showed that the Barail sandstones of the study area were poorly sorted fine grained sand.

A scattered bivariate plots like "Inclusive Graphic Mean size (M_z) vs Inclusive Graphic Skewness (S_k), Inclusive Graphic Skewness (S_k) vs Kurtosis (K_G),

Inclusive Graphic Skewness (S_k) vs Graphic Mean size (M_z)", etc., showed that the Barail sediments from Ngopa areas were "moderate to poorly sorted, fine to very fined grained" sediments deposited in "mixed environments of shallow marine, beach environment under influence of river action". Linear discriminant value of Y1&Y2 showed beach deposition and shallow marine deposits whereas Y3 value showed majority of the samples being deposited under fluvial environment. Y4 value showed that the sediments of the study areas were transported by turbidity current. Y1 vs Y2 plot suggested beach/shallow agitated environment of deposition and Y2 vs Y3 suggested fluvial/agitated and according to Y3 vs Y4 plot, the sediments were deposited by fluvial/turbidity currents.

CHAPTER 10
CONCLUSION

On the basis of various analyses using different proxies, the following conclusions can be enumerated with reference to the objectives of the present research work.

1. The sandstones are fine to very fine grained, poor to moderately sorted and mostly buff in colour. The lithological column of the study area indicated that the sedimentary profile of the study area is of normal grading with fining upward direction.
2. The systematic classification of the sandstones indicated that majority of the sandstones are litharenite followed by arkose, Fe-sandstones and wacke.
3. The paleoweathering history of the Barail sandstones was found out to be moderate to intensive weathering phenomena. The environment of deposition varies from fluviatile to beach and shallow marine environment. The paleoenvironment was also determined to be of humid climate.
4. The tectonic settings of the sandstone were inferred to be Active Continental Margin, Quartzose Recycled or Recycled Orogen, Continental Island Arc and Ocean Island Arc.
5. The lithological provenance of Barail sandstones have wide spectrum of sources which include acidic to mafic igneous rock, low rank to high rank metamorphic rocks and recycled sedimentary rocks.

FUTURE WORK

The present investigation targets at various sedimentological history of Barail sandstones from its classification to paleoweathering phenomenon, depositional environments, lithological provenance and tectonic settings. There are different scopes of study that may be carried out in the region. The following are few of the future works

that may be of significance in the context of complete documentation of geological history of the study area:

1. Geochronological investigation by isotope dating of the common heavy minerals such as zircon.
2. Studies on geodynamic evolution of the region with emphasis on Indo-Burmese tectonic history by detail analysis of surface and sub-surface structures.
3. Paleontological studies in terms of ichnology may also have good scope in this particular region of Ngopa and adjoining areas since there are common preservations of ichno-fossils in the areas where no works were recorded.
4. Hydrogeology, environmental studies, geotechnical investigation of landslides, morphotectonic analysis, etc. are also important research that may be taken up in future.

REFERENCES

Al-Juboury, A. (2012). A combine petrological-Geochemical study of the Paleozoic successions of Iraq. *Petrology- New Perspectives and Application.* 169-198.

Ali, S., Statteger, K., Garbe-Schonberg, D., Frank, M., Kraft, S. and Kuhnt, W., (2014). The provenance of Cretaceous sediments in the Tarfaya basin, SW Morocco: evidence from trace element geochemistry and radiogenic Nd-Sr isotopes. *J. Afr. Earth Sci.* **90**: 64-76.

Armstrong-Altrin, J. S. (2009). Provenance of sands from Cazones, Acapulco, and Bahı´a Kino beaches, Mexico. *Revista Mexicana de Ciencias Geolo ´gicas.* **26(3)**: 764-782.

Armstrong-Altrin, J. S., Nagarajan, R., Madhavaraju, J., Rosalez-Hoz, L., Lee, Y. I., Balaram, V., Cruz-Martinez, A. and Avila-Ramirez, G. (2013). Geochemistry of the Jurassic and Upper Cretaceous shales from the Molango Region, Hidalgo, Eastern Mexico: implications of source-area weathering, provenance, and tectonic setting. *C R Geosci*. **345**: 185-202.

Andel, V. (1950). Provenance, transport and deposition of Rhine sediments. Ph.D. thesis. Univ. Groningen.

Ashutosh, S. (2019). India State of Forest Report 2019. *Forest Survey of India.* **1(16).**

Babeesh, C., Achyuthan, H. and Sajeesh, T. P. (2018). Geochemical Signatures of Karlad Lake Sediments, North Kerala: Source Area Weathering and Provenance. *Jour. Geol. Soc. India*. **92**: 177-186.

Baruah, H., Lahkar, A. D., Bhagabati, B., Kar, R. and Das, P. K. (2017). Geochemistry of Tikak Parbat Sandstones and Tipam Sandstones Occurring in and around Dilli Area, Sivasagar District, Assam, India. *Open Journal of Geology*. **7**: 1238-1267.

Basu, A., Young, S., Suttner, L., James, W. and Mack, G. H. (1975). Re-evaluation of the use of undulatory extinction and crystallinity in detrital quartz for provenance interpretation. *J. Sediment. Petrol*. **45**: 873-882.

Behra, U. K., Mohanty, B. K., Lahiri, S., Ray, J. N., Gupta, G. D., Prakash, H. S. M. and Kesari, G. K. (2011). Geology and mineral resources of Manipur, Mizoram, Nagaland and Tripura. *Geol. Surv. India Misc. Pub.* No. **30(4) 1(2)**, 103.

Bhatia, M. R. (1983). Plate tectonics and geochemical composition of sandstones. *J. Geol*. **91**: 611-627.

Bhatia, M. R. (1985). Rare earth element geochemistry of Australian Paleozoic graywackes and mudrocks: Provenance and tectonic controls. *Sediment. Geol*. **45**: 97-113.

Bhatia, M. R. and Crook, K.A.W. (1986). Trace element characteristics of graywackes and tectonic setting discrimination of sedimentary basins. *Contrib Mineral. Petrol*. **92**: 181-193.

Bhuiyan, M. A. H., Rahman, M. J. J., Samuel, B. D. and Suzuki, S. (2011). Provenance, tectonic settings and source weathering of modern fluvial sediments of the Brahmaputra- Jamuna river, Bangladesh: Inference from Geochemistry. *J. Geochem. Explor*. **111**: 113-137.

Bharali, B., Borgohain, P., Bezbaruah, D., Vanthangliana, V., Phukan, P. P. and Rakshit, R. (2017). A geological study on Upper Bhuban Formation in parts of Surma Basin, Aizawl, Mizoram. *Sci. Vis.* **17(3)**: 128-147.

Blatt, H., Middleton, G. V. and Murray, R. C. (1980). "Origin of Sedimentary Rocks. Second Edition. *Prentice Hall, Englewood Cliffs, New Jersey*, 782p.

Blatt, H. (1967). Provenance determinations and recycling of sediments. *J. Sediment. Res*. **37**: 1031-1044.

Boggs, S. (2009). Petrology of Sedimentary Rocks. *Cambridge*, UK, 600p.

Bracciali, L., Marroni, M., Pandolfi, L. and Rocchi, S. (2007). Geochemistry and petrography of Western Tethys Cretaceous sedimentary covers (Corsica and Northern Apennines): from source areas to configuration of margins. In: Arribas J, Critelli S, Johnsson M J (eds) Sedimentary provenance and petrogenesis: perspectives from petrography and geochemistry. *Geol. Soc. Am. Spec. Pap*. **420**: 73-93.

Bracciali, L., Najman, Y., Parrish, R. R., Akhter, S. H. and Millar, I. (2015). The Brahmaputra tale of tectonics and erosion: Early Miocene river capture in the Eastern Himalaya. *Earth Planet. Sci. Lett.* **415**: 25-37.

Camire, G. E., Lafleche, M. R. and Ludden, J. N. (1993). Archean metasedimentary rocks from the northwestern Pontaic Subprovince of the Canadian Shield: chemical characterization, weathering and modelling of the source area. *Precambrian Res.***62**: 285-305.

Chaudhuri, A., Banerjee, S. and Gaurav Chauhan, G. (2020). Compositional evolution of siliciclastic sediments recording the tectonic stability of apericratonic rift: Mesozoic Kutch Basin, western India. *Mar. Pet, Geol*. **111**: 476-495.

Chenkual, L., Kataki, T. and Sarma, J. N. (2010). Heavy minerals of Tertiary Rocks exposed in Teidukhan Anticline, Kolasib, Mizoram, India. *Sci. Vis* **10(1)**: 8-19.

Chutia, A. and Sarma, J. N. (2013). A Study of Geochemical Composition and Source Area Weathering of the Tipam Sandstones from a Few Oil Fields of Upper Assam Basin, India. *Indian J. Appl. Res.* **3**: 332-334.

Condie, K. C., Noll (Jr), P. D. and Conway, C. M. (1992). Geochemistry and detrital mode evidence for two sources of early Proterozoic sedimentary rocks from the Tonto basin, Supergroup, central Arizona. *Sed. Geol*. **77**: 51-76.

Cox, R., Lower, D. R. and Cullers, R. L. (1995). The influence of sediment recycling and basement composition on evolution of mudrock chemistry in the southwestern United States. *Geochimi. Cosmochim. Acta.* **59**: 2919-2940.

Crook, K. A. W. (1974). Lithogenesis and geotectonics: The significance of compositional variation in flysch arenites (greywacke): in R.H. Dott., and R.H. Shavar (Eds.) Modern and ancient geosynclinals Sedimentation. *Soc. Econ. Palaeon. Mineral. Spec. Publ.* **19**: 304-310.

Cullers, R. L., Barrett, T., Carlson, R. and Robinson, R. (1987) Rare-earth distributions in size fractions of Holocene soil and stream sediment, Wet Mountains region, Colorado, USA. *Chem. Geol.* **63**: 275-297.

Cullers, R. L. (1994). The controls on the major and trace element variation of shales, siltstones and sandstones of Pennsylvanian-Permian age from uplifted continental blocks in Colorado to platform sediment in Kansas, USA. *Geochim. Cosmochim. Acta*. **58**: 4955-4972.

Cullers, R. L. (2000). The geochemistry of shales, siltstones and sandstones of Pennsylvanian- Permian age, Colorado, USA: Implications for provenance and metamorphic studies. *Lithos*. **51**: 181-203.

Cullers, R. L. and Podkovyrov, V. N. (2000). Geochemistry of the Mesoproterozoic Lakhanda shales in southeastern Yakutia, Russia: Implications for mineralogical and provenance control, and recycling. *Precamb. Res*. **104**: 77-93.

Cullers, R. L., Basu, A. and Suttner L. J. (1988). Geochemical signature of provenance in sand-size material in soils and stream sediments near the Tobacco Root Batholith, Montana, USA. *Chem. Geol*. **70**: 335-348.

Cullers, R. L. (1995). The controls on the major and trace element evolution of shales, siltstones and sandstones of Ordovician to Tertiary age in the Wet Mountain region, Colorado, USA. *Chem. Geol*. **123**: 107-131.

Dapples, E. C. (1967). Diagenesis of Sandstone, in G. Larson and G. Chilinar, eds., Diagenesis of sediments. *Amsterdam, Elsevier Pub. Co.* 91-215.

Das, D. and Pramanik, B. K. (2015). Ecological amplitude and Environmental impact on Flora and Fauna including society of Mizoram People in North-East India. *J. of Pharm. & Biol. Sci*. **10 (2):** 84-95.

Devi, S. R. and Mondal, M. E. A. (2008). Provenance and tectonic setting of Barail (origocene) and surma (Miocene) Group of surma-Barak Basin, Manipur, India: petrographic Constraints. *J. Geol. Soc. India*. **7**: 459-467.

Dickinson, W. R. and Suczek, C. A. (1979). Plate tectonics and sandstone compositions. *Amer. Assoc. Pet. Geol. Bull*. **63**: 2164–2182.

Dickinson, W. R. (1985). Interpreting provenance relations from detrital modes of sandstones. In: Zuffa, G.G. (Ed.), Provenance of Arenites. *D. Reidel Publ. Co., Dordrecht*, New York, 333-361.

Dickinson, W. R., Beard, L. S., Brakenridge, G. R., Erjavec, J. L., Ferguson, R. C., Inman, K. F., Knepp, R. A., Lindberg, F. A. and Ryberg, P. T. (1983). Provenance of North American Phanerozoic sandstones in relation to tectonic setting. *Geol. Soc. Am.Bull.* **94**: 222-235.

Evans, P. (1964). Tectonic framework of Assam. *J. Geol. Soc. India.* **48**: 17-26.

Fedo, C. M., Nesbitt, H. W. and Young, G. M. (1995). Unravelling the effects of potassium metasomatism in sedimentary rocks and paleosols, with implications for paleoweathering condition and provenance. *Geology*. **23**: 921-924.

Feo-Codecido, G. (1956). Heavy mineral techniques and their application to Venezuelan stratigraphy. *Am. Assoc. Petrol. Geol. Bull*. **40**: 979.

Fyffe, L. R. and Pickerill, R. K. (1993). Geochemistry of Upper Cambrian – Lower Ordovician black shale along a northeastern Appalachian transect. *Bull. Geol. Soc. Am.* **105**: 897-910.

Feng, R. and Kerrich, R. (1990). Geochemistry of fine-grained clastic sediments in the Archean Abitibi greenstone belt, Canada: Implications for provenance and tectonic setting. *Geochim. Cosmochim. Acta*. **54**: 1061-1081

Floyd, P.A., Winchester, J. and Park, R. G. (1989). Geochemistry and tectonic setting of Lewisian clastic metasediments from the Early Proterozoic Loch Maree Group of Gairloch, N.W. Scotland. *Precamb. Res.* **45(1–3)**: 203-214.

Folk, R. L. (1951). Stages of textural maturity in sedimentary rocks. *J. Sediment. Petrol.* **21**: 127-130.

Folk, R.L. (1974). Petrology of Sedimentary Rocks. *Hemphill Publishing Co.*, Austin, TX.

Folk, R. L. (1980). Petrology of Sedimentary Rocks. *Hemphill Austin, Tex.* 183p.

Ganguly, S. (1983). Geology and Hydrocarbon prospects of Tripura-Cachar-Mizoram region. *Jour. Petrol. Asia*. **6(IV)**: 105-109

Ganguly, S. (1975). Tectonic evolution of the Mizo Hills, Bull. *Geol. Min. Met. Soc. India* **48**: 28-40.

Ganju, J. L. (1975). Geology of Mizoram. Bull. *Geol. Min. Met. Soc. India* **48** 17-26.

Garzanti, E. (2017). The Maturity Myth in Sedimentology and Provenance Analysis. *J. Sediment. Res*. **87**: 353-365.

Govin, G., Najman, Y., Copley, A., Millar, I., van der Beek, P., Huyghe, P., Grujic, D. and Davenport, J. (2018). Timing and mechanism of the rise of the Shillong Plateau in the Himalayan foreland. *Geology*. **46**: 279-282.

Grantham, J. J. and Velbel, M. A. (1988). The influence of climate and topography on rock fragment abundance in modern fluvial sands of the southern Blue Ridge Mountains, North Carolina. *J. Sediment. Petrol*. **58**: 219-227.

Gumbel, C.W. Von (1888). Grundziige der Geologie, Kassel: Fischer. 1144p.

Harnois, L. (1988). The CIW index: a new chemical index of weathering. *Sediment. Geol*. **55**:319-322.

Hauhnar, M., Lalnunmawia, J. and Vanthangliana, V. (2018). Petrography of Barail sandstone of Champhai-Mualkawi section in Champhai district, Mizoram: Implication on provenance and tectonic setting. *Advances in Engineering Research,* **178**: 66-73.

Hayashi, K. I., Fujisawa, H., Holland, H. D. and Ohmoto, H. (1997). Geochemistry of 1.9Ga Sedimentary rocks from northeastern Labrador, Canada. *Geochim. Cosmochim. Acta.* **61**: 4115-4137.

Hazarika, I.M. (1984). Significance of heavy mineral studies in the Upper Tertiary Tipam Sandstone of the Kameng Foot Hills of Arunachal Himalaya. *Current Trends in Geology, Sedimentary Geology of Himalaya*. **5**: 83-89.

Herron, M. M. (1988). Geochemical classification of terrigenous sands and shales from core or log data. *J. Sed. Res*. **58:** 820-829.

Hossain, H. M. Z., Roser, B. P. and Kimura, J. I. (2010). Petrography and whole rock geochemistry of the Tertiary Sylhet succession, northeastern Bengal Basin, Bangladesh: Provenance and source area weathering. *Sediment. Geol.* **228**: 171-183.

Hussain, M. F. and Bharali, B. (2019). Whole-rock geochemistry of Tertiary sediments of Mizoram Foreland Basin, NE India: implications for source composition, tectonic setting and sedimentary processes. *Acta. Geochim.* **38**: 897-914.

Hubert, J. F. (1962). A zircon-tourmaline-rutile maturity index and independence of composition of heavy mineral assemblages with gross composition and texture of sandstone. *J. Sediment. Petrol*. **32**: 440-450.

Hubert, J.F. (1971). Analysis of heavy mineral assemblages. In, R.E. Carver (Ed.), Procedures in Sedimentary Petrology. *Wiley*, New York, 453-478.

Ingersoll, R. V., Bullard, T. F., Ford, R. L., Grimm, J. P., Pickle, J. D. and Sares, S. W. (1984). The Effect of Grain size on Detrital Modes: A Test of the Gazzi-Dickinson Point counting Method. *J. Sediment. Petrol.* **54**: 103-116.

Jinliang, Z. and Xin, Z. (2008). Composition and Provenance of Sandstones and Siltstones in Paleogene, Huimin Depression, Bohai Bay Basin, Eastern China. *J. China Univ. Geosci.* **19**: 252-270.

Johnsson, M. J. (1993). The system controlling the composition of clastic sediments in Johnsson, M. J. and Basu, A., eds., Processes Controlling the composition of Clastic Sediments Boulder, Colorado, *Geol. Soc. Am. Special Paper,* **284**.

Judd, J. W. (1886). Report on a series of specimens of the deposits of the Nile delta. *Proc. R. Soc.* **39**: 213-227.

Karunakaran, C. (1974). Geology and Mineral resources of the States of India. *Misc. Publ. Geol. Surv. India* **30(4)**: 93-101.

Kesari, G. K. (2011). Geology and Mineral Resources of Manipur, Mizoram, Nagaland and Tripura. *Geol. Surv. India Misc. Pub.*, No. 30 Pt 4, **1(2)**: 103.

Kichu, A. M. and Srivastava, S. K. (2018). Diagenetic Environment of Barail Sandstones in and around Jotsoma Village, Kohima District, Nagaland, India. *Jour. Geosci. Res*. **3(1)**: 31-35.

Kroonenberg, S. B. (1992). Effects of provenance, sorting and weathering on the geochemistry of fluvial sands from different tectonic and climatic environments. *Proc. 29th Int. Geol. Congr*. 69-81.

Krumbein, W.C. and Pettijohn, F. J. (1938). Manual of sedimentary petrography. *Appleton-Century- Crafts Inc*, New York. 549p.

Krynine, P. D. (1940). Petrology and Genesis of the Third Bradford Sand. *Pennsylvania State College Mineral Industries Experimental Station, Bulletin* 27.

Krynine, P. D. (1946). The tourmaline group in sediments. *J. Geol.* **54**: 65-87.

Krynine, P. D. (1984). The megascopic study and field classification of sedimentary rocks. *Jour. Geol*. **56**: 230-265.

Lalmuankimi, C., Kumar, S. and Tiwari, R. P. (2011). Geochemical study of upper Bhuban sandstone in Muthi, Mizoram, India. *Sci. Vis.,* **11(1)**: 40-46.

Lalnunmawia, J. and Lalhlimpuii, J. (2014). Classification and provenance studies of the sandstones exposed along Durtlang road section, Aizawl, Mizoram. *Sci. Vis.,* **14(3)**:158-167.

Lalnunmawia, J., Vabeihmo, Ch. and Lalremruatsanga, H. (2016). Petrography and heavy minerals as tools for reconstruction of provenance and depositional environment of Bhuban sandstones in Aizawl, Mizoram. *Sci. Vis*., **16(1)**: 1-9.

Lalremruatfela, C. (2019). Magnetostratigraphic Study of Barail Group in Champhai District, Mizoram. *Unpublished Thesis*. Mizoram Univ. 142p.

Lindholm, R. C. (1987). A Practical Approach to Sedimentology. *Allen and Unwin,* London.

Long, X., Yuan, C., Sun, M., Safonova, I., Xiao, W. and Wang, Y. (2012). Geochemistry and U-Pb detrital zircon dating of Paleozoic graywackes in East Junggar, NW China: Insights into subduction-accretion processes in the southern Central Asian Orogenic Belt. *Gondwana Res*. **21**: 637-653.

Mackie, W. (1896). The sands and sandstones of eastern Moray. *Edinburgh Geol. Soc. Trans*. **7**: 148-172.

Mackie, W. (1923). The principles that regulate the distribution of particles of heavy minerals in sedimentary rocks, as illustrated by the sandstones of the north-east of Scotland. *Edinburgh Geological Society, Transactions*. **11**: 138-164.

Mange, M. A. and Maurer, H. F. W. (1992). Heavy minerals in Colour. *Chapman and Hall, London,*147p.

McBride, E. F. (1963). A classification of common sandstone. *Jour. Sed. Petrol*., **33**: 664-669.

McLennan, S. M., Taylor, S. R. and Eriksson, K. A. (1983). Geochemistry of Archean shales from the Pilbara supergroup, Western Australia. *Geochimi. Cosmochim. Acta*. **47**:1211-1222.

McLennan, S. M., Hemming, S., McDaniel, D. K. and Hanson, G. N. (1993). Geochemical approaches to sedimentation, provenance and tectonics. *Geol. Soc. Am. Spec. Pap.* **284**: 295-303.

Mitchell, A. H. G. and Reading, H.G. (1986). Sedimentation and tectonics. Sedimentary Environments and Facies. (Reading, H. G., ed.). *Blackwell.*

Morton, A. C. (1985). Heavy minerals in provenance studies. In Provenance of arenites. *G. G. Zuffa (ed.)* 249-77.

Moss, A. J. (1972). Initial fluviatile fragmentation of granitic quartz. *Jour. Sed. Petrology*. **42**: 905-916.

Mongelli, G., Critelli, S., Perri, F., Sonnino, M. and Perrone, V. (2006). Sedimentary recycling, provenance and paleoweathering from chemistry and mineralogy of Mesozoic continental redbed mudrocks, Peloritani mountains, southern Italy. *Geochem. J.* **40**: 197-209.

Mukherjee, R. N. and Saxena, A. (1973): Systematic geological mapping in parts of Lungleh district Mizoram. *Unpublished GSI Progress Report*.

Najman, Y., Bickle, M., Fadel, B. M., Carter, A., Garzanti, E., Paul, M., Wijbrans, J., Willett, E., Oliver, G., Parrish, R., Akhterk, S. H., Allen, Allen R., Chisty, S. E., Reisberg, L. and Vezzoli, G. (2008). The Paleogene record of Himalayan erosion: Bengal Basin, Bangladesh. *Earth Planet. Sci. Lett.* **273**: 1-14.

Nandy, D. R., Gupta, S. G., Sarkar, K. and Ganguly, A. (1983). Tectonic Evolution of Tripura-Mizoram Fold Belt, Surma Basin, North East India. *Quart. Jour. Geol. Min. Met. Soc. Ind.*, **34(4)**: 186-194.

Nandy, D. R. and Sarkar, K. (1973). Geological mapping and mineral survey in parts of Aizawl District, Mizoram. *Geol. Surv. India. Prog. Rep. F.S.* 1971-72.

Nandy, D. R. (2017). Geodynamics of northeastern India and the adjoining Region. *Scientific Book Centre, Guwahati, Assam*. 272p.

Nesbitt, H. W. (1979). Mobility and fractionation of rare earth elements during weathering of a granodiorite. *Nature*. **279**: 206-210.

Nesbitt, H. W., Markovics, G. and Price, R. C. (1980). Chemical processes affecting alkalis and alkaline earths during continental weathering. *Geochim. Cosmochim. Acta*. **44**: 1659-1666.

Nesbitt, H. W. and Young, G. M. (1982). Early Proterozoic climates and plate motions inferred from major elements of lutites. *Nature*. **299**: 715-717.

Nesbitt, H. W. And Young, G. M. (1984). Prediction of some weathering trends of plutonic and volcanic rocks based upon thermodynamic and kinetic considerations. *Geochem. Cosmochim. Acta.* **48**: 1523-1534.

Nesbitt, H. W. And Young, G. M. (1989). Formation and diagenesis of weathering profiles. *J. Geol*. **97**: 129-147.

Oni, S. O. and Olatunji, A. S. (2017). Eurasian. *J. Soil. Sci.* **6(3)**: 259-274.

Omotoso1, O. A., Ojo, O. J. and Alebiosu, M. T. (2017). Geochemical characteristics of in river Niger fadama, central Nigeria. *Water Utility Journal.* **17**: 35-48.

Parker, A. (1970). An index of weathering for silicate rocks. *Geol Mag.* **107**: 501-504.

Pearson, K. (1895). Contributions to the Mathematical Theory of Evolution. II. Skew Variation in Homogeneous Material. Phil*os. Trans. R. Soc. A Math. Phys. Eng. Sci.* **186**: 343-414.

Pettijohn, F. J. Potter P. E. and Siever, R., (1972). Sand and Sandstone. *Springer-Verlag*. p241.

Pettijohn, F.J. (1975). Sedimentary Rocks, 3rd Edition. *Harper and Row*, New York. 624-629.

Pettijohn, F.J., Potter, P. E. and Siever, R., (1973). Sand and Sandstone. Springer Verlag, New Work.

Potter, P. E. (1978). Petrology and chemistry of modern big river sands. *J. Geol.* **86(4)**:423-449.

Rahman, J. J. M. and Suzuki, S. (2007). Geochemistry of sandstones from the Miocene Surma Group, Bengal Basin, Bangladesh: Implications for Provenance, tectonic setting and weathering. *Geochem. Jour*. **41**: 415-428.

Rahman, M. J. J., Sayem, A. S. M. and McCann, T. (2014). Geochemistry and provenance of the Miocene sandstones of the Surma Group from the Sitapahar Anticline, Southeastern Bengal Basin, Bangladesh. *J. Geol. Soc. India.* **83**: 447-456.

Ralte,V. Z. (2012). Heavy mineral analysis of Tipam sandstone near Buhchang village, Kolasib district, Mizoram, India. *Sci .Vis.* **12(1)**: 22 -31

Ramamoorthy, A. and Ramasamy, S. (2015). Petrography and Provenance of Surface Barail Sandstones, Kohima, Nagaland, India. *Int. Jour. Engr. Mgmt. and Economics.* **4(10)**: 35-41.

Rintluanga, Pachuau. (1994). Geology of Mizoram. 1st edition, *New Aizawl Press*, Chandmari, Aizawl. 54p.

Rollingson, Hugh. R. (1993). Using Geochemical Data: Evaluation, Presentation, Interpretation. *Harlow, Essex, England: New York: Longman Scientific & Technical*. 352p.

Roser, B. P. and Korsch, R. J. (1986). Determination of tectonic setting of sandstones-mudstone suites using SiO2 content and K_2O/Na_2O ratio. *Journal of Geology*. **94**: 635-650.

Roser, B. P. and Korsch, R. J. (1988). Provenance signatures of sandstone-mudstone suites determined using discrimination function analysis of major element data. *Chem. Geol*. **67**: 119-139.

Roser, B. P., Cooper, R. A., Nathan, S. and Tulloch, A. J. (1996). Reconnaissance sandstone geochemistry, provenance, and tectonic setting of the lower Paleozoic terranes of the West Coast and Nelson, New Zealand. *Jour. Geol. Geophys*. **39**: 1-16.

Roy, D. K. and Roser, B. P. (2012). Geochemistry of tertiary sequence in Shahbajpur-1 well, hatia trough, Bengal basin, Bangladesh: provenance, source weathering and province affinity. *J. Life Earth Sci.* **7**: 1-13.

Rudnick, R. L. and Gao, S. (2003). Composition of the continental crust. *Treatise on Geochemistry*. **3**: 1-64.

Sahoo, U. K. and Singh, S.L., Lalnundanga., Lalnuntluanga., Devi, A. S., and Zothanzama, J. (2018). Climate Change Impacts on Forest and its Adaption study in Mizoram. Mizoram University, Aizawl – 7986004, Mizoram.

Sarma, J. N. and Chutia, A. (2013). Petrography and heavy mineral analysis of Tipam sandstones exposed on the Tipam hill of Sita Kunda area, upper Assam, India. *South East Asian Journal of Sedimentary Basin Research* 1: 28-34.

Schoenborn, W. A. and Fedo, C. M. (2011). Provenance and paleoweathering reconstruction of the Neoproterozoic Johnnie Formation, southern California. *Chem. Geol*. **285**: 231 -255.

Schwab, F. L. (1975). Framework mineralogy and chemical composition of continental margin type sandstone. *J. Geol*.**3**: 487-490.

Sengupta, S. M. (2004). Introduction to Sedimentology. *Oxford*, New Delhi. 295p.

Sen, S., Das, P. K., Bhagaboty, B. and Singha, L. J. C. (2012). Geochemistry of Shales of Barail group Occuring in and around Mandardisa, North Cachar Hills, Assam; India: Its Implications. *Intr. Jour. Chem. and Applications*. **4(1)**: 25-37.

Shrivastava, B. P., Ramachandran, K. K. and Chaturvedi, J. G. (1979). Stratigraphy of Eastern Mizo Hills. *Bull. ONGC*. **16(2)**: 87-94.

Singh N. P., Singh K. P. and Singh D. K. (2002). Flora of Mizoram. *Botanical Survey of India*. 1.

Singh, P. K., Singh, M. P., Singh, A. K. and Naik, A. S. (2012). Petrographic and geochemical characterization of coals from Tiru Valley, Nagaland, NE India. *Energy Exploration and Exploitation.* **30(2)**: 171-192.

Slack, J. F. and Stevens, P. J. (1994). Clastics metasediments of the Early Proterozoic Broken Hill Group, New South Wales, Australia: geochemistry, provenance and metallogenic significance. *Geochim. Cosmochim. Acta*. **58**: 3633-3652.

Somasekhar, V., Ramanaiah, S. and Sarma, D. S. (2018). Geochemical characterization of the siliciclastic rocks of Chitravati Group, Cuddapah Supergroup: Implications for provenance and depositional environment. *J. Earth Syst. Sci.* 127:54.

Sorby, H. C. (1880). On the structure and origin of non-calcareous stratified rocks. *Proc. Geol. Soc. Lond*. **36**: 46-92.

Srivastava, S. K. and Pandey, N. (2011). Search for Provenance of Oligocene Barail Sandstones in and around Jotsoma, Kohima, Nagaland. *Jour. Geol. Soc. India*. **77**: 433-442.

Srivastava, S. K. (2013). Petrography and Major Element Geochemistry of Oligocene Barail Sediments in and around Jotsoma, Kohima, Nagaland. *Gond. Geol. Mag.* **28(2)**: 159-164.

Srivastava, S. K., Laskar, Keditsu, J. and Awomi, L. (2018). Petrography and major element geochemistry of palaeogene sandstones, South of Kohima town, Nagaland. *J. Appl. Geochem.* **20 (1)**: 41-49.

Suttner, L. J. (1974). Sedimentary petrographic provinces: An evaluation, in Ross, C. A, ed., Paleogeographic provinces and provinciality. *Society of Economic Paleontologists and Mineralogists. Special Publication* **21**: 75-84.

Suttner, L. J. and Dutta, P. K. (1986). Alluvial sandstone composition and paleoclimate, I. Framework mineralogy. *J. Sediment. Petrol.* **56**: 329-345.

Suttner, L. J., Basu, A. and Mack, G. H. (1981). Climate and the origin of quartz arenites. *J. Sediment. Petrol.* **51**: 1235-1246.

Taylor, S. R. and McLennan, S. M. (1985). The Continental Crust: Its composition and Evolution. *Blackwell, Oxford*. 312p.

Tiwari, R. P. and Kachhara, R. P. (2003). Molluscan biostratigraphy of the tertiary sediments of Mizoram, India. *Jour. Paleon. Soc. India.* **48**: 59-82.

Tortosa, A., Palomares, M. and Arribas, J. (1991). Quartz grain types in Holocene deposits from the Spanish Central System: some problems in provenance analysis; In: Developments in Sedimentary Provenance Studies (eds) A. C. Morton, S. P. Todd and P. D. W. Haughton. *Geol. Soc. Lon.*, Spec. Publ. **57**: 47-54.

Tucker, M. E. (2012). Sedimentary Petrology: An introduction to the Origin of Sedimentary Rocks. 3rd Edition. *Blackwell Publishing*. 262p.

Uddin, A. and Lundberg, N. (1998). Unroofing history of the Eastern Himalaya and the Indo–Burman ranges: Heavy mineral study of Cenozoic sediments from the Bengal Basin, Bangladesh. *J. Sediment. Res*. **68(3)**: 465-472.

Uddin, A. and Lundberg, N. (1999). A paleo-Brahmaputra, Subsurface lithofacies analysis of Miocene deltaic sediments in the Himalayan-Bengal system, Bangladesh. *Sediment. Geol.* **123**: 239-254

Uddin, A., Kumar, P., Sarma, J. N. and Akhter, S. H. (2007). Heavy mineral constraints on the provenance of Cenozoic sediments from the foreland basins of Assam and Bangladesh: Erosional history of the Eastern Himalayas and the Indo–Burman ranges. *Developments in Sedimentology*. **58**: 823-847.

Weljte, G. J. (1994). Provenance and dispersal of sand-sized sediments: recognition of dispersal pattern and sources of sand-sized sediments by means of inverse modelling techniques. *Geol. Ultraiectina*. 121, 208p.

Worden, R. H. and Burley, S. D. (2003). Sandstone diagenesis: the evolutionof sand to stone, in Burley, S.D. and R.H. Worden (eds.), Sandstone Diagenesis: Recent and Ancient: *Blackwell*, Malden, M. A. 3-44.

Wronkiewicz, D. J. and Condie, K. C. (1987). Geochemistry of Archean shales from the Witwatersrand Supergroup, South Africa: source-area weathering and provenance. *Geochim. Cosmochim. Acta*. **51(9)**: 2401-2416.

Xeujing, X., Mingcai, Y., Lianzhong, L. and Huijun, S. (2007). Useable values for Chinese Standard Reference Samples of Stream Sediments, Soils and Rocks: GSD 9-12, GSS 1-8 and GSR 1-6. *Geostand. Geoanal. Res*. **9(2)**: 277-280.

Zoramthara, C., Ralte, V. Z. and Lalramdina. (2015). Grain size analysis of Tipam sandstones near Buhchang village, Kolasib district, Mizoram. *Sci. Vis*. **15**: 42-51.

BRIEF BIO-DATA OF THE CANDIDATE

1. NAME OF THE CANDIDATE : ORIZEN MS DAWNGLIANA
2. FATHER'S NAME : SANGMAWIA
3. DATE OF BIRTH : 06.07.1989
4. PERMANENT ADRESS : PWD ROAD, MUALPUI, CHHINGCHHIP
5. E-MAIL : orizen18@gmail.com
6. MOBILE NO. : 9612660599/8118944941
7. STATE OF DOMICILE : MIZORAM
8. NATIONALITY : INDIAN
9. CATEGORY (G/OBC/SC/ST) : ST
10. QUALIFICATIONS : M.Sc. (Applied Geology) with NET (Lectureship)

Sl. No.	Examination passed	Year	Board/University
1	HSLC	2007	MBSE
2	HSSLC	2010	MBSE
3	B.Sc.	2014	MZU
4	M.Sc.	2016	MZU
5	NET	2017	CSIR-UGC

(ORIZEN MS DAWNGLIANA)

Research Scholar

LISTS OF PUBLICATIONS

1.	Hauhnar, M., Jimmy Lalnunmawia and Orizen MS Dawngliana. Geochemistry of Barail sandstone in Champhai, Mizoram: Implications on provenance and weathering history. J. Earth Sys. Sci. MS received 13 March 2020; revised 22 September 2020; accepted 29 September 2020.
2.	Jimmy Lalnunmawia, Hauhnar, M, Orizen MS Dawngliana, Zoramthara C. Geochemical Appraisal on History and Evolution of Barail sandstones of Zote-Ngur, Champhai District. Science and Technology Journal Vol.9 Issue 1, January 2021 ISSN: 2321-3388.
3.	Jimmy Lalnunmawia, Hauhnar, M., and Orizen MS Dawngliana. 2020. Provenance studies of Barail sandstone in Ngur village, Champhai District, Mizoram: Constraints from heavy mineral analysis. In Singh, K.K. (eds): Advances in Environmental Research in Northeast India. South Eastern Book Agencies, pp. 241-254. ISBN: 978-9389262-10-0.
4.	Jimmy Lalnunmawia, Hauhnar, M., Laltluanpuii, Orizen MS Dawngliana, and Lalrochani, T. 2020. Petrographic analysis of Surma sandstones in Reiek Hill area, Mizoram, India. In Singh, K.K. (eds): Advances in Environmental Research in Northeast India. South Eastern Book Agencies, pp. 241-254. ISBN: 978-9389262-10-0.

PRESENTATIONS

1.	Depositional Environment of Barail Sandstones Exposed in and Around Ngopa Village, Mizoram, India. International Seminar on Recent Advances in Science and Technology (ISRAST) (16th -18th November 2020).
2.	Provenance studies of Barail Sandstones in Ngur Village, Champhai District, Mizoram: Constrains from Heavy Mineral Analysis. National Conference on Emerging trends in Environmental Research (NACETER) (31 October 2019.

SEMINAR/ TRAINING etc ATTENDED

1.	Emerging Trends in Environmental Research. (Dept. Of Environmental Science, PUC, Aizawl, Mizoram).
2.	International Seminar on Recent Advances in Science and Technology (ISRAST-NEAST)
3.	International Workshop on ‘Landslide Hazards in Mizoram’. (DGM, PUC&GSM)
4.	Refresher course on: Modern and ancient environment and ecology: Sediments and Biota. (Science Academics’ Education Programme)

5.	5 Days National workshop on ‘Surveying by Total Station’.
6.	Science Academies’ Refresher course in Geology, ‘Mineralogy, Petrology, Thermodynamics, Ore Geology, Structural Geology and Tectonics’.
7.	National workshop on Sequence stratigraphy and Basin analysis
8.	Advanced training programme on ‘ Analytical Geochemistry’ (Under CSIR Integrated skill initiative programme).
9.	e-Training on ‘ Fundamentals of Sedimentology and Mapping in Sedimentary terrain’ (GSITI-Hyderabad).
10.	e-Training on “Art of Publication, Effective Writing and Presentation Skills in Earth Sciences” (RTD, NR, GSITI, Lucknow)
11.	e-Training on “Basics of Structural Geology” (T.C. Division, GSIT I, Hyderabad)
12.	e-Training on “Basics of Geographical Information System and its Applications” (CGMT Div., GSITI, Hyderabad).
13.	webinar on ‘Earthquake versus Landslide with special reference to Mizoram’ (Mizoram University)
14.	e-Training on “Engineering Geology and Landslide Studies’’. (RTD, SR, GSITI, Hyderabad)
15.	GEOCHRON- An Online Lecture Series on various aspects of Geology. (Geological Institute, Department of Geology, Presidency University, Kolkata)
16.	Geological Research in Indo_Burma Ranges. Org. By- Geology Dept. PUC, Geol. Society of Mizoram (GSM) supported by DST-NRDMS-Delhi.
17.	21 days Online GIS Training Program using QGIS. (Department of Geography, School of Earth Sciences, Central University of Karnataka).
16.	International virtual workshop on ‘Global Seismology and tectonics’. (Geoscience and Tecnology Division, CSIR-NEIST, Jorhat, Assam.
19.	‘Understanding our Rivers of Hilly Region and its Conservation’ (Conducted by Mizoram University).
20.	Mapping in Tertiary Terrain (Regional TrainingDivision, NE Region, Shillong).

PARTICULARS OF THE CANDIDATE

NAME OF THE CANDIDATE	:	ORIZEN MS DAWNGLIANA
DEGREE	:	PH.D
DEPARTMENT	:	GEOLOGY
TITLE OF RESEARCH	:	SEDIMENTOLOGICAL AND GEOCHEMICAL STUDIES OF BARAIL SANDSTONES IN AND AROUND NGOPA VILLAGE, SAITUAL DISTRICT, MIZORAM.
DATE OF PAYMENT OF ADMISSION	:	27.07.2018

APPROVAL OF RESEARCH PROPOSAL

1	DRC	:	08.03.2019
2	BOS	:	05.04.2019
3	SCHOOL BOARD	:	26.04.2019

MZU REGISTRATION NO.	:	1807389
Ph.D REGISTRATION NO.	:	MZU/Ph.D/1291 of 27.07.2018

HEAD
DEPARTMENT OF GEOLOGY
MIZORAM UNIVERSITY

ABSTRACT

SEDIMENTOLOGICAL AND GEOCHEMICAL STUDIES OF BARAIL SANDSTONES IN AND AROUND NGOPA VILLAGE, SAITUAL DISTRICT, MIZORAM.

AN ABSTRACT SUBMITTED IN PARTIAL FULFILMENT OF THE REQUIREMENTS FOR THE DEGREE OF DOCTOR OF PHILOSOPHY.

ORIZEN MS DAWNGLIANA

MZU REGD. NO.: 1807389

PH.D. REGD. NO.: MZU/Ph.D/1291 of 27.07.2018.

DEPARTMENT OF GEOLOGY

SCHOOL OF EARTH SCIENCES AND NATURAL RESOURCES MANAGEMENT

DECEMBER, 2022.

SEDIMENTOLOGICAL AND GEOCHEMICAL STUDIES OF BARAIL SANDSTONES IN AND AROUND NGOPA VILLAGE, SAITUAL DISTRICT, MIZORAM.

BY

Orizen MS Dawngliana
Department of Geology

Dr. Jimmy Lalnunmawia
Supervisor

Submitted
In partial fulfilment of the requirement of the Degree of Doctor of Philosophy in Geology of Mizoram University, Aizawl.

ABSTRACT

Mizoram is a part of the Neogene Surma Basin, It is now surrounded by a belt of folded, elongated hill ranges with an arcuate shape that are convex to the west. It is considered Surma valley's southern extension. Mizoram's whole territory is covered in a thick Neogene succession that is a component of the Assam-Arakan basin (Evan 1964). In addition to a few pockets of shell-limestone, calcareous sandstone, and intra formational conglomerates, the sediments are composed of arenaceous and argillaceous rocks such as sandstone, silty-sandstone, siltstone, and silty-shale. The basin, where a 7 km thick deposit of sediments was made, is situated between the Indian and Burmese plates. The Barail, Surma, and Tipam groups of rocks make up Mizoram's tertiary sequence. With a thickness of around 3000m and an Oligocene age, “Barail group of rocks represents the oldest lithostratigraphic unit among the three groups”.

The Tertiary succession exposed in the study area is situated in the northeastern corner of Mizoram, close to the border with Manipur and Myanmar. The distance of the Study area from Aizawl, the Mizoram state capital, is around 170 kilometers. The study area is covered by “Survey of India toposheet No.84 E/1 and 84 E/2” (Between Tuiphal bridge 23°48'32.53"N, 93° 9'39.46"E and Kawlbem Village 23°52'16.13"N, 93°18'27.76"E). To reconstruct and interpreted the underlying environmental conditions and processes during the formation of Barail sandstones, numerous field and laboratory studies had been conducted. For the interpretation of provenance, age, and geochemical history of any sedimentary basin, geochemical methods are particularly reliable. The interpretation of the tectonic settings of the source location can be done using a variety of petrographical, geochemical, and other isotopic approaches. A detailed history of tectonic settings is also provided by trace and other REE analysis. The age of the provenance can potentially be constrained by the use of various isotopic analyses. Data on major and trace components aid in making predictions about the provenance's composition. The understanding of various secondary processes, such as diagenesis, weathering, sorting, etc., is greatly aided by geochemistry. The palaeo-environmental conditions can also be recreated with the aid of granulometric analysis.

The majority of the geological research that has been done in Mizoram during the past few years has been based on various approaches, including petrography, geochemistry, magnetostratigraphy, stratigraphy, and palaeontology. However, the Barail sandstones of the Saitual District have not been properly studied in terms of petrological and geochemical techniques. This justifies the necessity to suggest a study on a specific topic in order to improve our understanding of Mizoram's geological frameworks as a whole. In order to find out “depositional settings, paleoweathering history, and to understand the tectonic setting and provenance of Barail sandstones in the research area, “Grain size analysis, petrographyh and geochemical investigations” have been conducted.

Barail sandstones observed in the study area are composed of “sandstone, siltstone, and shale” and their admixture in varying proportions has various lithological thicknesses. Shales are fragile and prone to crumpling, but sandstones are tough, compact, buff in color, and have extremely fine to fine-grained grains. Sedimentary beds contain sedimentary structures such as “ripple marks, ball and pillow structures, load structures, rain drop structures, ripped-up clasts, and sandstone lenses”. There are bioturbated preservation burrows in some of the sandstone strata, they suggest and support the hypothesis of “a shallow depositional environment with an oxidizing environment and supportive environment for the living organisms”.

The thesis is categorized into nine (9) chapters. The first chapter's introduction covering few previous researches on the area nearby, study area location, coordinates, definition of sample names, accessibility of the study area, the physiography, the climate, and Geological importance of the study area. A thorough field assessment has been conducted along the study area Tuiphal River to Kawlbem Village, Saitual District. Field analysis on sedimentary structures, lithology and detailed mapping of the litho units exposed in these sections. Gathering rock samples, field data (such as GPS location, dip and strike) and images taken in the field. These important data collected were further used to make a lithological column of the study area. Chapter 2 includes “Regional geology, general geology and stratigraphy of Mizoram and the study areas’ geology and lithological column”. Chapter 3 contains review of literatures. A review of

the literature was conducted using old and new journal articles and book publications as well as related Thesis topics.

Chapter 4 contains methodology, the materials used and Techniques employed to achieve the objectives of the present study. For grain analysis, sieving method is used using Mechanical Sieve Shaker Machine (Krumbein and Pettijohn, 1938). To adhere to the necessary grade scale 1/2Φ, ASTM sieves are employed. Ssieve meshes 35, 45, 60, 80, 120, 170, 230, 325 and collecting pan was used. For petrography, Modal analysis using Point counting technique after "Gazzi-Dickinson method. (cf. Ingersoll et al., 1984)" was employed. After thin section were made from the sample collected from the study area, they were analysed using "LeicaDM4500 P polarizing microscope attached with Leica DFC420 camera and Leica Image Analysis software (LAS- v4.6)" microscope installed in "Department of Geology, Mizoram University". Each thin section has been counted for 300 steps using PETROGLITE Stepping Stage (cf. Ingersoll *et al*., 1984). For Heavy mineral separation and analysis, Gravity settling method is used for Heavy mineral separation using Bromoform as liquid medium. (Funnel separation method of Krumbein and Pettijohn, (1938). ZTR Index by Hubert (1962) is used to express the maturity of the investigated samples. For Geochemical study, "major, trace, and rare earth elements" are examined in represented rock samples at CSIR- National Geophysical Research Institute, Hyderabad, India. "Trace and rare earth elements" are examined using HR-ICP-MS and the "major elements" are examined using XRF.

In this chapter, more detailed procedures and methods employed for each analysis performed were highlight.

Chapter 5 contains Grain size analysis (Granulometric analysis). The data obtained from the laboratory were systematically used to calculate various grain parameters. These grain parameters calculated were further used to obtain grain size distribution patterns and to interpret the environment that is avail during the time of sediment deposition. Based on many discrimination diagram plots and other determining functions, it is found out from grain analysis that the Barail sandstone from

the study area are deposited in a “Shallow marine, Beach environment under the influence of river action”.

“The provenance, weathering history, and tectonic settings of the source area” were revealed by the investigation of Barail sandstones' petrography in chapter 6. Among the detrital grains, Quartz is the most abundant (average 67.34%) which is followed by Rock fragments (average 67.34%) and Felspars (average 5.42%). Other accessory minerals like Micas and Heavy mineral inclusions etc. are also observed. According to Pettijohn et al. (1972) and Folk (1980), Barail sandstones are classed as Litharenite and sub Litharenite. The Barail sandstones analysed are assumed to come from “mixed provenance” like “low-ranked metamorphic and Granirtic rocks under sub-humid to humid climatic conditions” based on several provenance and paleoclimatic condition diagrams.

Heavy mineral analysis, Chapter 6 discusses how heavy minerals separated were identified using a petrological microscope and counted. The source area's maturity and origin were identified by the composition and properties of the minerals present. The heavy minerals observed in the samples were “opaque and non-opaque”. Non opaque minerals like “Zircon, Tourmaline, Rutile, garnet, Apatite, Chlorite, Monazite, Epidote, Chloritoid, Enstatite, Diopsite, Augite, Kyanite, Clinozoisite, Hypersthene, Staurolite, Silliminite, Zoisite and Muscovite” are identified. Based on the heavy minerals identified, the studied sandstones are considered to be derived from “mixed sources” and are originated from “sub-mature sediments” according to the mineral assemblages and the ZTR maturity index. The majority of the sediments revealed igneous and metamorphic origins as their sources. Rounded to subrounded minerals shape also suggests reworked sediments.

The geochemistry of the Barail sandstones is covered in Chapter 7. Based on geochemical constituents, the sandstone of the Barail formation is classed as litharenite and Fe-sandstone and lithic sandstone according to classification schemes after Pettijohn et al. (1972), Blatt et al. (1980) and Herron (1988). The REE chondrite normalised pattern shows a slight enrichment of light rare earth elements (LREE: La-Sm) and a slight depletion of heavy rare earth elements (HREE: Gd-Lu) with a negative

Eu anomaly (average of 1.42%), suggesting that the Barail sandstones were derived from fractionated felsic to intermediate source rocks (granitoid) (Slack and Stevens, 1994). The Barail sandstones are believed to have originated from a variety of sources, including “recycled sedimentary terrain, intermediate sources, and felsic sources” based on multiple provenance plots of the geochemical data. The A-CN-K plot reveals that the Barail sandstones are subject to “mild to moderate weathering conditions”. Zr/Sc vs. Th/Sc graph (McLennan et al. 1993) suggests sediment recycling with zircon addition. The Barail sediments have undergone “immature to weak weathering” in the source region, according to chemical weathering indices like CIA and PIA. The studied sediments were deposited in an “active continental margin with sediment input from the Continental Island Arc and Oceanic Island arc” according to several tectonic setting discrimination diagrams using major oxides and trace elements.

The entire body of research is summarized and concluded in Chapter 9. It is possible to infer from field observations, several laboratory studies, and interpretations that the Barail sandstones were likely deposited in a “shallow marine environment” based on grain size analysis as well as various sedimentary structures and the preservation of burrows observed in the field. In terms of mineralogy, the investigation of “heavy mineral assemblages, ZTR maturity index, and petrographic analysis”, the analysed Barail sandstones were formed from sub mature sediments that are derived from “mixed sources i.e., metamorphic, igneous sources with some reworked sediment” whereas the geochemical makeup of the investigated sandstone leads to sediments that are immature in character and gradually become mature. The Barail sandstones have been generated from a wide range of provenances, including recycling sedimentary terrain, intermediate, and felsic source of sediments, according to petrography, heavy mineral analysis, and geochemical study. It is hypothesized that the “Continental Island Arc”, which is connected to the “Active Continental Margin” is where the tectonic settings of the Barail sandstones originated. The sediments were hypothesized to have been carried from “Himalayan orogenic belts uplifted and eroded terrain, the crystalline Proterozoic upliftments in northeast India as well as the nearby Indo-Myanmar tectonic belt”.